INSTITUTO SUPERIOR TÉCNICO
Universidade Técnica de Lisboa

INESC MN Microsistemas & Nanotecnologias

Microfluidic Devices for single-cell analysis and gradient generation

Marta Isabel Magalhães Mota do Amaral

Dissertação para obtenção do Grau de Mestre em

Engenharia Biomédica

Júri

Presidente:	Professora Maria de Fátima Reis Vaz
Orientadores:	Professor João Pedro Estrela Rodrigues Conde
	Doutor Tiago Fleming de Oliveira Outeiro
Vogal:	Professor Duarte Miguel de França Teixeira dos Prazeres

Setembro de 2008

Acknowledgments

I would like to express my deepest gratitude to my supervisor, Professor João Pedro Conde for his valuable support and precious guidance and for giving me the opportunity to work on this project. His capacity to transmit his vast knowledge gave me motivation to work hard and to improve my skills every day.

Sincere acknowledgments also go to Doctor Virginia Chu and Doctor Tiago Fleming Outeiro for their constructive advice and support.

I am particularly thankful to Doctor Sandra Tenreiro who so kindly supported me during all the project with her constant motivation and encouragement.

A very special thanks goes to Master Diogo Martins for his understanding and for sharing his knowledge whenever I needed it.

I am grateful to MEMS group which offered me the opportunity for many interesting discussions and advice.

I would like to express my gratitude to Virginia Soares for her excellent technical support.

Over and above all, I am sincerely thankful to all people around me, particularly my family for their patience and support.

Resumo

Este projecto teve como objectivo principal a criação de um dispositivo microfluido para a análise de células individualmente. Durante este projecto foi implementada uma nova técnica de microfabricação que permite a fabricação de microcanais com larguras coincidentes com o tamanho das células de interesse, nomeadamente células da levedura *Saccharomyces cerevisiae* (5-10μm). Foram igualmente desenvolvidas metodologias para localizar a mesma célula ao longo de vários períodos de tempo, bem como técnicas de vácuo capazes de forçar as células a entrar nos microcanais.

O dispositivo híbrido microfluido PDMS/vidro foi fabricado pela técnica de Soft Lithography e o molde foi desenvolvido por uma nova técnica de microfabricação no qual este é criado directamente por dupla exposição a 100% de energia na DWL (Direct Laser machine) sem a necessiadade de recurso a uma máscara.

A plataforma concebida foi aplicada ao estudo de leveduras geneticamente modificadas, exprimindo proteínas fluorescentes, uma das quais fusionada a uma proteína envolvida na doença de Parkinson, a α-sinucleina.

Os resultados obtidos demostraram a eficiência do dispositvo em estabelecer um microambiente adequado para o crescimento celular e expressão proteica, bem como a capacidade de visualizar células individualmente e não em colónias.

Neste projecto foi igualmente desenvolvida uma abordagem que permite gerar gradientes químicos estáveis durante 2 a 3 horas no interior dos microcanais, pela disposição prependicular dos mesmos a dois reservatórios principais, e que foi testado com o fluoroforo FITC.

Palavras-chave:

Dispositivo Microfluido
PDMS
Microcanais
Soft lithography
Alfa-Sinucleína
Gradientes químicos

Abstract

The main goals of this project were to develop a microfluidic device for single-cell analysis and to serve as a gradient-generator.

During the project a new microfluidic fabrication technique was developed that allowed the fabrication of microchannels with widths coincident to that of the cells of interest (5-10μm) namely *Saccharomyces cerevisiae* yeast cells. Approaches to localize the same cell over long periods were improved as well as a new methodology that forced cells to enter the microchannels.

A hybrid PDMS/glass microfluidic device was fabricated using the Soft Lithography process. The master mold was fabricated using a new technique of Rapid Prototyping in which the mold is directly fabricated by double exposure on a Direct Laser machine (DWL) without the need of any photomask.

The conceived microfluidic platform was then applied to study yeast cells carrying fluorescent proteins, one of them fused with αSyn, a protein related to Parkinson's disease.

The results obtained demonstrate the effectiveness of the device to establish a suitable environment for cell growth and protein expression as well as the capacity to visualize individual cells.

This work also demonstrates an approach to generate chemical gradients by using microchannels featured alongside two main reservoirs. The creation of a stable gradient inside the channels using the fluorophore FITC was achieved for 2-3 hours despite being different from what was theoretically expected.

Keywords:

Microfluidic device
PDMS
Microchannels
Soft lithography
Alpha-Synuclein
Chemical Gradients

Contents

1 INTRODUCTION 1

1.1 MOTIVATION BEHIND THE DEVELOPMENT OF MICROFLUIDIC DEVICES 1
1.2 BACKGROUND OF THE DEVELOPMENT OF MICROFLUIDICS AND NEW MATERIALS FOR ITS FABRICATION 3
1.3 BASIC PRINCIPLES OF MICROFLUIDICS 5
1.4 APPROACHES TO MICROFABRICATION TECHNIQUES 6
1.5 MICROFLUIDICS FOR BIOLOGICAL APPLICATIONS 9
1.5.1 MICROFLUIDIC DEVICES FOR SINGLE GENE EXPRESSION 10
1.5.2 MICROFLUIDICS FOR GRADIENT GENERATION 11
1.6 PHYSICAL BACKGROUND OF DIFFUSION 13
1.7 YEAST CELLS 14
1.8 ALPHA-SYNUCLEIN AND ITS RELATION TO PARKINSON'S DISEASE 15
1.9 WORK GOALS 16
1.10 WORK STRUCTURE 17

2 MICROFABRICATION TECHNIQUES 19

2.1 MATERIALS 19
2.1.1 MICROFLUIDIC FABRICATION 19
2.2 METHODS 22
2.2.1 MICROFABRICATION ENVIRONMENT 22
2.2.2 FABRICATION OF MICROFLUIDIC CHANNELS 23
2.2.2.1 Fabrication of Microfluidic channels using the negative photoresist SU-8 2015 23
2.2.2.2 Methods to increase the adhesion between SU-8 2015 photoresist and Si substrate 27
2.2.2.3 Fabrication of microfluidic channels using polymeric materials as substrate 29
2.2.2.4 Fabrication of microfluidic channels using the positive photoresist AZ 4562 29
2.2.2.5 Microfluidic channels using four layers of positive photoresist PFR 7790G 27cP 30
2.2.3 PDMS REPLICA MOLDING 31
2.2.4 OPTIMIZATION OF THE MICROFLUIDIC DEVICE 32
2.2.5 OPERATION MODE OF THE MICROFLUIDIC DEVICE 35

2.3 RESULTS AND DISCUSSION 37
2.3.1 FABRICATION OF MICROFLUIDIC CHANNELS USING THE PHOTORESIST SU-8 2015 37
2.3.2 METHODS TO INCREASE THE ADHESION BETWEEN SU-8 AND SI SUBSTRATE..... 38
2.3.3 FABRICATION OF MICROCHANNELS USING POLYMERIC MATERIALS AS SUBSTRATE 40
2.3.4 FABRICATION OF MICROCHANNELS USING THE POSITIVE PHOTORESIST AZ 4562..... 41
2.3.5 MICROFLUIDIC CHANNELS USING FOUR LAYERS OF POSITIVE PHOTORESIST PFR 7790G 27CP 42
2.3.6 GENERAL CONSIDERATIONS ABOUT THE MICROFLUIDIC DEVICE 43

3 YEAST CELL EXPERIMENTS 46

3.1 MATERIALS 46
3.1.1 STRAINS AND PLASMIDS 46
3.1.2 GROWTH CONDITIONS AND MEDIA..... 47
3.2 METHODS..... 47
3.2.1 INTRODUCTION OF THE CELLS INTO MICROCHANNELS 47
3.2.2 CELL GROWTH WITHIN MICROCHANNELS 47
3.2.3 αSYN-GFP/GFP-αSYN EXPRESSION INDUCTION WITH GALACTOSE..... 48
3.3 RESULTS AND DISCUSSION 49
3.3.1 INTRODUCTION OF THE CELLS INTO MICROCHANNELS AND OPTIMIZATION OF THE OPTICAL DENSITY 49
3.3.2 APPROACHES TO IDENTIFY A PARTICULAR CELL OVER LONG PERIODS 51
3.3.3 CELLS GROWTH WITHIN MICROCHANNELS 52
3.3.4 THE IMPORTANCE OF THE TEMPERATURE CONTROL IN BIOLOGICAL STUDIES..... 54
3.3.5 αSYN-GFP/GFP-αSYN EXPRESSION INDUCTION WITH GALACTOSE..... 55

4 GENERATION OF A STABLE GRADIENT INSIDE THE CHANNELS 61

4.1 MATERIALS AND METHODS 61
4.1.1.1 Generation of stable gradients using the fluorophore FITC 62
4.1.1.2 Generation of Methionine and Galactose gradients 62
4.2 RESULTS AND DISCUSSION 63
4.2.1 GENERATION OF A STABLE GRADIENT USING FLUOROPHORES 63
4.2.2 GENERATION OF A METHIONINE + GALACTOSE GRADIENT WITHIN MICROCHANNELS .. 67

5 GENERAL CONSIDERATIONS 68

5.1.1 HYDROPHOBIC SURFACE OF THE PDMS 68

5.1.2 FLUIDIC RESISTANCE AT THE ENTRANCE OF THE MICROCHANNELS 69
5.1.3 MICROFLUIDIC COMPONENTS WHICH COULD BE INCORPORATED IN THE MICROFLUIDIC DEVICE 70

6 CONCLUSION 71

7 FUTURE WORK PERSPECTIVES 73

8 REFERENCES 75

9 ANNEX 1 81

List of Figures

FIGURE 1.1 - INTEGRATED CELL ANALYSIS SYSTEM. DNA EXTRACTION AND PURIFICATION CHIP WITH ADVANCED INTEGRATED FLUIDIC HANDLING OF CELL SAMPLES AS WELL AS THE NECESSARY BUFFERS AND REAGENTS (EXTRACTED FROM [5]). 3

FIGURE 1.2 - PDMS STRUCTURAL FORMULA AND THREE DIMENSIONAL STRUCTURE (FROM [7]). 4

FIGURE 1.3 - FLOW PROFILES IN MICROCHANNELS. A PRESSURE GRADIENT, $-\nabla P$, ALONG A CHANNEL GENERATES A PARABOLIC OR POISEUILLE FLOW PROFILE IN THE CHANNEL. THE VELOCITY OF THE FLOW VARIES ACROSS THE ENTIRE CROSS-SECTIONAL AREA OF THE CHANNEL. ON THE RIGHT IS AN EXPERIMENTAL MEASUREMENT OF THE DISTORTION OF A VOLUME OF FLUID IN A POISEUILLE FLOW (FROM [12]) 6

FIGURE 1.4 - SCHEME OF THE SOFT LITHOGRAPHY TECHNIQUE (FROM [13]). 7

FIGURE 1.5 - DIFFERENCES BETWEEN POSITIVE AND NEGATIVE PHOTORESIST IN TERMS OF LITHOGRAPHY PROCESS (EXTRACTED FROM [17]). 8

FIGURE 1.6 - EXAMPLES OF MICROFLUIDIC DEVICES FOR BIOLOGICAL APPLICATIONS. A) MICROFLUIDIC CELL-TRAPPING DEVICE. TRAPPING IS CONTROLLED BY ALTERING FLUID FLOW USING VALVES CONNECTED TO THE FOUR OUTLETS [22]. B) MICROFLUIDIC CULTURE PLATFORM FOR CNS AXONAL INJURY, REGENERATION AND TRANSPORT [23]. C) MICROFLUIDIC DEVICE FOR SINGLE CELL STUDIES USING HYDRODYNAMIC TRAPS [24]. 9

FIGURE 1.7 - MICROFLUIDIC DEVICES FOR SINGLE CELL ANALYSIS. A) DEVICE FOR SINGLE-CELL GENE EXPRESSION OVER MULTIPLE CELL CYCLES. SCHEMATIC DESIGN OF THE DEVICE (UPPER IMAGE) AND SINGLE-CELL YELLOW FLUORESCENT PROTEIN (YFP) DYNAMICS FOR 119 CELLS (LOWER IMAGE) [26]. B) MICROFLUIDIC DEVICE FOR SINGLE CELL GENE EXPRESSION ANALYSIS IN *SACCHAROMYCES CEREVISIAE*. ELECTRON MICROGRAPH OF SILICON MASTER FOR PDMS DEVICES SHOWING THE JAIL DESIGN (UPPER IMAGE) AND EXPERIMENTAL RESULTS (LOWER IMAGE) [27]. C) MICROFLUIDIC DEVICE FOR TEMPORALLY CONTROLLED GENE IN *SACCHAROMYCES CEREVISIAE*. SKETCH OF THE SETUP (UPPER IMAGE) AND GROWTH CURVES OF WT CELLS DURING A TIME-LAPSE EXPERIMENT (LOWER IMAGE) [28]. . 11

FIGURE 1.8 - EXAMPLES OF STEADY-STATE GRADIENT GENERATORS. A) SCHEMATIC OF A PDMS DEVICE WITH RED REGION DESIGNATING THE GRADIENT- GENERATION REGIO AND BLUE HIGHLIGHTING FLOW INLETS AND OUTLET [40]. B) SCHEMATIC DESIGN OF A REPRESENTATIVE GRADIENT-GENERATING MICROFLUIDIC NETWORK (UPPER IMAGE) WITH FLUORESCENCE MICROGRAPHS OF SOLUTION GRADIENT OF FITC AT THE OUTLET CHANNEL REGION (LOWER IMAGE) [41]. C) REPRESENTATION OF A LAMINAR MICROFLUIDIC DIFFUSION DILUTER (UPPER IMAGE) AND AN

EPIFLUORESCENCE MICROGRAPH OF 23 PARALLEL MICROCHANNELS DURING THE OPERATION OF THE DIFFUSION DILUTER DEVICE WITH LINE PROFILES OF FLUORESCENCE INTENSITY [42]. 13
FIGURE 1.9 - A) YEAST CELLS. THE LARGE CELL ON THE BOTTOM IS CURRENTLY BUDDING. THE LARGE CELL IN THE TOP MIDDLE HAS ALREADY BUDDED SEVERAL TIMES (FROM [50]). B) VARIOUS ASPECTS OF METABOLIC ENGINEERING IN YEAST CELLS (FROM [49]). 15
FIGURE 1.10- FLUORESCENCE MICROSCOPY OF YEAST CELLS EXPRESSING A-SYN-GFP (FROM [53]). 16
FIGURE 1.11 – SCHEMATIC DESIGN SHOWING THE GRADIENTS PRETENDED INSIDE THE MICROCHANNELS. 17
FIGURE 2.1 - PHOTOLITHOGRAPHY EQUIPMENT. A), B) DIRECT WRITER LASER (DWL) LITHOGRAPHY 2.0 SYSTEM. C) SVG 88 SERIES TRACK SYSTEM. D) UV HANDMADE CHAMBER. 20
FIGURE 2.2 - EQUIPMENT USED TO CONFIRM THE PROFILE OF THE CHANNELS. A) PERFILOMETER. B) SCANNING ELECTRON MICROSCOPE. 20
FIGURE 2.3 - A) OVEN FORM MEMMERT. B) VACCUM DESSICATOR. 21
FIGURE 2.4 - CORONA PORTABLE SYSTEM. 21
FIGURE 2.5 - A) FLUORESCENCE MICROSCOPE. B) SYRINGE PUMP. 22
FIGURE 2.6 - AUTOCAD DESIGN OF THE CHANNELS AND THEIR DIMENSIONS. THREE CHANNELS OF EACH WIDTH WERE DESIGNED. 23
FIGURE 2.7 - SCHEMATICS OF MASK FABRICATION. A), ALUMINIUM DEPOSITION OVER QUARTZ SUBSTRATE. B) PR SPIN COATING. C) DWL EXPOSURE. D) PR DEVELOPMENT. E) AL ETCHING. F) PR STRIP. 24
FIGURE 2.8 - SU- 8 2000 SPIN SPEED VS. THICKNESS (FROM [55]). 25
FIGURE 2.9 - SAMPLE EXPOSURE TO UV LIGHT. A) MASK WITH ALUMINIUM LAYER FACED SU-8. B) MASTER MOLD AFTER DEVELOPMENT. 26
FIGURE 2.10 - GOLD DEPOSITION BY SPUTTER COATING TO MAKE THE SURFACE OF THE MASTER MOLD ELECTRICALLY CONDUCTIVE. 26
FIGURE 2.11 - HMDS DEPOSITION TO PROMOTE CHEMICAL ADHESION ON ORGANIC SUBSTRATES (FROM [57]). 27
FIGURE 2.12 - POLYMERIC MATERIALS THAT WERE USED AS SUBSTRATE FOR MASTER MOLD FABRICATION. A) POLYETHYLENE (PET) AND B) POLYIMIDE (PI). 29
FIGURE 2.13 - MASTER MOLD FABRICATION USING THE POSITIVE PHOTORESIST PFR 7790G 27CP. A) COATING OF 4 LAYERS OF POSITIVE PR. B) DWL DOUBLE EXPOSURE. C) MASTER MOLD AFTER DEVELOPMENT. 30
FIGURE 2.14 - REPLICA MOLDING TECHNIQUE. A) PDMS (BLUE) IS POURED OVER THE MASTER MOLD (ORANGE) AND CURED. B) PDMS REPLICA IS OBTAINED BY PEELING FROM THE MOLD. C) MASTER MOLD CAN BE USED MANY SEVERAL TIMES TO PRODUCE MANY REPLICA MOLDS. 32

FIGURE 2.15 – FIRST VERSION OF THE MICROFLUIDIC DEVICE. 33
FIGURE 2.16 - FLUORESCENCE MICROGRAPHS OF MICROCHANNELS WITH FITC.....33
FIGURE 2.17 - MICROCHANNELS WITH DIFFERENT WIDTHS WITH YEAST CELLS INSIDE IT. A) WIDTH= 50 µM, B) 20 µM, C) 10 µM AND D) 5 µM. 33
FIGURE 2.18 - AUTOCAD DESIGN OF THE RULER NEAR EACH CHANNEL TO FACILITATE THE LOCALIZATION OF A PARTICULAR CELL OVER LONG PERIODS OF OBSERVATION. 34
FIGURE 2.19 – MASTER MOLD WITH TWO PIECES OF SILICON ACTING AS THE MOLD FOR THE RESERVOIRS. 35
FIGURE 2.20 - PHOTOS OF THE REPLICA MOLDING TECHNIQUE. A) MASTER MOLD. B) PDMS WAS POURED OVER THE MASTER MOLD AND C) WAS TAKEN TO REST FOR 2-3 MINUTES. D) PDMS WAS HEAT CURED FOR 1 HOUR AT 60ºC. C) PDMS REPLICA WAS THEN REMOVED FROM THE MOLD, AND F) CUT TO FORM THREE DISTINCT PDMS DEVICES. 35
FIGURE 2.21 - OPERATION MODE OF THE MICROFLUIDIC DEVICE. A) MICROFLUIDIC DEVICE PRIOR TO THE INSTALLATION OF THE EXTERNAL TUBING RESPONSIBLE FOR THE OUTSIDE FLUIDIC SYSTEM. B) APPLICATION OF THE CORONA DISCHARGE INSIDE THE RESERVOIRS. C) 1 ML SYRINGE CONNECTED TO THE MICROFLUIDIC DEVICE TO MAKE THE VACUUM STEP. D) MICROFLUIDIC DEVICE FILLED WITH WATER WITH BOTH CONNECTORS AFTER THE VACUUM STEP. 36
FIGURE 2.22 - MASTER MOLD MADE OF SU-8 2015 WITH MICROCHANNELS PATTERNED. A) GROUP OF MICROCHANNELS WITH A WIDTH OF 100 µM. B) GROUP OF MICROCHANNELS WITH A WIDTH OF 50µM. C) MICROCHANNELS WITH INCREASING WIDTHS (10, 20, 50 AND 100 µM) IN WHICH THE FIRST CHANNEL IS BROKEN. D) MICROCHANNELS WITH A VARIETY OF WIDTHS IN WHICH MANY OF THEM ARE BROKEN. 37
FIGURE 2.23 - SEM PHOTOGRAPHS OF MICROCHANNELS MADE OF SU-8 2015. A) MICROCHANNELS WITH WIDTHS OF 50 µM, B) 20 µM AND 10 µM. 38
FIGURE 2.24 - MASTER MOLD MADE OF SU-8 USING HF TO MAKE THE SURFACE OF SI HYDROPHOBIC. A) MICROCHANNELS WITH DECREASING WIDTHS (FROM LEFT TO RIGHT, 100, 50, 20,10 µM). B) MICROCHANNELS, THE THREE ON THE LEFT WITH WIDTHS OF 10 µM AND THE ONE ON THE RIGHT 5 µM WIDE. 39
FIGURE 2.25 - MASTER MOLD MADE OF SU-8 USING AN AMORPHOUS SILICON FILM OVER THE SI SUBSTRATE BEFORE COATING THE NEGATIVE PHOTORESIST. MICROCHANNELS WITH DECREASING WIDTHS (FROM LEFT TO RIGHT, 100, 50, 20 AND 10 µM).....40
FIGURE 2.26 - MASTER MOLD MADE OF SU-8 2015 USING PET (A) TO C)) AND PI (D) AND E)) AS SUBSTRATES. A) MICROCHANNELS WITH DECREASING WIDTHS (100,50,20 AND 10µM). B) MICROCHANNELS WITH WIDTHS OF 10µM AND THE LAST ONE WITH A WIDTH OF 20µM. C) THE FIRST CHANNEL HAS A WIDTH OF 20MM AND THE LAST

ONES (WITH IRREGULAR SHAPES) HAVE WIDTHS OF 10µM. D) MICROCHANNELS WITH A 100µM WIDE. E) MICROCHANNELS WITH 100µM WIDE PRESENTING IRREGULARITIES. 41

FIGURE 2.27 - MASTER MOLD MADE OF AZ-4562. A) MICROCHANNELS WITH DIFFERENT WIDTHS. C) SEM PHOTOGRAPH SHOWING THE PROFILE OF A MICROCHANNEL. 42

FIGURE 2.28 - MICROCHANNELS MADE OF 4 LAYERS OF PHOTORESIST PFR 7790G 27CP. A) MICROCHANNEL WITH A WIDTH OF 5 µM. B) MICROCHANNEL WITH A WIDTH OF 10 µM. C) SEM PHOTOGRAPH SHOWING THE PROFILE OF A MICROCHANNEL. 43

FIGURE 2.29 - EVOLUTION OF THE MASTER MOLD AND THE MICROFLUIDIC DEVICE. A) MASTER MOLD ONLY WITH MICROCHANNELS AND B) ITS MICROFLUIDIC DEVICE. C) FINAL MASTER MOLD WITH RESERVOIRS MADE OF RECTANGULAR PIECES OF SILICON AND D) ITS MICROFLUIDIC DEVICE WITH EXTERNAL TUBAGE. 44

FIGURE 3.1 - CLUSTER OF CELLS ACCUMULATED AT THE ENTRANCE OF A MICROCHANNEL. 49

FIGURE 3.2 - CLUSTERS OF YEAST CELLS INSIDE A MICROCHANNEL WITH 5 µM WIDE. .. 50

FIGURE 3.3 - YEAST CELLS INSIDE MICROCHANNELS WITH AN OD_{600} OF 3.4 AND AFTER A VIGOROUS VORTEX. 50

FIGURE 3.4 - HYDRODYNAMIC TRAPS. A) MICROCHANNEL WITH 2 TRAPS. B) YEAST CELLS TRAPPED INSIDE A MICROCHANNEL**.** 51

FIGURE 3.5 - CELLS GROWTH WITHIN MICROCHANNELS. INDIVIDUAL CELLS WERE SELECTED (A) AND C)) AND THE SAME CELLS WERE VISUALIZED AFTER 3 HOURS RESPECTIVELY IN (B) AND D)). 52

FIGURE 3.6 - YEAST CELL GROWTH WITHIN MICROCHANNELS EXPRESSING α–SYN-GFP FUSION PROTEIN. A) VISIBLE MICROGRAPH OF CELLS PREVIOUSLY SELECTED WITHIN MICROCHANNELS AT T=0H. B) FLUORESCENCE MICROGRAPHS OF THE SAME CELLS AT T=0H AND C) T=18H. 53

FIGURE 3.7 - YEAST CELL GROWTH WITHIN MICROCHANNELS EXPRESSING α-SYN-GFP FUSION PROTEIN. A) VISIBLE MICROGRAPH OF CELLS PREVIOUSLY SELECTED WITHIN MICROCHANNELS AT T=0H. B) FLUORESCENCE MICROGRAPHS OF THE SAME CELLS AT T=0H AND C) T=18H. 53

FIGURE 3.8 - EXAMPLES OF EXPERIMENTAL SETUPS TO CONTROL THE TEMPERATURE IN MICROFLUIDIC DEVICES. A) HEATED ALUMINIUM ALLOY STAGE USING THERMOELECTRIC MODULES IN WHICH THE MICROFLUIDIC DEVICE WAS CLAMPED [28]. B) MICROFABRICATED HEATING ELELMENTS MADE OF TI/PT [65]. 55

FIGURE 3.9 – YEAST W303.1A EXPRESSION LEVELS OF RFP AND GFP-αSYN PROTEINS WITHIN MICROCHANNELS. A) VISIBLE MICROGRAPH OF CELLS PREVIOUSLY SELECTED WITHIN MICROCHANNELS AT T=0H.B) FLUORESCENCE MICROSCOPY OF CELLS EXPRESSING RFP PROTEIN AT T=0H. C) FLUORESCENCE MICROGRAPHS OF YEAST CELLS EXPRESSING GFP-αSYN PROTEIN AT T=0H D) 1.5H AND E) 3H AFTER GALACTOSE INDUCTION. 56

FIGURE 3.10 - YEAST W303.1A EXPRESSION LEVELS OF RFP AND GFP-αSYN PROTEINS WITHIN MICROCHANNELS A) VISIBLE MICROGRAPH OF CELLS PREVIOUSLY SELECTED WITHIN MICROCHANNELS AT T=0H.B) FLUORESCENCE MICROSCOPY OF CELLS EXPRESSING RFP PROTEIN AT T=0H. C) FLUORESCENCE MICROGRAPHS OF YEAST CELLS EXPRESSING GFP-αSYN PROTEIN AT T=0H D) 1.5H AND E) 3H AFTER GALACTOSE INDUCTION.....56

FIGURE 3.11 - YEAST W303.1A EXPRESSION LEVELS OF RFP AND GFP-αSYN PROTEINS WITHIN MICROCHANNELS A) VISIBLE MICROGRAPH OF CELLS PREVIOUSLY SELECTED WITHIN MICROCHANNELS AT T=0H.B) FLUORESCENCE MICROSCOPY OF CELLS EXPRESSING RFP PROTEIN AT T=0H. C) FLUORESCENCE MICROGRAPHS OF YEAST CELLS EXPRESSING GFP-αSYN PROTEIN AT T=0H D) 1.5H AND E) 3H AFTER GALACTOSE INDUCTION.....57

FIGURE 3.12 - FLUORESCENCE MICROSCOPY OF *S. CEREVISIAE* VSY72 CELLS EXPRESSING A α-SYN-GFP FUSION PROTEIN UNDER THE CONTROL OF *GAL1* PROMOTER, GROWN IN A) RAFFINOSE (NEGATIVE CONTROL OF α-SYN-GFP FUSION PROTEIN EXPRESSION) OR IN B) GALACTOSE MEDIUM (POSITIVE CONTROL OF α-SYN-GFP INDUCTION BY GALACTOSE).....58

FIGURE 3.13 - EXPRESSION LEVELS OF α-SYN-GFP PROTEIN IN VSY72 YEAST CELLS WITHIN A MICROCHANNEL (WIDTH= 6μM) WHEN SUBJECT TO GALACTOSE INDUCTION. A) VISIBLE MICROGRAPH OF CELLS PREVIOUSLY SELECTED WITHIN A MICROCHANNEL AT T=0H.B) FLUORESCENCE MICROSCOPY OF CELLS AT T=0H, C) T= 1.5H D) T= 3H AND E) T= 4.5H WITH AN EXPOSURE TIME OF 114MS. F) FLUORESCENCE MICROSCOPY OF CELLS AT T=4.5H WITH AN EXPOSURE TIME OF 23MS WITH THE AIM OF LOCATING THE SOURCE OF FLUORESCENCE INSIDE THE CELLS. 58

FIGURE 3.14 - CHART SHOWING THE EVOLUTION OF THE FLUORESCENCE INTENSITY OF α-SYN-GFP FUSION PROTEIN OF THE VSY72 CELLS OF FIGURE 3.23 ALONG TIME WHEN INDUCED BY THE GALACTOSE INDUCER FLUORESCENCE MEASUREMENTS WERE OBTAINED WITH IMAGEJ SOFTWARE. 59

FIGURE 3.15 - EXPRESSION LEVELS OF α-SYN-GFP PROTEIN IN VSY72 CELLS WITHIN A MICROCHANNEL (WIDTH= 5μM) WHEN SUBJECT TO GALACTOSE INDUCTION. A) VISIBLE MICROGRAPH OF CELLS PREVIOUSLY SELECTED WITHIN A MICROCHANNEL AT T=0H.B) FLUORESCENCE MICROGRAPHS OF CELLS AT T=0H, C) T= 1.5H D) T= 3H AND E) T= 4.5H WITH AN EXPOSURE TIME OF 194MS. F) FLUORESCENCE MICROSCOPY OF CELLS AT T=4.5H WITH AN EXPOSURE TIME OF 87MS WITH THE AIM OF LOCATING THE SOURCE OF FLUORESCENCE INSIDE THE CELLS. 59

FIGURE 3.16 - CHART SHOWING THE EVOLUTION OF THE FLUORESCENCE INTENSITY OF αSYN-GFP FUSION PROTEIN OF THE CELLS OF FIGURE 3.25 ALONG TIME WHEN

INDUCED BY WITH THE GALACTOSE INDUCER. FLUORESCENCE MEASUREMENTS WERE OBTAINED WITH IMAGEJ SOFTWARE. 60
FIGURE 4.1 - MICROFLUIDIC DEVICE WITH THE TUBING RESPONSIBLE FOR THE EXTERNAL FLUIDIC SYSTEM. 61
FIGURE 4.2 - EXPERIMENTAL SETUP: 1 SYRINGE PUMP CARRYING TWO SYRINGES, EACH ONE CONNECTED TO THE RESERVOIRS OF THE MICROFLUIDIC DEVICE BY POLYETHYLENE TUBES....62
FIGURE 4.3 - FITC GRADIENT INSIDE A MICROCHANNEL. 63
FIGURE 4.4 - SYRINGE PUMP CARRYING TWO SYRINGES WITH DIFFERENT CAPACITIES (1ML AND 3ML). 64
FIGURE 4.5 - CHART SHOWING THE FLUORESCENCE INTENSITY PROFILE ACROSS A MICROCHANNEL (WIDTH=6 μM) AT DIFFERENT TIMES. A STABLE GRADIENT WAS ESTABLISHED AFTER 16 MINUTES. 65
FIGURE 4.6 - CHART SHOWING THE EVOLUTION OF THE FLUORESCENCE INTENSITY IN THE SAME MICROCHANNEL IN A) X = 194μM AND X = 2134 μM. 65
FIGURE 4.7 - FLUORESCENCE MICROGRAPH OF TWO MICROCHANNELS SHOWING A DEFECT IN THE PDMS WALLS IN ONE MICROCHANNEL WHICH STOPS THE PASSAGE OF THE FLUID ALONG THE REST OF THE MICROCHANNEL. 67
FIGURE 5.1 - GRAPH OF WATER CONTACT ANGLE VS. AGING TIME FOR PDMS MODIFIED WITH OXYGEN PLASMA, O2 + C2F6 PLASMA AND HEMA (FROM [72]). 69
FIGURE 5.2 - SCHEMATIC REPRESENTATION OF A METHOD FOR FILLING MICROFLUIDIC CHANNELS IN A PDMS DEVICE (FROM [76]). 70
FIGURE 7.1 - MICROFLUIDIC DEVICE WITH MICROCHANNELS OF DIFFERENT LENGTHS TO TEST THE INFLUENCE IN THE GRADIENT PROFILE. 73
FIGURE 7.2 - LONG TERM MICROFLUIDIC PLATFORM. 74

Abbreviations

αSyn	Alpha-Synuclein
Si	Silicon
PR	Photoresist
Al	Aluminium
IPA	Isopropanol alcohol
UV	Ultraviolet
HF	Hydrofluoridric acid
DI	Deionized
PMMA	Poly(methyl methacrylate)
PI	Polyimide
PET	Polyethylene
HCl	Hydrochloric acid
PDMS	Polydimethylsiloxane
FITC	Fluorescein isothiocyanate

1 Introduction

The main goal of this work is to develop of a microfluidic device to study single cells and to generate stable gradients inside microchannels.

In the first part of this chapter (**1.1**), an outlook of the promising and rapidly expanding area of microfluidics will be presented as well as some basic definitions. Afterwards, the background of the development of microfluidic systems and new materials for their fabrication will also be elucidated (**1.2**). To understand the differences in terms of fluid physical properties between macro and microscopic systems a brief explanation will be given about the main properties that distinguish such behaviour (**1.3**). After that, the main approaches to microfabrication techniques will be described, particularly the *Soft Lithography* Technique (**1.4**). After this general overview, we will focus particularly on the microfluidics for biological applications, namely for single-cell analysis and gradient-generation (**1.5**). Since there have been a large number of newly reported microfluidic devices for cell research in the last years, we will only review a few more relevant devices to provide the current state-of-the-art technology in this field. In section **1.6**, due to the fact that the gradient inside the microchannels will be formed mainly by diffusion, we will present the physical background of this type of transport phenomena and its relation to the concentration gradient. In the last sections of this chapter, we will provide brief information about the importance of *Saccharomyces cerevisiae* as a model organism to understand the biology of the eukaryotic cell and hence, human biology (**1.7**). Since we focus our work on a particular protein, alpha-synuclein, some basic concepts about it will be described and also its relation to Parkinson's disease (**1.8**).

1.1 *Motivation behind the development of microfluidic devices*

One of the most important and interesting scientific developments of the last years has been the development of new methods of miniaturization of chemical and biological instrumentation with the aim of creating integrated *lab-on-a-chip* systems. These systems allow the reduction of reagent consumption and the uncomparable automation which makes them more advantageous compared to the usual industrial laboratory equipment. Behind the *lab-on-a-chip* technology is an exciting new field of science and engineering that enables very small-scale fluid control and analysis using channels with dimensions of tens to hundreds of micrometers This science is called Microfluidics [1,2]. According to Urbanskiet and colleagues [1], microfluidics provides for the experimental sciences what the integrated circuit provided for electronics more than 50 years ago due to the fact that it provides us with the opportunity to create a single fabrication process composed of several micro-components.

Microfluidics systems have the potential for wide applications, including advances in point-of-care diagnostics, bioterrorism detection, drug discovery, biotechnology, pharmaceuticals and life sciences [3].

One of the main reasons for the enormous development of the microfluidics area came from the field of molecular biology, due to the emergence of new techniques with higher sensitivity and resolution after the explosion of genomics in the 1980s. Another contribution was from microelectronics because the main techniques associated with this field, particularly photolithography, could be directly applicable to microfluidics [2].

The great development of this new distinct field lies in the fact that microfluidic devices require small amounts of sample and reagent for each process leading to greater efficiency of use of chemical or biochemical reagents. Other advantages include low production costs per device thereby allowing for disposability; high throughput synthesis and screening of biological species and drug targets; parallel processing of samples; fast sampling times; portability for in situ use; accurate and precise control of samples; low power consumption; and versatile format for integration of various detection schemes thereby leading to greater sensitivity. One major advantage is the potential for parallel operation and for integration with other miniaturized devices. Other major factors that contribute to the increasing application of these miniaturized systems are the automation of these type of technologies with little human intervention, and therefore allowing the combination of multiple functions on a single chip (see Figure 1.1), including for example purification, labelling, reaction, separation, and detection. Furthermore, some studies are difficult or impossible in larger scale devices. For example, microfluidic channels can create in a very similar way the conditions in terms of size and flow parameters (~10mm, 0.1cm/s) found in *in vivo* capillaries [4].

Microfluidics allows experiments to be carried out that cannot be performed simply by miniaturizing conventional laboratory equipment. The traditional methodologies to manipulate small volumes of a particular solution are not exact and can lead to high losses, making them very expensive. In contrast, besides the cost savings, the ability to produce many copies of microfluidic devices in only step, the small reagent volumes and the automation associated with microtechnology are other key aspects that make this new field so attractive, creating opportunities for portable and point-of-care devices that are becoming important in the personalization of medical care [5].

At present, almost all the institutions doing research and development are aware of this miniaturization progress due to the unquestionable characteristics that these systems have such as low cost and little maintenance and space, less time consuming, in contrast with the robotic systems that are very expensive and require much more space and height [3].

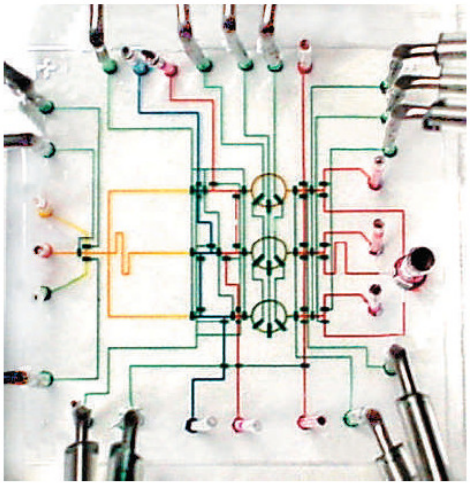

Figure 1.1- Integrated cell analysis system. DNA extraction and purification chip with advanced integrated fluidic handling of cell samples as well as the necessary buffers and reagents (from [5]).

1.2 *Background of the development of microfluidics and new materials for its fabrication*

Microfluidic devices were first developed in the 1990s and were initially fabricated in silicon and glass using the traditional techniques borrowed from the semiconductor industry, specifically photolithography and etching techniques, because these technologies were available and highly developed [6]. One of the main reasons that explain the utilization of silicon and glass in microfluidics is the vast knowledge about their surface properties and chemistries. Moreover, these substrates are mechanical strength, present high chemical resistance and low conductivity. Microchannels made of these materials are fabricated using etching techniques and therefore allow the surfaces cleaning while produce the channels. Glass systems have proved to be especially suitable for DNA separating and sequencing [4].

Despite photolithography and etching techniques being very precise, they are also expensive and inflexible. Furthermore, such technologies require that each device be fabricated in a cleanroom environment and the sealing processes require high voltages and temperatures. The conventional chemical etching techniques should also be performed with extremely safety precautions [3].

Among the drawbacks of the use of silicon and glass is the fact that the first, in particular, is opaque to visible and ultraviolet light so cannot be used with conventional optical methods of detection. On the other hand, although glass is transparent but, because it is amorphous, vertical side walls are more difficult to obtain by etching than in Si. The major disadvantage of glass and silicon materials is the relatively high cost for mass production, which is especially important in medical applications because a particular device should only be used one time to avoid any cross contamination. These and other limitations have motivated researchers to seek

other alternatives such as ceramics, plastics, and polymer-based materials. General speaking, an ideal substrate material for microdevices (for biological applications) is one that is relatively inexpensive, mechanically strong, chemically and thermally stable, and biocompatible. Seeking these characteristics, there has been a rapid expansion into new types of materials, especially polymers. In contrast to silicon and glass, polymers are inexpensive and allow low cost fabrication; channels can be formed by molding or embossing rather than etching; and sealing methods do not require cleanrooms or high temperatures. Another attractive feature to use polymer and plastic substrates is the ability to mass produce devices with high aspect ratios which facilitate the production of disposable microdevices appropriate for several applications such as in biomedical applications, clinical, environmental, and biological analyses.

Disadvantages of polymers for microfluidics applications are that more attention must be taken to control their surface, since there is a small knowledge about their surface chemistries; they are often incompatible with organic solvents (ex: PDMS and PMMA), and low molecular weight organic solutes and they are usually incompatible with high temperatures [3,4]. Nonetheless, polymers remain attractive for bioanalytical application and their use is growing.

Much of the exploratory research in microfluidic systems has been carried out in poly(dimethylsiloxane), PDMS, based on Soft Lithography Technique, which will be explained in section **1.4**.

PDMS is a silicon-based organic polymer with the following structure:

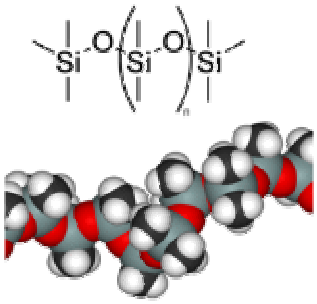

Figure 1.2 - PDMS structural formula and three dimensional structure (from [7]).

PDMS is an excellent material for the fabrication of microsystems for a number of reasons [4, 8, 9]:

- It is optically transparent down to 280 nm so it can be used for a number of detection schemes.
- It cures at low temperatures.
- It is non-toxic thus most cells can be cultured directly on it and devices made form it can be implanted *in vivo*.
- Its surface chemistry can be controlled by reasonable well-developed techniques. PDMS is elastic and provides a surface that has low interfacial free energy (~21.6 dyn/cm) with good chemical stability. Most molecules or polymers being patterned or molded do not adhere irreversibly to, or react with, the surface of PDMS.

- Features on the micron scale can be reproduced with high fidelity in PDMS by Replica Molding.
- A PDMS stamp or mold can be used repeatedly with minimal degradation.
- PDMS membranes are permeable to nonpolar gases, including O_2, N_2, and CO_2. This property is essential to its use in channel systems for mammalian cell culture.
- PDMS is not hydroscopic and does not swell with humidity.
- Because it is elastomeric, it will conform to smooth, nonplanar surfaces, and it releases from delicate features of a mold without damaging them or itself.
- It is intrinsically very hydrophobic, but its surface can be converted to a hydrophilic form by a brief treatment with a plasma, corona discharge, etc.

1.3 *Basic Principles of Microfluidics*

At this point, it is important to understand the main differences in terms of fluid physical properties between macro and microscopic systems in order to comprehend the importance of microfluidic devices. The behaviour of fluids at the microscale can differ from *macrofluidic* behaviour in many factors such as surface tension, energy dissipation, and fluidic resistance. Microfluidics studies how these behaviours change, and how they can be worked around, or exploited for new uses.

At small scales (channel diameters of around 100 nanometers to several hundred micrometers) there are important physical properties that differ from large scale behaviours. The ratio between the moment of inertia and the viscous forces in a fluid system is described by the Reynolds number:

$$Re = \rho v l / \eta \quad (1)$$

where ρ, v, l, and η are the fluid density, fluid velocity, characteristic length scale, and dynamic viscosity, respectively.

Within microchannels, Re is usually much less than 100, often less than 1.0 and therefore the flow is laminar and no turbulence occurs (Figure 1.3). In the laminar flow, molecules can be transported in a relatively predictable manner through microchannels in which the fluid flow is governed mainly by viscous forces and pressure gradients, with a low moment of inertia. In microsystems, with water as a fluid, fluids do not mix convectively but they flow in parallel without any turbulence. The only mixing that could occur is the result of diffusion of molecules across the interface between the fluids. The transition to turbulent flow generally occurs in the range of Reynolds number 2000.

On large scales fluids mix convectively due to the fact that in macroscopic fluids inertia is often more important than viscosity.

Besides laminar flow, there are also other important properties that distinguish the behaviour of

fluids in microsystems, such as high surface-to-volume ratios, small diffusion distances, and small heat capacities. The surface tension of the fluid and the wetting properties of the system can also be significant forces.

Specifically, the difference in physical behaviour between microscopic and macroscopic systems allows for the construction of functionalities that are difficult or even impossible to access on the macroscopic scale. Taking all these properties into account, one should take advantage of the differences in the physical behaviour between macro and microsystems and develop new microfluidic platforms that benefit from such characteristics, rather than just making a downsized copy of a macroscopic system [2,10,11].

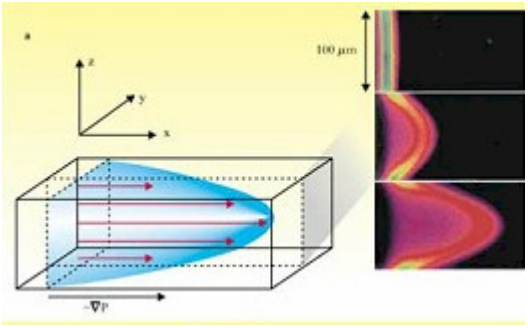

Figure 1.3 - Flow profiles in microchannels. A pressure gradient, −∇P, along a channel generates a parabolic or Poiseuille flow profile in the channel. The velocity of the flow varies across the entire cross-sectional area of the channel. On the right is an experimental measurement of the distortion of a volume of fluid in a Poiseuille flow (from [12]).

1.4 *Approaches to microfabrication techniques*

Together with the progress of the use of plastics and polymeric materials in the fabrication of microfluidic devices, in the last decade several microfabrication methods have been developed for the production of microfluidic devices in polymers with high precision and aspect ratios. The main approach to the fabrication of microfluidic devices is based on the techniques of Soft Lithography (Figure 1.4), especially Rapid Prototyping and Replica Molding.

Soft lithography was originally developed in order to overcome the limitations of photolithography, which has been the basic technology used for making all microelectronic systems, and silicon/glass-based microfluidic devices. Soft lithography is a general term of nonphotolithographic methods for replicating a pattern. The key element of this technique is an elastomeric block with patterned relief structures on its surface. This elasticity is why these techniques are called *soft* [4].

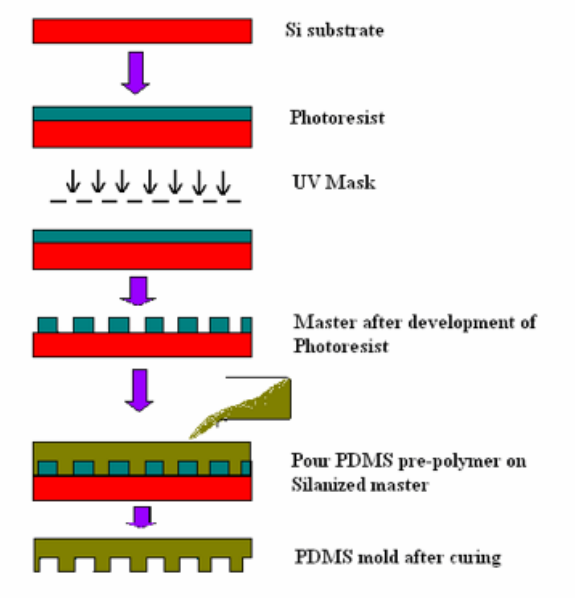

Figure 1.4 - Scheme of the Soft Lithography technique (from [13]).

Briefly, Soft Lithography starts with the mask preparation and mold fabrication (Rapid Prototyping). Rapid prototyping begins with the creation of a design for the future device using a CAD program. This design will then be patterned by photolithography on a substrate to serve as the photomask and this photomask by contact photolithography will then produce a positive relief of photoresist on silicon wafer (master) [14].

One key element in the master mold fabrication is the photoresist, a light-sensitive material used in several industrial processes. Photoresists are classified into two groups, positive and negative resists (Figure 1.5):

- A *positive resist* is a type of photoresist in which the portion of the photoresist that is exposed to light becomes soluble to the photoresist developer and the portion that is unexposed remains insoluble to the photoresist developer.
- A *negative resist* is a type of photoresist in which the portion of the photoresist that is exposed to light becomes insoluble to the photoresist developer. On the other hand, the unexposed areas are dissolved by the photoresist developer [17,18].

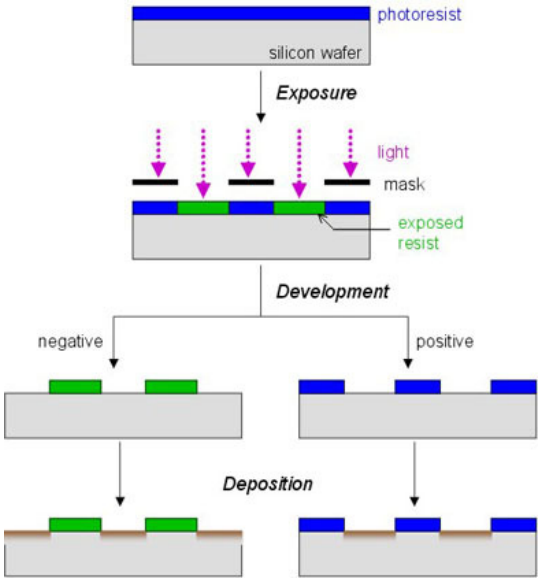

Figure 1.5 - Differences between positive and negative photoresist in terms of Lithography process (extracted from [17]).

Once the master is fabricated, the patterned is formed in PDMS using the technique of replicate molding. PDMS is firstly poured onto the master and then hardened using heat or ultraviolet light. Finally, the cured elastomer is peeled off to yield an exact structural inverse replica of the master mold [15,16]. After PDMS replica was made, it is necessary to seal it to a flat surface. The elastomer can either bond to another elastomer to form all-elastomer microchannel or bond to glass using many different techniques such as UV-ozone cleaning, oxygen plasma or Corona discharge, to form hybrid elastomer-glass microchannels. The main drawback of using all-elastomer microchannels is the fact that these materials usually present native fluorescence and porosity and do not readily permit surface modification [3].

Soft lithography has several advantages in applications in which photolithography falters or fails such as:

- Lower cost than traditional photolithography in mass production;
- easy to learn, straightforward to apply, and accessible to a wide range of users
- the softness of these materials allows the device areas to be reduced by more than two orders of magnitude compared with silicon-based devices;
- well-suited for applications involving large or nonplanar (non-flat) surfaces due to the flexibility of the stamp;
- can be used with a wide variety of materials and surface chemistries;
- well-suited for applications in biotechnology and in plastic electronics [16,19].

1.5 *Microfluidics for biological applications*

Microfluidic devices are a powerful tool for biological applications, especially in cell biology, tissue and biomedical engineering, and pharmacokinetics for drug development due to their ability to approach the size and volume of single cells.

Eukaryotic cells have dimensions of 3–100 μm that are appropriate to study in microfluidic devices. Furthermore, as it has already been said, PDMS is a material that presents exceptional features that make this material suitable for the fabrication of microchambers in which to grow and observe cells, as well as the opportunity to understand fundamental aspects in biochemical and mechanical processes that are responsible for changes in cell behaviour [20,21]. Microfluidic platforms can present cells almost in their normal environment that cannot easily be achieved by conventional tissue cultures, creating for example gradients of cytokines or direct cell-cell contacts [5]. There are also many important cell processes that occur over long periods, such as cell differentiation, and proliferation, in which microfluidic systems are capable to reproduce accurately and in a very controllable way [21].

Traditional cell studies are performed on the scale of millions of cells and therefore, measurement can only reflect average values summed over the responses of many cells. For this reason, the stochastic behaviour of individual cells is lost. What is more, such studies mask the behaviour of individual cells and are often insufficient for characterizing biological processes in which cellular heterogeneity plays a key role. Due to the ability of the photolithography process to create highly parallel structures, it is possible to study many individual cells in the same experiment, while still sampling a sufficient number to characterize the group dynamics [3].

Here, we review some of the interesting devices with applications in many general cell analysis techniques (Figure 1.6).

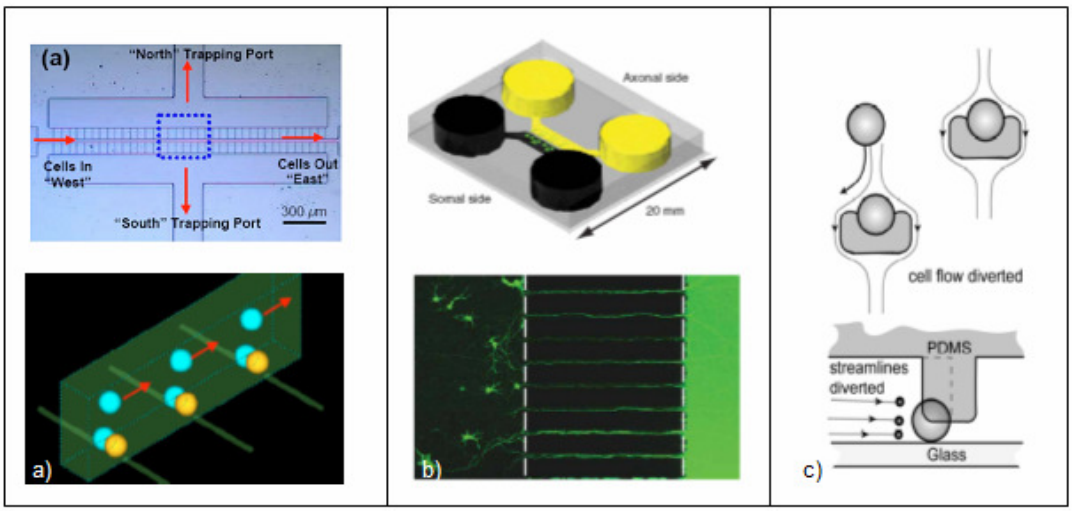

Figure 1.6 - Examples of microfluidic devices for biological applications. a) Microfluidic cell-trapping device. Trapping is controlled by altering fluid flow using valves connected to the four outlets [22]. b) Microfluidic culture platform for CNS axonal injury, regeneration and transport [23]. c) Microfluidic device for single cell studies using hydrodynamic traps [24].

Lee and co-workers [22] have developed a microfluidic device for selective trapping of cell-pairs and simultaneous optical characterizations for the analysis of molecular mechanisms of gap junctions that underlie intercellular communication (Figure 1.6a)). Taylor and colleagues [23] created a microfluidic platform to isolate and direct growth of CNS axons into a fluidically isolated environment without the use of neurotrophins. This platform also serves as a platform to study axonal injury and regeneration (Figure 1.6b)). A microfluidic was also fabricated to quantify single cell studies that require perfusion of drugs or switching of solutions, by hydrodynamically trapped cells [24] (Figure 1.6c)).

1.5.1 Microfluidic devices for single gene expression

Cellular heterogeneity has been observed in a wide variety of cell types ranging from simple bacterial cells to more complex mammalian cells. Any population of cells exhibit some degree of variability, and genetic differences are one of the main factors responsible for cellular heterogeneity.

The recent development of fluorescent proteins allowed the quantification of protein production, localization, and the monitorization of individual mRNA molecules. Fluorescent fusion proteins are created by fusing the coding sequence of a protein of interest to the coding sequence of a fluorescent protein. For the fluorescent fusion protein to be functional, both the fluorescent protein and the host protein must fold correctly [25].

Flow cytometry is an example of a technique that can be used to obtain information about gene expression for thousands of cells, but only provides a snapshot of gene expression at single time points. Traditional microscopy experiments can track gene expression dynamics in individual cells, but can only monitor a relatively small population of cells. On the other hand, microfluidic systems gathers the advantages of both techniques described above in a single device, allowing the study of gene expression changes in individual cells, but also the monitoring of large populations of cells.

Balaban and co-workers [26] employed a microfluidic device to observe phenotypic switching of growth rates in individual E. coli cells (see Figure 1.7a)). A microfluidic device containing narrow PDMS grooves was developed to force the formation of linear microcolonies during cell growth, thus allowing growth rates of the progeny of individual cells to be determined from the lengths of the linear microcolonies. Another example of a microfluidic device for single cell gene expression was developed by Ryley and co-workers [27], in which a platform was designed to trap individual yeast using μm-sized structures, to determine the variability of gene expression levels among cells over time (Figure 1.7b)). A novel microfluidic setup for yeast cells was reported [28] and a dialysis membrane was used to separate the cells from the external flow. They had studied the induction of the regulatable promotors *GAL1* and *MET3* (Figure 1.7c)).

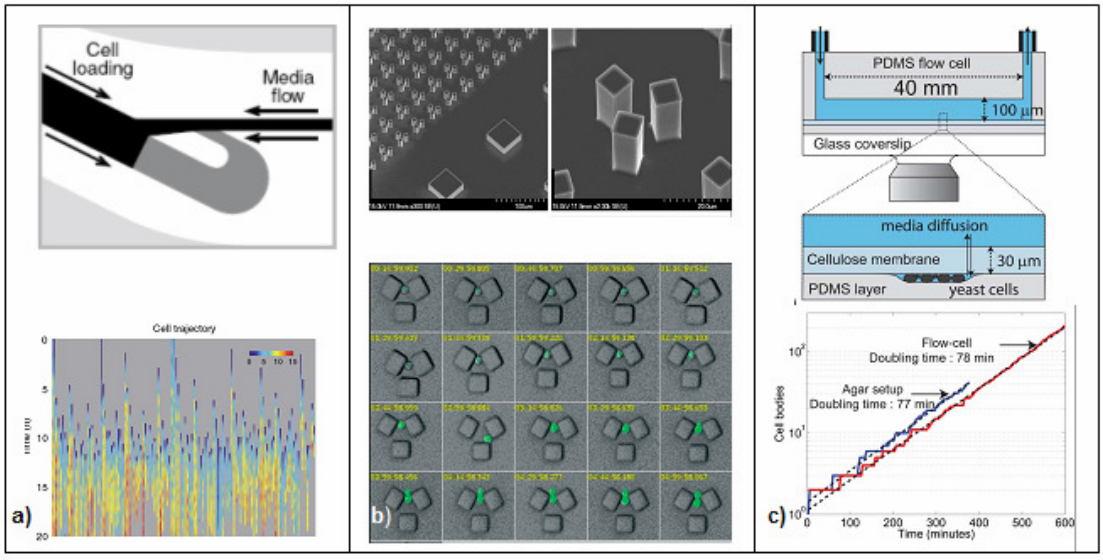

Figure 1.7 - Microfluidic devices for single cell analysis. a) Device for single-cell gene expression over multiple cell cycles. Schematic design of the device (upper image) and single-cell yellow fluorescent protein (YFP) dynamics for 119 cells (lower image) [26]. b) Microfluidic device for single cell gene expression analysis in *Saccharomyces cerevisiae.* Electron micrograph of silicon master for PDMS devices showing the jail design (upper image) and experimental results (lower image) [27]. c) Microfluidic Device for Temporally Controlled gene in *Saccharomyces cerevisiae.* Sketch of the setup (upper image) and growth curves of WT cells during a time-lapse experiment (lower image) [28].

1.5.2 Microfluidics for Gradient generation

Much of the work in microfluidics for biological applications developed to date has focused on testing the effects of a soluble component on the cell behaviour using a wide range of techniques.

Biomolecular gradients are an important mechanism for guiding the growth, migration, and differentiation of cells within the environment of living tissue and thus, the interest in comprehending these phenomena has led to the development of several methods for exposing the cells to chemical gradients and to develop microfluidic platforms capable to produce different microenvironments on a single device, that is not possible using traditional culture methods [29].

Defined chemical gradients have been used in many different fields, for example to generate gradients of mechanical stiffness [30], to examine the effects of various biomolecule gradients on the chemotaxis of neutrophils [31], bacteria [32,33] sperm [34], breast cancer cells [35], or to infect cells with graded concentrations of virus [36].

There are a wide range of gradient-generators, each one adapted to the desired applications. For example, it is possible to create a depletion gradient by adsorbing chemical molecules within the channels in which the gradient is formed with highest concentrations nearest the inlet reservoir [37]. On the other hand, some microfluidic gradient generators are developed in such

a way that they do not have control on the distribution of chemical species within the device and thus, the gradient will change along space and time [38,39]. Finally, there are also gradient generator platforms that aim to create a steady-state gradient in which distinct regions have constant biomolecules concentrations along time and therefore it is possible to form time-invariant gradients across a cell culture area, providing detailed information about how this gradient profile influences cell behaviour [29].

Due to the fact that in this project one of the objectives will be the formation of a steady state gradient within microchannels, in the following paragraphs only the state-of-art relative to these gradient generators will be presented.

Steady-state gradient platforms employed two main strategies. In the first strategy, different chemical gradients could be formed parallel to each other due to the lack of convective mixing that occurs between adjacent fluid streams under laminar flow. The gradients could be kept constant if the flow rates and the compositions are constant. In the second strategy, stable gradients are formed between source and sink reservoirs due to the utilization of fluidic resistance elements between these reservoirs. The fluidic resistance elements allow the minimization or even the elimination of convection and therefore the stable gradient could be established based only on biomolecules diffusion. The main approaches to eliminate convection are the connection of the source and the sink with hydrogel-filled compartment, or using microchannels [29].

Mosadegh and colleagues [40] developed a microfluidic device that can generate an array of steady-state soluble molecular gradients in flow-free two and three-dimensional environments. By designing different profiles in the gradient generating region and placing them in series, located between the source and the sink, they were able to establish different steady-state gradients at the same time that could be useful in a number of biological and chemical experiments (Figure 1.8a)). Jeon and colleagues [41] invented a parallel flow gradient generator that has been used to study the effects of soluble biomolecule gradients. This method is based on controlled diffusive mixing of species in solutions that are flowing laminarly, at low Reynolds number, inside a network of microchannels (Figure 1.8b)). Another interesting gradient generator was created by Holden and co-workers [42] for the combinatorial study of concentration dependent phenomena. The platform consists of a Y-junction that allows inflow of two different streams into a main channel, which splits into a linear array of independent microchannels (Figure 1.8c)).

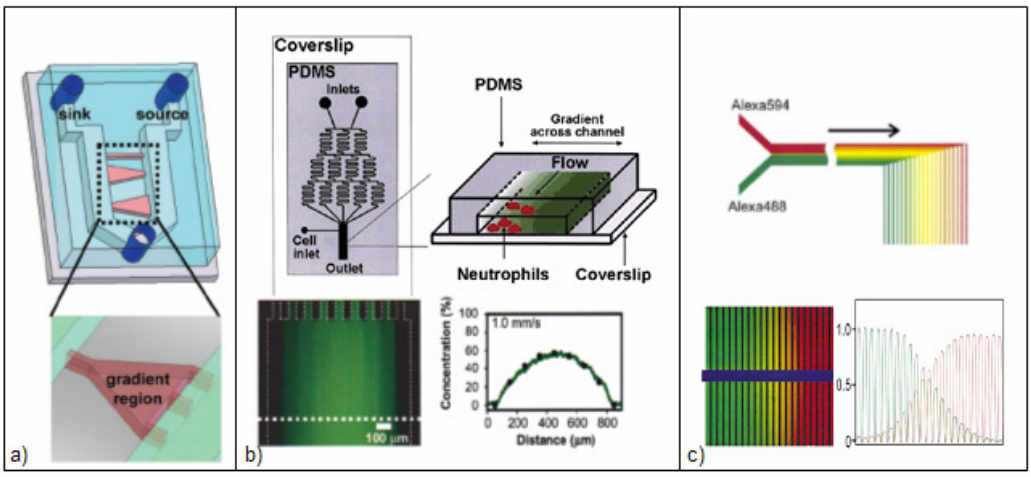

Figure 1.8 - Examples of steady-state gradient generators. a) Schematic of a PDMS device with red region designating the gradient- generation regio and blue highlighting flow inlets and outlet [40]. b) Schematic design of a representative gradient-generating microfluidic network (upper image) with fluorescence micrographs of solution gradient of FITC at the outlet channel region (lower image) [41]. c) Representation of a laminar microfluidic diffusion diluter (upper image) and an epifluorescence micrograph of 23 parallel microchannels during the operation of the diffusion diluter device with line profiles of fluorescence intensity [42].

1.6 *Physical background of Diffusion*

At this point, due to the fact that the gradient inside the microchannels will be formed mainly by diffusion, it is important to recall some important equations that describe this type of transport phenomena and its relation to the concentration gradient.

Diffusion is the process by which molecules spread from areas of high concentration to areas of low concentration as a result of their kinetic energy of random motion. When the molecules are even throughout a space it is called equilibrium [43].

To describe the diffusion process, the Fick's Law, derived by Adolf Fick in the year 1855, is used. Fick's first law is used in steady-state diffusion, i.e., when the concentration within the diffusion volume does not change with respect to time $(J_{in} = J_{out})$. In one dimension, this is:

$$J = -D\frac{\partial \phi}{\partial x} \tag{2}$$

where J is the diffusion flux in $\frac{mol}{m^2.s}$, D is the diffusion coefficient in $\frac{m^2}{s}$, ϕ is the concentration in $\frac{mol}{m^3}$ and x is the position in m.

D is proportional to the velocity of the diffusing particles, which depends on the temperature, viscosity of the fluid and the size of the particles according to the Stokes-Einstein relation:

$$D = \frac{k_B T}{6\pi\eta r} \tag{3}$$

where k_B is the Boltzmann's constant, T is the absolute temperature, η is the viscosity of the

medium and r is the radius of spherical particles.

In dilute aqueous solutions the diffusion coefficients of most ions are similar and have values that at room temperature are in the range of 0.6×10^{-9} to 2×10^{-9} m^2/s. For biological molecules the diffusion coefficients normally range from 10^{-11} to 10^{-10} m^2/s.

In microfluidic systems operating at low values of the Reynolds number *Re*, as it has already been said streams of reagents flow laminarly. Diffusive mixing across laminar streams is slow because the mixing time t_{diff}[s] is proportional to the square of the initial striation length *L* [m], the distance over which the mixing occurs by diffusion with a diffusion coefficient *D* [m^2s-1] [44,45]:

$$t_{diff} = \frac{L^2}{2D} \quad (4)$$

1.7 *Yeast cells*

Yeasts are a growth form of eukaryotic microorganisms classified in the kingdom Fungi, with about 1,500 species currently described. *Saccharomyces cerevisiae* is a species of yeast whose cells are round to ovoid and present 5–10 micrometers in diameter. They reproduce by a division process known as budding (the formation of a new organism by the protrusion of part of another organism). The genome is composed of about 13,000,000 base pairs and 6,275 genes, compactly organised on 16 chromosomes. Only about 5,800 of these are believed to be true functional genes and it is estimated that yeast shares about 23% of its genome with that of humans [46].

Saccharomyces cerevisiae is the most thoroughly investigated eukaryotic microorganism and it has been the model system for much of molecular genetic research because the basic cellular mechanics of replication, recombination, cell division and metabolism are generally conserved between yeast and larger eukaryotes, including mammals [47]. Many proteins important in human biology were first discovered by studying their homologs in yeast; these proteins include cell cycle proteins, signalling proteins, and protein-processing enzymes [46].

One of the most important reasons for the applicability of *S. cerevisiae* within the field of biotechnology is its susceptibility to genetic modifications by recombinant DNA technology, which has been even further facilitated by the availability of the complete genome sequence of *S. cerevisiae*, published in 1996 [48].

Developments of sophisticated methods in the field of recombinant DNA technology have enabled the manipulation of a given pathway of interest and hence to improve the cell by a more directed approach (Figure 1.9). Thus, it is now possible to introduce specific genetic perturbations in terms of modifying the promoter strength of a given gene, to perform gene deletions, or to introduce whole new genes or pathways into the cell [49].

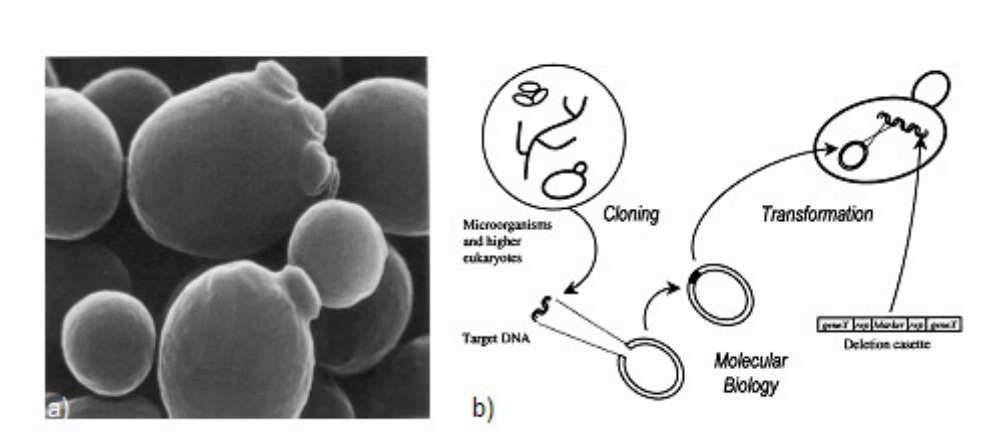

Figure 1.9 - a) Yeast cells. The large cell on the bottom is currently budding. The large cell in the top middle has already budded several times (from [50]). b) Various aspects of metabolic engineering in Yeast cells (from [49]).

1.8 *Alpha-Synuclein and its relation to Parkinson's disease*

In this project a particular protein was studied to test the effectiveness of the microfluidic device to visualize and quantify the expression levels of proteins, encoded by genes under the control of inducible promoters, when subject to the action of a soluble component (inducer).

Alpha-synuclein (α-syn) is a protein implicated in the regulation of dopamine release and transport. It is a soluble protein, expressed principally in the brain but also expressed in low concentrations in all tissues examined (except liver). In the nervous system, α-syn is primarily located at pre-synaptic terminals and is found membrane bound in dopaminergic neurons [50,51]. Recent studies indicate that negative influences can turn the protein α-syn into a major contributor of the movement-impairing disorder, Parkinson's disease (PD).

PD is a neurodegenerative movement disorder that is characterized by the loss of dopaminergic neurons from the substantia nigra, and the formation of fibrillar intraneuronal inclusions (called Lewy bodies). Missense mutations (A53T, A30P and E46K) and triplication of the α-syn gene have been found to cause autosomal dominant PD. Thus, both increased α-syn gene dosage and mutations favouring its conversion to abnormally folded species forming oligomers appear to cause PD. It was observed that in transgenic mice and *Drosophila* expressing human wild-type (WT) α-syn, the mutants are characterized by α-syn inclusions that resemble Lewy bodies. In both models, the formation of these inclusions is correlated to the onset of disease phenotype. Additionally, the PD-linked mutations (A30P and A53T), promote in vitro α-syn oligomerization, suggesting that the process of α-syn fibrillization may initiate neurodegeneration [52,53].

Outeiro and Lindquist [53] had used *Saccharomyces cerevisiae* to uncover and establish basic aspects of both normal and abnormal α-syn biology due to the strong conservation of protein

folding and membrane trafficking between yeast and higher eukaryotes (Figure 1.10).

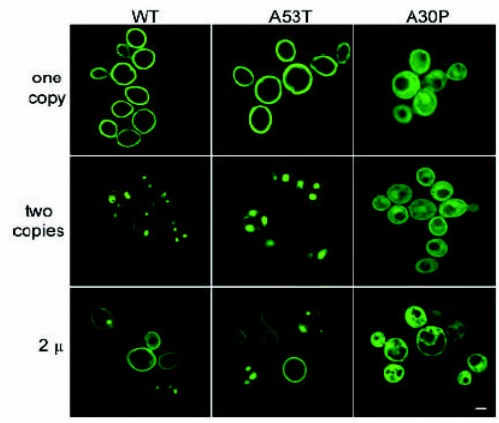

Figure 1.10- Fluorescence microscopy of yeast cells expressing α-Syn-GFP (from [53]).

They found that, when expressed in yeast, α-syn is associated with the plasma membrane in wild-type cells (see figure 1.10), but in the α-syn point mutants (A53T and A30P) their distribution varied and showed a diffuse cytoplasmic distribution in the α-syn A30P. What is more, if cells were overexpressing α-syn (two copies), such protein showed cytoplasmic inclusions and reduced membrane localization and also inhibited growth.

The study of α-syn and other proteins related to neurodegenerative diseases in yeast and other eukaryote cells could also be improved when studied inside microchannels. In a very controlled environment as in microfluidic devices, it is possible to analyse single cells and thus many aspects such as its growth and protein expression levels that would not be possible to study in the traditional *macrocultures*. What is more, in microfluidic devices it could be possible to form gradients inside the channels that could not be possible to form in any other platform. These gradients could be very important to have yeast cells expressing a certain protein in different levels along the same channel when subject to an inducer gradient. It could also possible to analyse the action of a certain supressor in different concentrations across the microchannel.

1.9 *Work Goals*

The present work focused on the field of microfluidic devices and the main goals of this project were the following:

- Develop a new microfabrication technique in which it is possible to fabricate microchannels with widths coincident to that of cells of interest (5-10μm).
- Develop a methodology to force cells to enter the microchannels.
- Create a stable gradient inside microfluidic channels.
- Use the microfluidic platform to analyse single *S. cerevisiae* cells carrying α–syn-GFP fusion protein, in terms of cell growth and protein expression levels.
- Create an inducer gradient inside the channel that will stimulate *S. cerevisiae* to express α-

syn at different levels depending on the location of these cells along the microchannel.

The goals described above have in mind the future utilization of this microfluidic platform to test different proteins that are known to suppress α–syn toxicity [54], by having the genes encoding these proteins under the control of repressible promoters. The subsequent creation of a new gradient of the respective repressor in the same channel will make it possible to analyse cell growth and generation time according to different levels respectively of α-syn and suppressors (Figure 1.11). Accordingly, the final goal would be to find the optimal suppressor that would be able to recover cells sensing advance stages of α-syn toxicity.

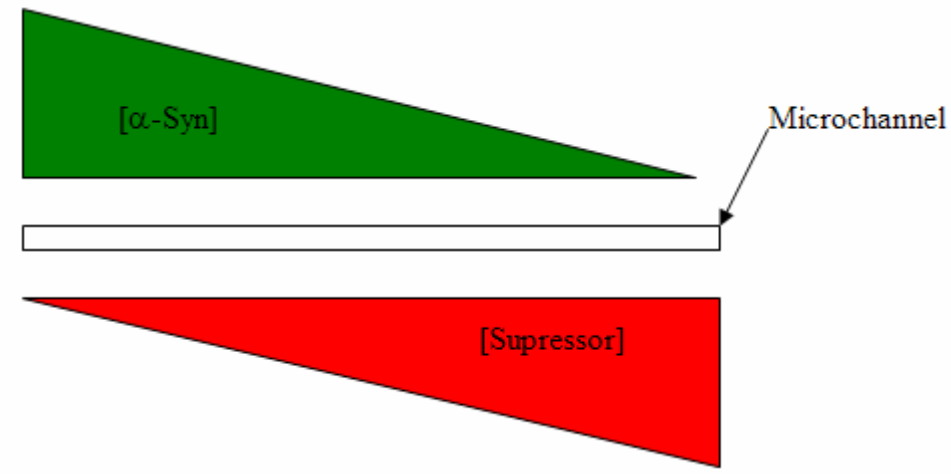

Figure 1.11 – Schematic design showing the gradients pretended inside the microchannels.

1.10 *Work structure*

The present work focuses on three distinct themes:

- Microfabrication Techniques
- Cell experiments using genetically modified *S. Cerevisiae*
- Gradient Generation

Since the topics listed above present specific methodologies, which independent from each other, each theme will be presented and discussed separately by chapters in order to allow a better understanding of each topic.

Chapter 2 will be dedicated to the Microfabrication Techniques developed in this project to fabricate the microfluidic device with microchannels with the appropriate configuration. In the first sections of this chapter, the materials (**2.1**) and the methodologies (**2.2**) will be described. Afterwards, some results will be presented and discussed in depth (**2.3**).

In the present project, several preliminary experiments using genetically modified *S. Cerevisiae* yeast cells were performed. Therefore, in **Chapter 3**, we will start by briefly describing the process of cell transformations as well as the different strains used during the project (**3.1**). Afterwards, the results of the experiments using cells in the microfluidic structures will also be described (**3.2**) and discussed (**3.3**), including the difficulties that we had to face when working with genetically modified cells.

In chapter 4, we will describe the methodology developed to generate stable gradients in the microfluidic structures (**4.1**) and the results related to such methodology will be presented and discussed (**4.2**).

General considerations about the project will be made in **chapter 5** where will also present suggestions regarding improvements in future projects.

In the last two chapters, we will present the main conclusions of the present project (**chapter 6**) and the future work perspectives (**chapter 7**).

2 Microfabrication Techniques

This chapter will be dedicated to the microfabrication techniques developed to fabricate a microfluidic device for single cell analysis and gradient generation.

The main equipment necessary for the microfluidic fabrication will be presented in section **2.1**. To obtain a microfluidic device with channels between one hundred and five micrometers wide, several methods to produce the master mold were tested to find the one in which all channels were perfectly defined, with vertical walls. These methods will be explained in section **2.2** and afterwards, once the channels have been made, we will describe the rest of the process by which the microfluidic device was fabricated. Some steps that were made in order to optimise the device, including changes in the mask design, will also be elucidated. Finally, the operation method of the microfluidic device, namely the process of introducing the cells within the microchannels, will be explained.

Since a major part of the work was dedicated to developing novel microfabrication techniques to create a new method to fabricate microchannels with the appropriate configuration, in section **2.3** the advantages/disadvantages related to each process will be discussed in detail. In this section we will also compare the microfluidic device developed in this work to the microfluidic platforms reported in the literature in terms of microfabrication techniques, design structure and operation mode employed.

2.1 *Materials*

2.1.1 Microfluidic Fabrication

The microfluidic devices developed in this project were performed inside the INESC MN cleanroom. In Figure 2.1 photographs of the main equipment necessary for the fabrication of such devices are shown.

The deposition of thin metallic films, such as the aluminium patterned over the quartz substrate to fabricate the photomask, was performed in the Nordiko 700 sputtering system. All the exposure steps during microfluidic fabrication were performed in the Direct Writer Laser (DWL) lithography 2.0 system (Figure 2.1a) and b)). During microfluidic chip fabrication, all the spin coating steps were carried out in the SVG 88 series track system (see Figure 2.1c)).

The first methodologies to fabricate the master molds were generated by using the photomask in contact lithography to produce a positive relief of photoresist on a silicon wafer. The process of contact lithography was performed in a UV chamber and the sample was exposed to UV light (UV 250 W hand lamp. Power supply specifications: 230V AC, 50Hz, 4A, from UV light technology Ltd) (Figure 2.1d)).

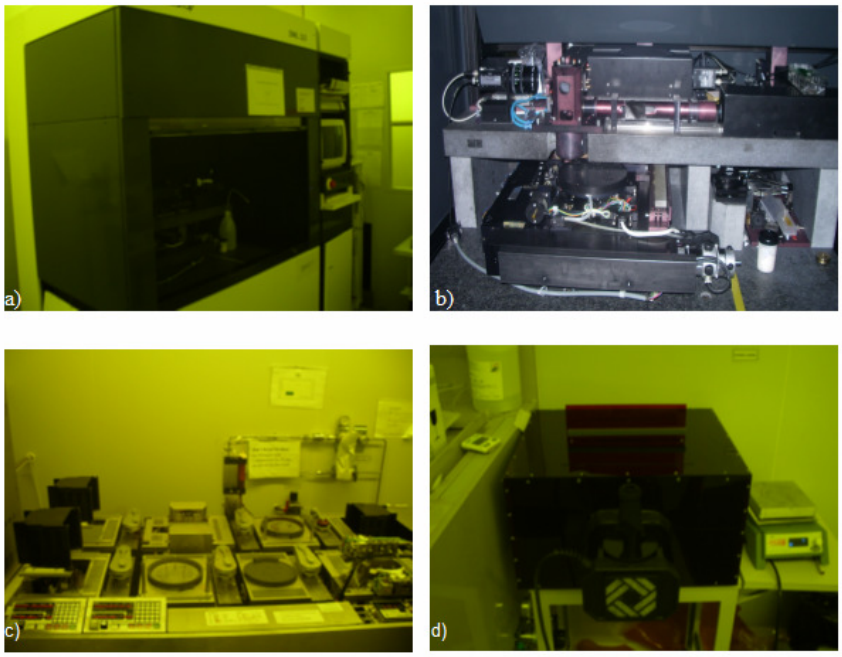

Figure 2.1 - Photolithography equipment. a), b) Direct Writer Laser (DWL) lithography 2.0 system. c) SVG 88 series track system. d) UV handmade chamber.

The profile of the channel walls was confirmed using the perfilometer DEKTAK 3030ST Surface Texture analysis system from SLOAN and the Scanning Electron Microscope S-2500 from HITACHI (Figure 2.2).

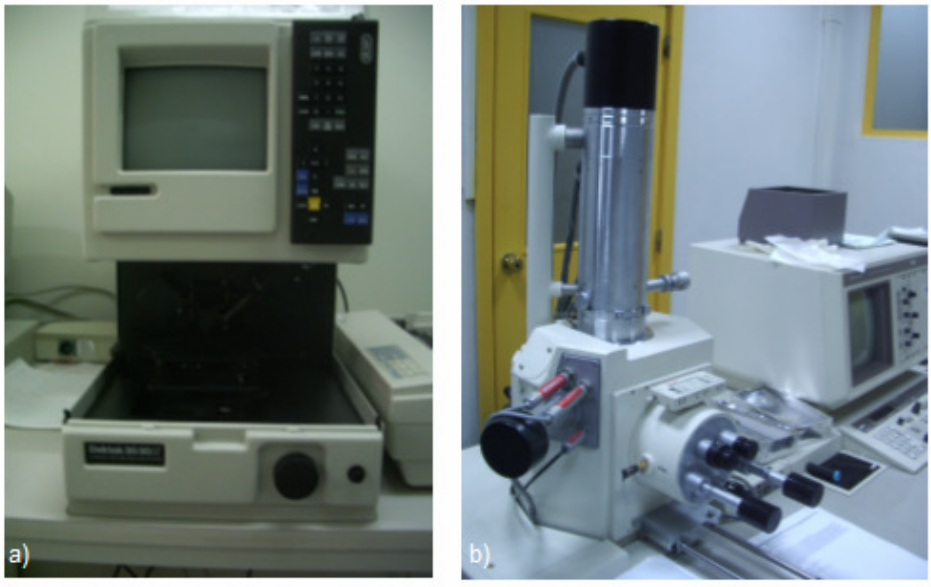

Figure 2.2 - Equipment used to confirm the profile of the channels. a) Perfilometer. b) Scanning Electron Microscope.

PDMS was used to perform the Replica Molding Technique. Before curing the PDMS in a model 400 oven from Memmert, the elastomer was degassed in a desiccator under vacuum (Figure 2.3).

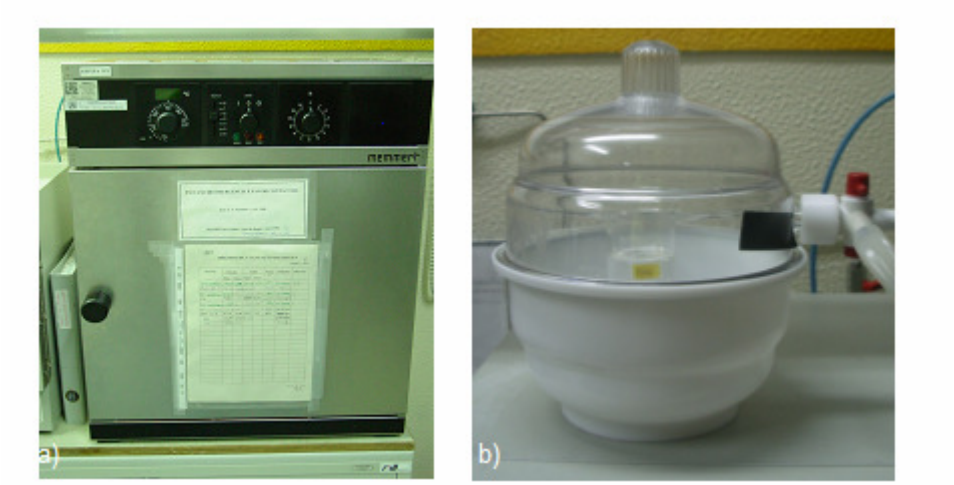

Figure 2.3 - a) Oven form Memmert. b) Vaccum Dessicator.

A Corona system model BD-20AC from Electro-Technique Products Inc was used to irreversibly bond the PDMS replica molding on a glass microscope slide and to hydrophilize the microchannels (Figure 2.4).

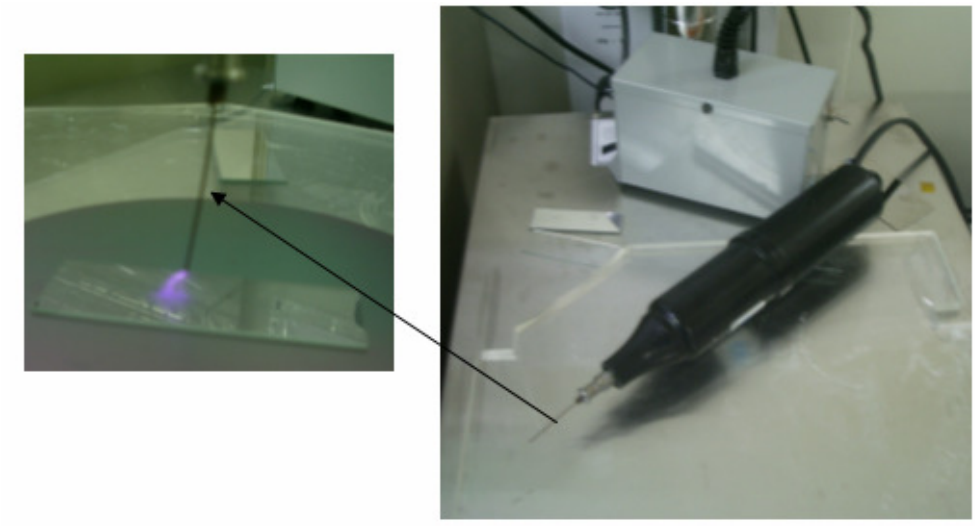

Figure 2.4 - Corona Portable System.

The cell and the gradient experiments were carried out both in INESC MN and in IMM. The microscope used in INESC MN was a DMLM model fluorescence microscope from Leica Microsystems Ltd (Figure 2.5a)). Images were captured by a digital colour camera Leica DFC300 FX. The fluorescence microscope used in IMM was an Axiovert 200M inverted microscope from Zeiss. Images were acquired by a digital camera Axiocam MRm form Zeiss.

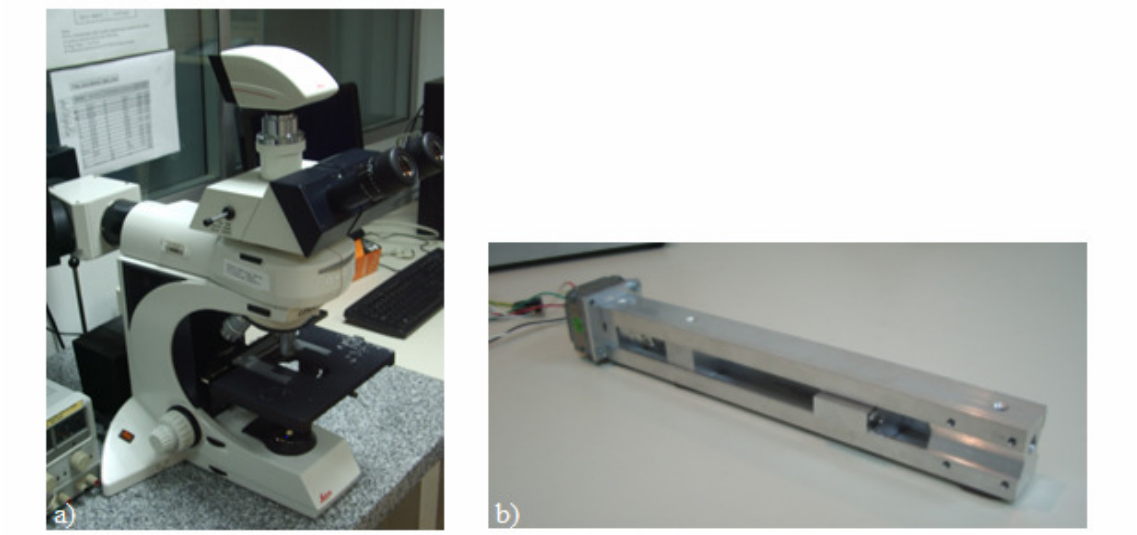

Figure 2.5 - a) Fluorescence Microscope. b) Syringe pump.

For the generation of a stable gradient within microchannels a syringe pump with a 16HS Series Size 16 Hybrid Stepper Motor, from RS, was used (Figure 2.5b)).

Due to the fact that several different methods were used to fabricate the final microfluidic device, and many different reagents were used for specific applications, to facilitate the comprehension of the methodology applied, all materials, reagents and other tools will be detailed in section **2.2**.

2.2 *Methods*

2.2.1 Microfabrication environment

Since the dimensions of the structures are of the order of micrometers, all the microfabrication processes were carried out in a very controlled environment. INESC-MN has a 250 m^2 cleanroom that fulfils these requirements helping to assure the quality and reproducibility of all the process [55]. Only the cell experiments were performed outside the cleanroom.

The air that enters the cleanroom from outside is filtered to exclude dust, and the air inside is constantly recirculated through high efficiency particulate air and ultra low penetration air filters to remove internally generated contaminants. Temperature (20ºC), humidity (70%), vibrations and electrical disturbances are under stringent control. This clean room has different areas classified as 100 and 10, referring to the maximum number of particles of size less than 4 µm per cubic inch of air inside the room.

People enter and wear protective clothing such as hats, face masks, gloves, boots and over-alls. INESC-MN also has an adjoining 250 m^2 grey area (nominally class 10,000) with

microelectronic facilities for backend microelectronics processing, magnetic recording head and MR sensor fabrication, thin film semiconductor device and MEMS processing [55].

2.2.2 Fabrication of Microfluidic channels

2.2.2.1 Fabrication of Microfluidic channels using the negative photoresist SU-8 2015

The first method used to fabricate microfluidic channels included the negative photoresist SU-8 2015 (Microchem Corp.) that was used as a master mold on Si wafers, and the steps are described bellow.

Step 1: Mask Design

The mask design was created using the AutoCAD 2005 program. The design included 4 groups of channels, each group with channels with widths between one hundred and five microns (see Figure 2.6).

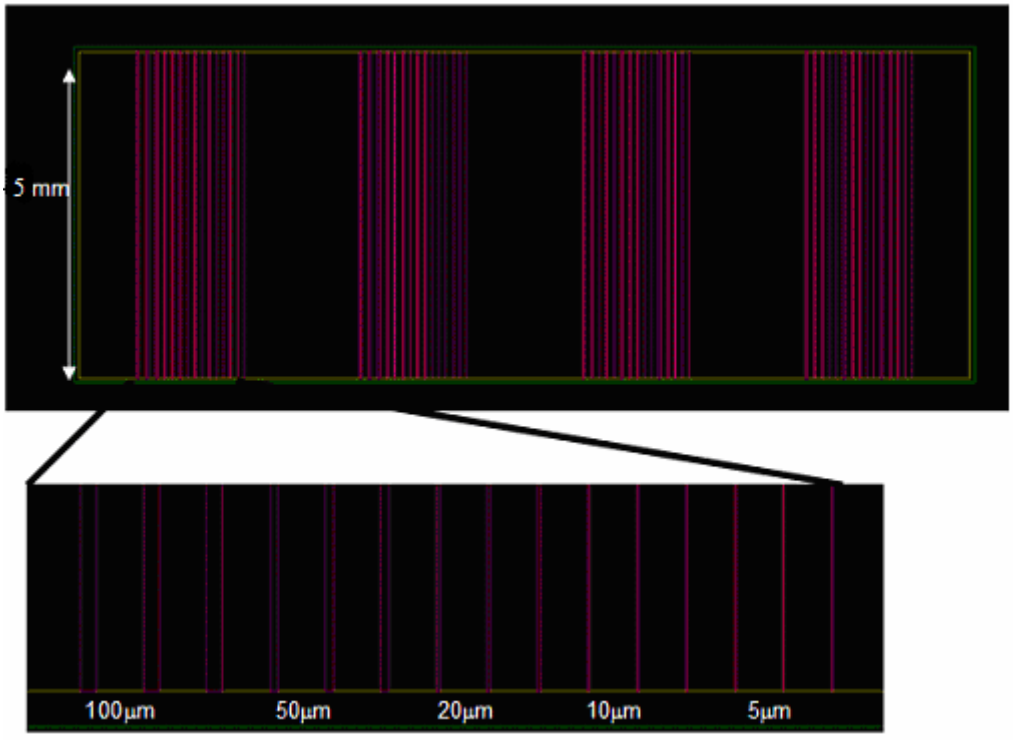

Figure 2.6 - AutoCAD design of the channels and their dimensions. Three channels of each width were designed.

The fabrication of microchannels with a wide range of widths aims to find out the optimal size for which the cells can be introduced and circulate one at the time. In each group of microchannels,

three of each width was designed to compare the final results in statistical terms.

Step 2: Mask Fabrication

The hard mask was composed by the channels patterned in Aluminium over a clean quartz substrate using the standard photolithography process according to the Figure 2.7.

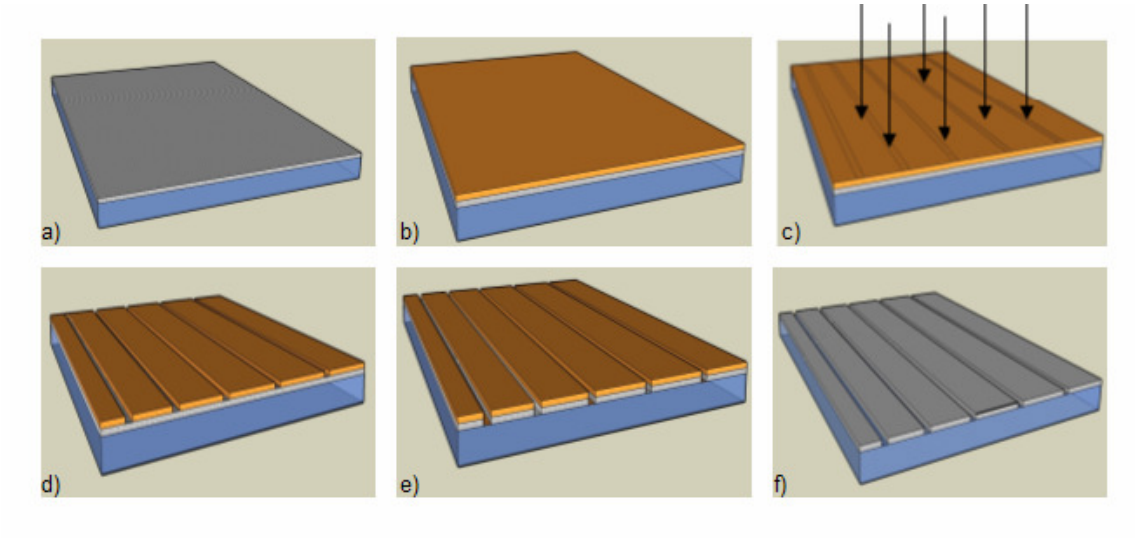

Figure 2.7 - Schematics of mask fabrication. a), Aluminium deposition over quartz substrate. b) PR spin coating. c) DWL exposure. d) PR development. e) Al etching. f) PR strip.

The quartz substrate (Vitreosil® UV-VIS Optical Fused Quartz 50 mm x 25 mm x 2 mm thickness) was cleaned with IPA (acquired from José M. Vaz Pereira, S.A.), rinsed with deionised water, and dried with nitrogen to remove the organic materials from its surface. In the next step a 200 nm thick layer of Aluminium was deposited over a quartz substrate in the Nordiko 7000 machine by Physical Vapor Deposition. After Aluminium deposition it was necessary to coat the Aluminium with a positive photoresist (PFR 7790G 27cP from JSR) with a spin speed of 2800 rpm for 40 seconds to achieve a layer of 1.5 µm thick of PR, and baked at 85 ºC for 1 minute to set its dissolution properties. The photoresist coating was used to transfer the desired pattern to the Al layer using photolithography.

The sample was exposed in DWL using a 422 nm wavelength laser. Under such exposure, irradiated areas of the resist undergo structural/chemical modifications such that they have differential solubility in a developing solution with respect to unexposed areas. These exposed/unexposed areas are directly related to the pattern created in the AutoCAD file. Because a positive photoresist was used, after development, the irradiated areas were etched selectively. This step is followed by an etching process to selectively remove Aluminium from areas not coated with photoresist creating the desired microstructure in the Aluminium layer. The sample was immersed for 3 minutes in Al Etchant. During etching, the resist needs to adhere well to the Aluminium layer to avoid excessive under-cut (etching under the photoresist layer). One has to be careful because this is an isotropic etch, which means that the protected

areas can still suffer a small removal. To stop the chemical etching the sample was immersed in water for 1 minute. Finally, after etching was complete, unwanted resist was stripped away by immersing the sample in microstrip (MICROSTRIP® 2001 from FUJIFILM) for 30 minutes, and cleaned with IPA, water and dried with pressurized N_2.

Step 3: Master Mold Fabrication

Master mold was fabricated by patterning thin negative photoresist SU-8 2015 on Silicon substrate.

Before coating the photoresist, a pre-step was necessary to clean the Si substrate to obtain maximum process reliability. According to MicroChem SU-8 datasheets [56] substrates should be cleaned with a Piranha wet etch (using H_2SO_4 and H_2O_2 4:1). Afterwards, about 1.5 ml of resist was spilled to coat a 5 cm x 2,5 cm piece of Silicon. To achieve the desired film thickness it was necessary to adjust the optimal spin conditions according to the information below (Figure 2.8):

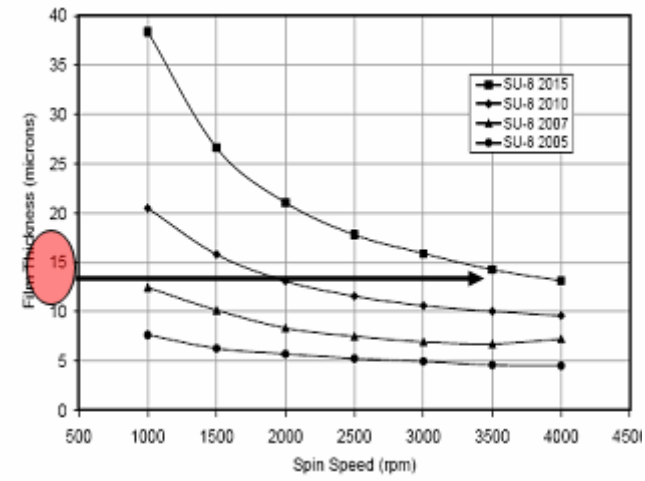

Figure 2.8 - SU- 8 2000 Spin Speed vs. Thickness (from [55]).

SU-8 is available in many standard viscosities according to the desired film thickness. Due to the goals of this work, and because the model of photoresist available in INESC-MN was SU-8 2015, the spin coater was set to spin at 500 r.p.m. for 5 seconds and at 3500 r.p.m. for 30 seconds in order to get a photoresist layer with a thickness of 15µm, the minimum layer of thickness possible to get using this PR. After coating silicon with SU-8 2015, it was necessary to do a soft bake step to evaporate the solvent for 5 minutes. Soft bake times were according to the data sheet of the fabricant [56]. The SU-8 photoresist was then patterned by UV exposure for 20 s. The mask was placed over the photoresist sample with aluminium facing down in a way that the Al layer faced SU-8. The set was inserted into the UV chamber and using the UV light the sample was exposed with the desired channels pattern. Immediately after exposure, a post bake took place to allow cross-linking by baking on a hotplate (95ºC for 5 min). Finally the mold was developed in PGMEA (form Sigma-Aldrich) for 3 min then rinsed with IPA and dried. A

hard bake (150 ºC for 15 minutes) was added to ensure that SU-8 2015 properties do not change in actual use.

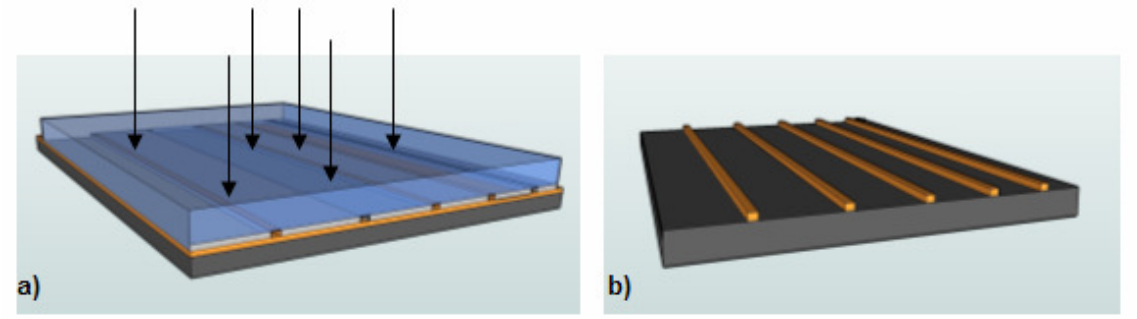

Figure 2.9 - Sample exposure to UV light. a) Mask with Aluminium layer faced SU-8. b) Master mold after development.

Step 4: Profile of the channels

The profile of the channel walls was confirmed using a perfilometer and a Scanning Electron Microscope.

In a perfilometer, the depth and the width of the channels can be measured electromechanically by moving the sample under a contact of a 12.5 micron diameter stylus.

SEM is a type of electron microscope that images the sample surface by scanning it with a high-energy beam of electrons in a raster scan pattern. The electrons interact with the atoms that make up the sample producing signals that contain information about the surface topography of the sample, composition and other properties such as electrical conductivity. For conventional imaging in the SEM, specimens must be electrically conductive, at least on the surface, and electrically grounded to prevent the accumulation of electrostatic charge at the surface. The sample was therefore coated with an ultra thin coating of electrically-conducting material, gold, deposited on the sample by sputter coating (Figure 2.10).

Figure 2.10 - Gold deposition by sputter coating to make the surface of the master mold electrically conductive.

2.2.2.2 Methods to increase the adhesion between SU-8 2015 photoresist and Si substrate

Using the method described in **2.2.2.1**, it was not possible to achieve the channels with smaller widths, namely the ones with 10 and 5 µm wide, possibly due to the weak adherence between the photoresist and the Si substrate. For this reason, new methods were implemented in order to increase such adhesion, which will be briefly described below.

- **Increasing the soft bake and exposure times**

Despite being referred on the data sheet of the fabricant [56] soft bake and exposure times were increased in order to verify if the adhesion of the SU-8 in the Si substrate would increase.

- **HMDS Vapor Prime**

The coating of the photoresist was preceded by HMDS vapor prime deposition to promote the resist adhesion.

In wafer fabrication, hexametyldilizane (HMDS) deposition is typically used to promote the chemical adhesion of an organic compound (photoresist) and non-organic substrate (wafer). The silane acts as a sort of "bridge", with properties that will bond to both photoresist and wafer surface (Figure 2.11). To promote a strong silane bond to the substrate, first, wafers must be completely dehydrated and therefore a process combining heat with low pressure was developed in the HMDS vapor prime oven, from YES. Once dehydrated, wafers were then primed with an HMDS vapor, from Fluka, to strengthen photoresist adhesion. The process was performed at 130 ºC in an ambient of hexamethyldisilazane (HMDS) vapor [57].

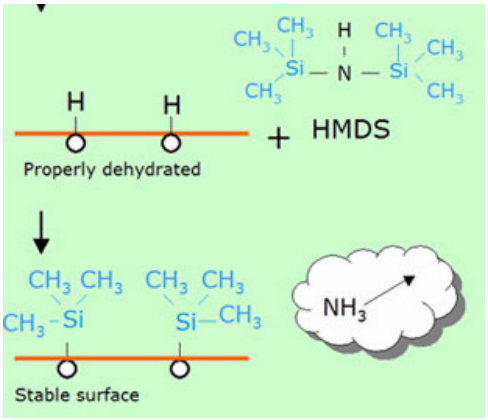

Figure 2.11 - HMDS deposition to promote chemical adhesion on organic substrates (from [57]).

- **HF treatment of Silicon wafers**

When silicon is exposed to oxygen (air) under ambient conditions a thin layer of native oxide (silicon dioxide) is formed, approximately 1 nm or 10 Å which makes the silicon surface hydrophilic. Due to the fact that it was not known what kind of surface (hydrophilic or hydrophobic) will improve the adhesion between the PR and the substrate, both surfaces were tested. The hydrophobic surface was obtained removing the native oxide layer, using for this purpose Hydrofluoric Acid (HF). Silicon dioxide is attacked by HF to produce "hexafluorosilicic acid":

$$SiO_2 + 6HF \rightarrow H_2SiF_6 + 2H_2O$$

Hydrofluoric Acid (HF) is a corrosive and a contact poison thus, an extremely dangerous material because it produces severe *delayed* tissue damage without necessarily producing pain [58]. For this reason, it should be handled with extreme care, using rubber gloves, apron and protection glasses. The sample was first immersed in Ammonium Hydrogendifluoride solution, from Arch Chemicals Inc., for 20 seconds and then immersed in water for 1 minute. The negative photoresist was spin-coated and exactly the same steps described in **2.2.2.1**. were followed.

- **Deposition of an amorphous silicon layer**

Amorphous silicon is a semiconductor that can be deposited as thin films and for this reason this form of silicon has become widely used in MEMs, Photodiodes and Transistors fabrication. The thin film of amorphous silicon is not completely uniform, presenting some irregularities that could improve the adhesion between PR and silicon wafers.

A piece of silicon was carefully cleaned with IPA, rinsed with deionised water and dried with pressurized N_2. Then, a 1000Å layer of amorphous silicon was deposited over the substrate in the Electrotech Delta Chemical Vapor Deposition System. SU-8 was spin-coated and the procedure was done by following the same steps described in **2.2.1.1.**

- **Coating of PMMA layer**

Bubendorfer and colleagues [59] found that using PMMA as a substrate instead of silicon the adhesion between PMMA and the overlying SU-8 is enhanced. The PMMA used in this experiment was liquid E-Beam Resist PMMA 600K from Allresist. A pre-bake was done at 100ºC for 5 minutes before spin coating PMMA over the silicon wafer at 3000 r.p.m. for 30 seconds.. Another bake step was performed at 150ºC for 30 minutes. Finally, the procedure

continued with the spin coating of SU-8 2015 and all the further steps described in **2.2.2.1.**

2.2.2.3 Fabrication of microfluidic channels using polymeric materials as substrate

A new method to fabricate the microchannels was implemented using polymeric materials such as Polyimide (PI) and Polyethylene (PET) instead of the usual silicon substrate (Figure 2.12).

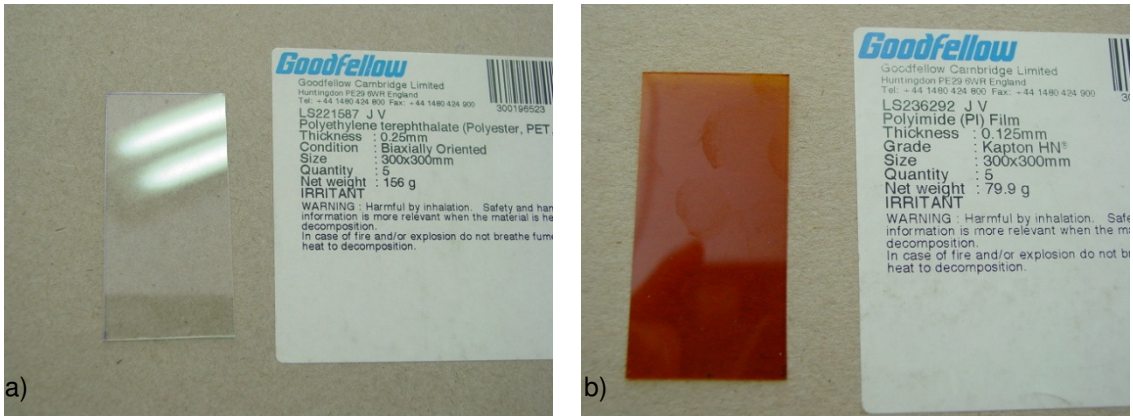

Figure 2.12 - Polymeric materials that were used as substrate for master mold fabrication. a) Polyethylene (PET) and b) Polyimide (PI).

PI (from Goodfellow, thickness: 0,125 mm) and PET (from Goodfellow, thickness: 0,125 mm) were firstly cleaned with Alcanox in order to remove the organic materials from their surfaces. It is important to refer that, because polymeric substrates tend to deform when heated, after cleaning them a tape was placed all around the substrates to keep them flat over a piece of silicon. After this step, the procedure was done by following the same steps described in **2.2.2.1.**

2.2.2.4 Fabrication of microfluidic channels using the positive photoresist AZ 4562

The fabrication process of the master mold was very similar to that of point **2.2.2.1** with the difference that in this case the positive photoresist AZ 4562 (from Clariant) was used [60]. The run sheet was already optimized by a colleague in INESC-MN and kindly provided for this experiment.

Step 1: Mask Design

The mask design was the same as the one used for the process described in **2.2.2.1** with the difference that this time the AutoCAD file had to be saved in such a way that the mask was inverted, which means that the laser acts outside the pattern in order to create an inverted mask.

Step 2: Mask fabrication

This step followed exactly the same procedure as described in **step 2 (2.2.2.1.)**

Step 3: Mold Fabrication

This step was also very similar to the one described in **2.2.2.1.** Before resist coating, the Si substrate was primed with HMDS to improve the adhesion of the resist to the substrate. The sample was then spin coated with the AZ4562 photoresist and before baking it was left to degas for 15 minutes in order to evaporate the solvent. The sample was baked at 100°C to harden the photoresist. The quartz mask was then placed over the thick resist (with the Aluminium facing down) and using the UV light, the sample was exposed with the desired channel pattern. The thick resist mold was developed in AZ 400K developer (form Clariant) and then it was rinsed with DI and dried with N_2.

Step 4: Profile of the channels

SEM was used to confirm the profile of the channels.

2.2.2.5 Microfluidic channels using four layers of positive photoresist PFR 7790G 27cP

The methods described in sections **2.2.2.1** to **2.2.2.4** were not adequate for the final purpose of this work which involved the fabrication of microchannels with a wide range of widths in order to verify which of them was the most adequate for use in the final experiments involving cell insertion and gradient generation. A new method to fabricate the microchannels was implemented using the positive photoresist PFR 7790G 27cP, and the key steps are given by the following figure:

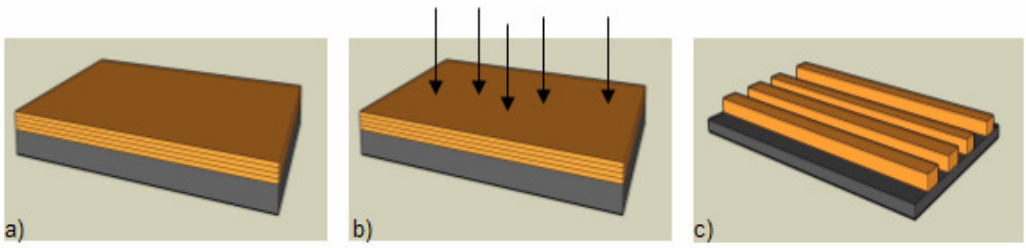

Figure 2.13 - Master mold fabrication using the positive photoresist PFR 7790G 27cP. a) Coating of 4 layers of positive PR. b) DWL double exposure. c) Master mold after development.

Firstly the silicon wafer was cleaned with IPA and rinsed with deionised water and dried with N_2. Before resist coating, the sample was vapor primed with HMDS for 30 minutes to improve the

adhesion of the resist to the substrate. Afterwards, the spin coating step (2800 rpm for 40 s to have a thickness of 1.5 μm) and the bake step (85ºC) were repeated four times to achieve a thickness layer of 6 μm. After each bake step, the Si sample needed to cool for 10 minutes until room temperature was reached again. The substrate used was the whole wafer and not only a piece of silicon with a size coincident with the desired pattern, to guarantee a uniform coating of the 4 layers of photoresist. After resist coating the sample was cut to have the dimensions match the dimensions of the designed pattern. The sample was exposed in DWL using a 422 nm wavelength laser (near ultra-violet light) but due to the higher thickness of the photoresist layers, it was necessary to increase the power of the machine to 100%. Furthermore, the sample was subjected to two consecutive exposures to ensure that all the layers were affected by the laser beam. Finally, the development step was made in short steps of 20 seconds, and the pattern was checked in the microscope to verify if the sample was perfectly developed. It is very important to avoid overdevelopment because when the pattern created has very small structures like the microchannels with very small widths, these structures could disappear when overdeveloped.

In this new method to fabricate the master mold, it was not necessary to produce a photomask because the pattern is directly created on the photoresist layers using the laser beam due to the fact that the machine used for exposure (Direct Write Laser) is perfectly adjusted to work with the positive photoresist PFR 7790G 27cP.

2.2.3 PDMS Replica Molding

The PDMS formulation used, SylgardTM 184 (Dow Corning; Midland, MI), is composed by a liquid silicon rubber base and a curing agent. The base and curing agent were measured in a 10:1 ratio by weight, according to the Sylgard 184 silicone elastomer datasheet [61], and mixed thoroughly by hand for about 2 minutes. Since bubbles were always present after mixing, the mixture was then degassed in a desiccator under vacuum for 1 hour, until all air bubbles were removed. The mold was put over a flat surface (plastic container) and, after degassing, PDMS was poured over the mold and cured in an oven for 1 hour at 60 ºC. After curing the elastomer, the device was released by peeling from the mold yielding a complementary structure of the pattern in the mold (Figure 2.14). The PDMS was finally cut with the right dimensions in order to be assembled and bonded to a glass microscope slide.

Before mounting the PDMS replica on a glass microscope slide both pieces were cleaned with HCl 32% from Merck (1:5 ratio by volume) for 8 minutes and then rinsed with IPA. The next step involved the irreversible bonding between these two surfaces using the Corona Portable System, which will oxidize PDMS and thus allow a permanent bond between the PDMS replica and substrate to be formed. Applying the Corona discharge to its surface starts to make it more hydrophilic, which means that silanol groups are being developed on the PDMS surface. Each

surface was scanned for 30 seconds (in the case of PDMS the pattern was facing up), and immediately afterwards such layers were brought into contact. The device was allowed to rest for 2-3 hours and after that time it was ready to use.

As it was said before, the hydrophobic surface of PDMS, when exposed to electrical discharge, such as corona discharge, becomes hydrophilic but after a certain relaxation time PDMS gradually regains its hydrophobicity [62]. Therefore, it was important to bond PDMS on the glass substrate immediately after corona treatment to avoid hydrophobicity recovery.

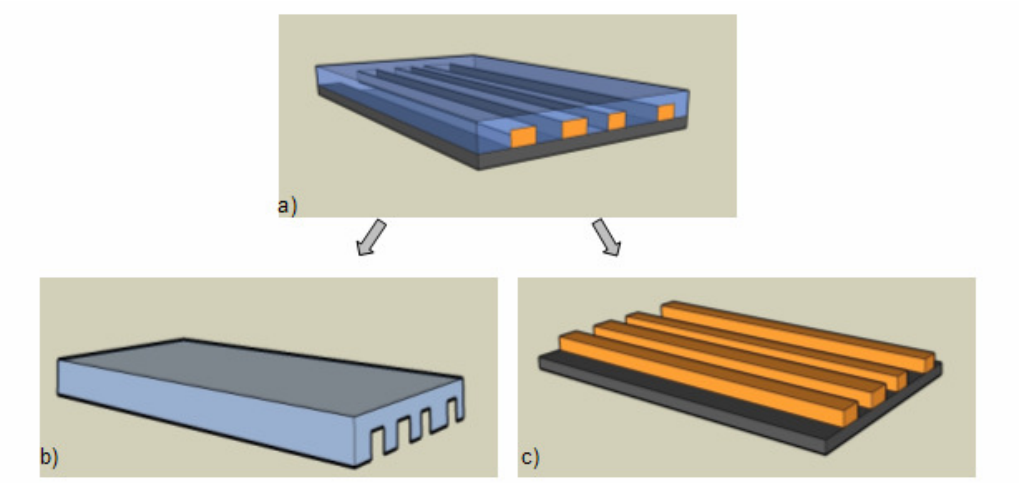

Figure 2.14 - Replica Molding Technique. a) PDMS (blue) is poured over the master mold (orange) and cured. b) PDMS replica is obtained by peeling from the mold. c) Master mold can be used many several times to produce many replica molds.

2.2.4 Optimization of the microfluidic device

This section will be dedicated to the description of the main approaches developed during the project to improve the microfluidic device. To clarify the reasons why these approaches were developed, one will present in this section some results of preliminary tests using the fluorophore FITC as well as some basic experiments using *Saccharomyces cerevisiae* cells because they justify the reason why it was necessary to make adjustments to improve the microfluidic device.

The first version of the microfluidic device was only constituted by microchannels with a range of widths between one hundred and five micrometers (figure 2.15).

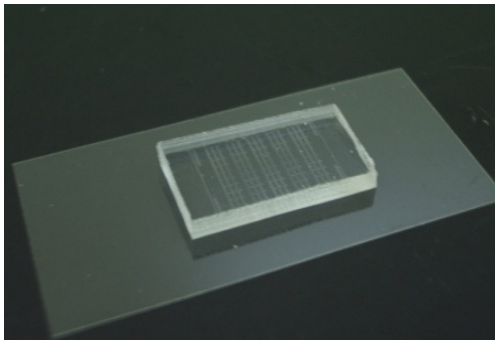

Figure 2.15 – First version of the microfluidic device.

Before starting with the cell experiments, some tests were performed to confirm the functionality of the microchannels. FITC fluorophore was used for this purpose because of its high fluorescence intensity (see Figure 2.16).

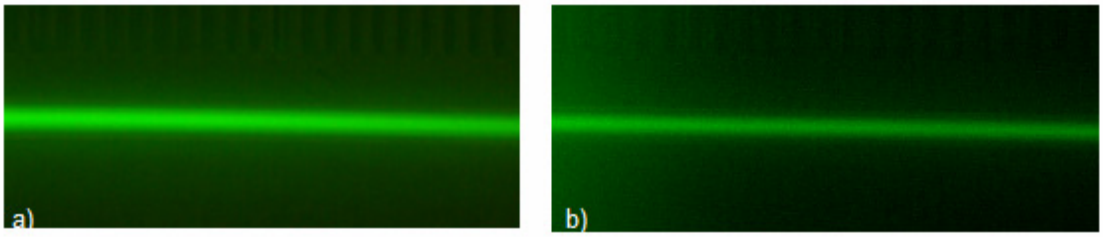

Figure 2.16 - Fluorescence micrographs of microchannels with FITC.

When it was proved that the microchannels had the optimum conditions to begin operations, with both entrances open and the PDMS walls not collapsed, some basic experiments were performed to see if the cells could enter the channels by capillarity and which size would be the optimal one to visualize them. A single drop of the solution with the cells was placed at the entrance of the microchannels and the results are shown in the following figure:

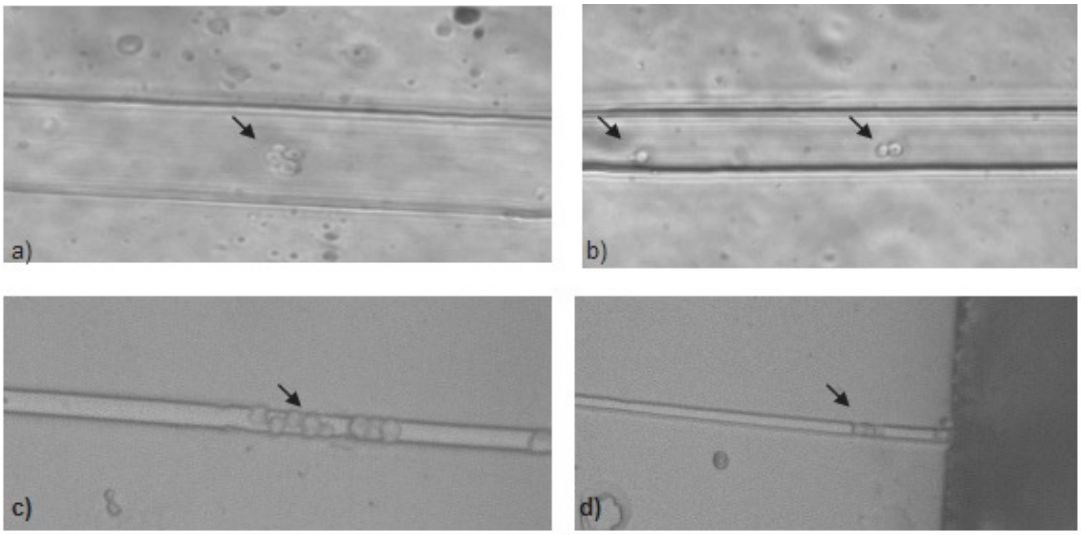

Figure 2.17 - Microchannels with different widths with yeast cells inside it. a) Width= 50 µm, b) 20 µm, c) 10 µm and d) 5 µm.

It is important to refer that before doing the cell experiment described above, the size of the *Saccharomyces cerevisiae* cells (3-4 μm) was already known, however it was not clear if it would be possible to visualize the cells in microchannels with widths matching that of the cells of interest, therefore microchannels with a wide range of widths were made.

Looking at the figure 2.17, we can clearly see that the optimal channel size to analyse single yeast cells should be between 10 and 5 μm. It was also possible to verify that the cells in the microchannels with widths up to 10 μm did not adhere on the glass substrate or on the PDMS sidewalls but simply went along the channel without stopping. In the microchannels with widths down to 10 μm, the cells entered the channels but these channels offered more resistance when they passed, which prevented these cells from leaving the channels. Furthermore, the PDMS sidewalls usually present some irregularities that reduce the brownian motion of the cells. In this experiment it was also possible to verify that the phenomenon of capillarity in the small channels (with widths down to 10 μm) was not sufficient for the cells to go through them and they stayed at the beginning of the channels.

With the results presented above, the mask design was improved having this time only microchannels with widths between 10 and 5 μm. Along the length of all the channels a *ruler* was added to the mask design so that it could be easier to localize a particular cell along the time (Figure 2.18).

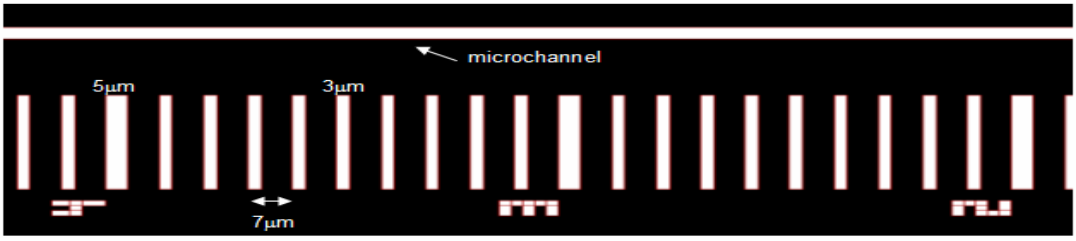

Figure 2.18 - AutoCAD design of the ruler near each channel to facilitate the localization of a particular cell over long periods of observation.

Since one of the goals of this work was to test the effect of an inducer/repressor in the protein expression levels, it was necessary to have reservoirs connected to the microchannels in the microfluidic device to store the soluble components. Having this goal in mind, two rectangular reservoirs were added in the mask design (15 mm x 15 mm) each one with a capacity of 1,575μl. After bonding the PDMS on the glass substrate, it was found that both reservoirs collapsed and it was not possible to fill them with liquid. This fact was due to the small height/area ratio of the reservoirs and therefore a way to overcome this problem had to be developed. Two pieces of silicon (15 mm x 5 mm x 0,7 mm) were cut using an automatic dicing saw DAD 321, form DISCO to act as the mold for the inlet and outlet reservoirs. With a thickness of 700 μm the capacity of each reservoir increased to 70 μl. The mask design was changed in such a way that the channels had 1 cm length instead of 0,5 cm initially established.

The silicon pieces were bonded to the master mold, using double-face tape, according to the alignment marks in the mold, as it is shown in figure 2.19. The microchannels, after the Si pieces having been bonded, have a final length of 0,5 cm.

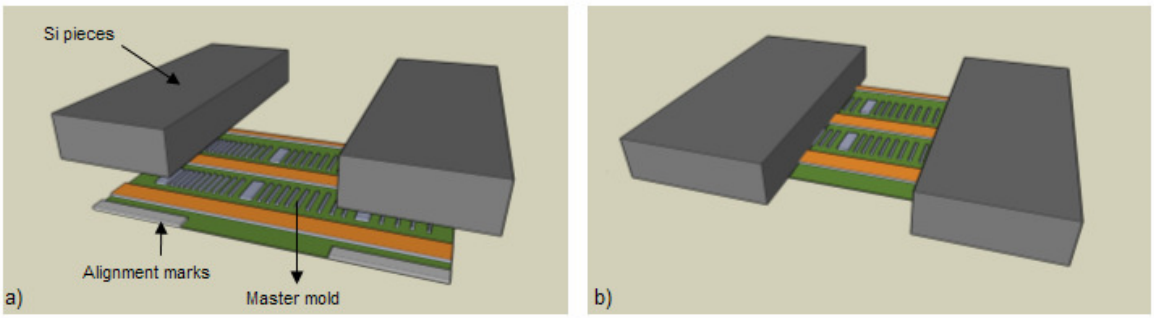

Figure 2.19 – Master mold with two pieces of silicon acting as the mold for the reservoirs.

In Figure 2.20 the key steps of the Replica Molding Technique that were performed to obtain the final microfluidic devices are shown. To improve the efficiency of the mold fabrication the mold had three dies to allow the fabrication of three PDMS replicas at the same time, thus decreasing the time spent on the microfluidic device fabrication.

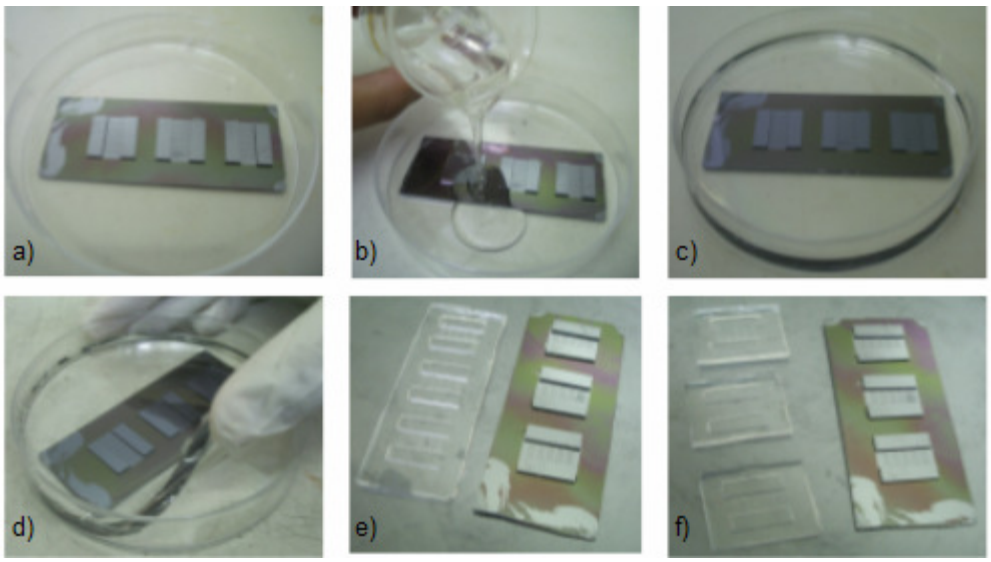

Figure 2.20 - Photos of the Replica Molding Technique. a) Master mold. b) PDMS was poured over the master mold and c) was taken to rest for 2-3 minutes. d) PDMS was heat cured for 1 hour at 60ºC. c) PDMS Replica was then removed from the mold, and f) cut to form three distinct PDMS devices.

2.2.5 Operation mode of the microfluidic device

After the PDMS/glass microfluidic device was made with close reservoirs (Figure 2.21a)), it was necessary to open vias in order to connect the microfluidic device with the tubes that constitute the external fluidic system. First, two openings were punched using a 20 gauge blunt needle to

insert metal connectors (20 ga x15 mm (ref. SC 20/15) from INSTECH) in the PDMS. Before connecting the PDMS to the outside fluidic system it was important to do a Corona Discharge to transform the hydrophobic surface of the channels/reservoirs into a hydrophilic one. This treatment was made introducing a small electrode (a needle-type electrode) inside the reservoirs and the power supply was turned on for 10 seconds (see Figure 2.21b)). Immediately after corona discharge both wells were completely filled with water using a 1 ml syringe to prevent the recovery of the hydrophobicity. Because microchannels were hydrophilic due to the Corona treatment, the liquid should have entered by capillarity through the channels. However, it was found that some channels did not present water inside then. To overcome this situation one metal connector was inserted in one of the reservoirs and connected to the outside by a 20 ga polyethylene catheter tube. Vacuum was made in that reservoir, using a 1 ml syringe and pulling on the plunger carefully, to force the liquid to enter through the channels (Figure 2.21c)). After this step, it was confirmed by microscope observation if all the channels were completely filled with water or not. If not, it was necessary to repeat the vacuum step to ensure the presence of the liquid inside it. After that, the reservoir that was subjected to the vacuum was filled with water again in order to keep the entire device hydrophilic. The other connector was then inserted in the opposite reservoir (jointly with the polyethylene tube) and both connectors were glued with silicone gel to avoid any fluidic leak (Figure 2.21d)). The connectors were placed sideways to the device to facilitate the visualization on the microscope. If the connectors were placed perpendicularly it would be difficult to move the device on the microscope stage due to steric hindrance between the connectors and the microscope objectives.

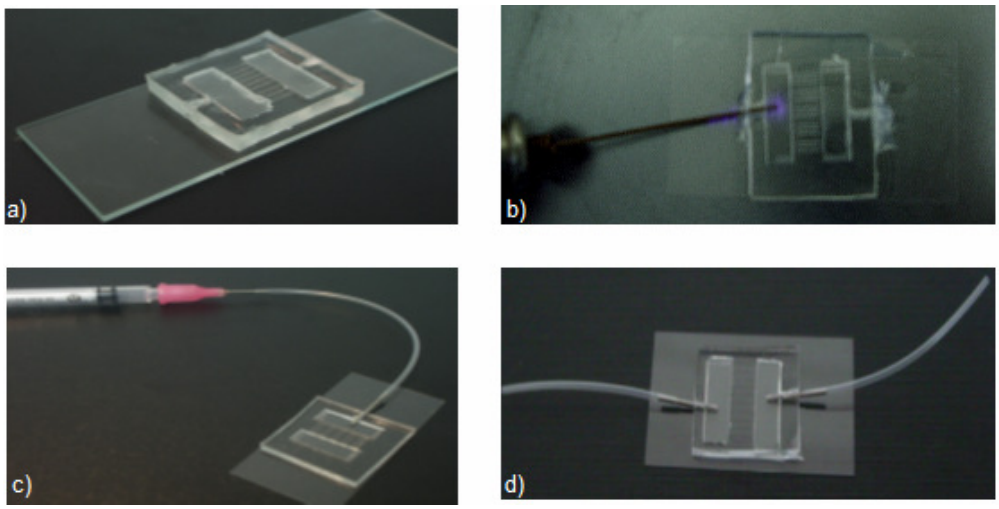

Figure 2.21 - Operation mode of the microfluidic device. a) Microfluidic device prior to the installation of the external tubing responsible for the outside fluidic system. b) Application of the corona discharge inside the reservoirs. c) 1 ml syringe connected to the microfluidic device to make the vacuum step. d) Microfluidic device filled with water with both connectors after the vacuum step.

2.3 *Results and Discussion*

The main technique involved in the fabrication of the microfluidic device was Soft Lithography. This process provides several major advantages when compared to other forms of microfluidic microfabrication such as those referred in section **1.4.** The main goal in Soft Lithography is to obtain an elastomeric block, for example using PDMS, with patterned relief structures on its surface.

PDMS has become one of the materials extensively used in Microfluidics, due to its biocompatibility, low toxicity, high oxidative and thermal stability, optical transparency, low permeability to water, and low electrical conductivity. The influence of PDMS composition on the attachment and growth of several different types of cells was investigated thoroughly by Whitesides and co-workers [8]. Their results showed that the ability of different PDMS surfaces to support cell attachment, growth and proliferation was cell-type dependent.

Soft Lithography had already been used at INESC MN for the fabrication of microfluidic structures. In the Rapid Prototyping Technique, in which the mold is generated and contains the inverse of all the features and microstructures of interest, epoxy photoresist SU-8 is the most widely used material and for this reason it was the first photoresist used in the project to produce the master mold (**2.3.1**).

2.3.1 Fabrication of microfluidic channels using the photoresist SU-8 2015

SU-8 photoresist is a multifunctional, highly branched novolac glycidyl ether containing 8 epoxy groups. The large quantity of epoxy groups produces a high degree of cross-linking and thus excellent sidewall resolution. SU-8 also confers excellent mechanical properties, chemical resistance, thermal stability and is optically transparent for wavelengths above 350 nm [59]. These properties enable patterning of thick layers with high aspect ratios and vertical walls.

MicroChem SU-8 datasheets [56] were followed and some results were shown in Figure 2.22.

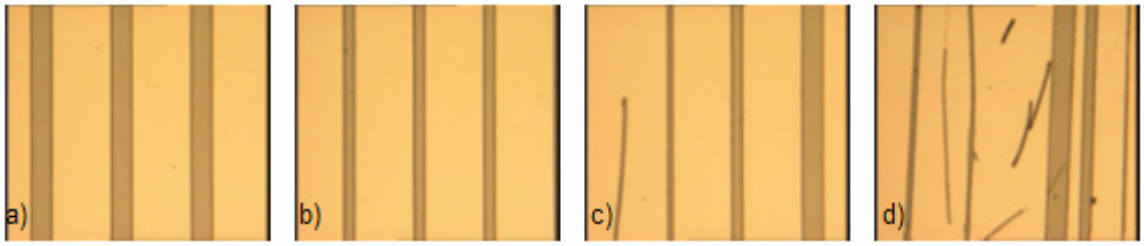

Figure 2.22 - Master mold made of SU-8 2015 with microchannels patterned. a) Group of microchannels with a width of 100 µm. b) Group of microchannels with a width of 50µm. c) Microchannels with increasing widths (10, 20, 50 and 100 µm) in which the first channel is broken. d) Microchannels with a variety of widths in which many of them are broken.

The channels with larger widths, namely the ones with widths of 100 μm, 50 μm and most of 20 μm, were obtained with vertical sidewalls. The structures were confirmed using SEM microscope (Figure 2.23).

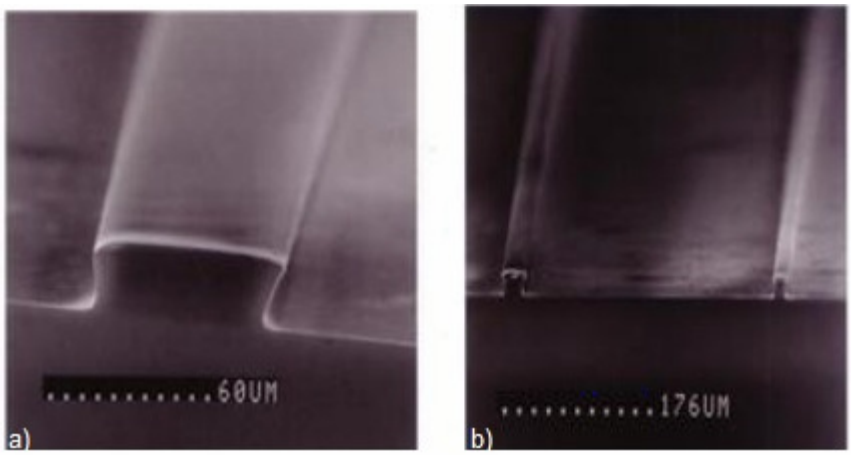

Figure 2.23 - SEM photographs of microchannels made of SU-8 2015. a) Microchannels with widths of 50 μm, b) 20 μm and 10 μm.

By checking the previous figures, one can say that the method to fabricate the master mold based on the photoresist SU-8 2015 was highly efficient to fabricated microchannels with larger widths. However, to fabricate structures down to 20 μm this method was not appropriate. During the development step in PGMEA it was observed that, after approximately 30 seconds, the channels with smaller widths (down to 20 μm) started to peel off, which revealed a weak adherence of the photoresist on the silicon substrate.

The methods previously described in section 2.2.2.2 were performed to improve the adhesion between the PR and the Si substrate and some results are shown in the following section.

2.3.2 Methods to increase the adhesion between SU-8 and Si substrate

- **Increasing the soft bake and exposures times**

The first method used to improve the adhesion between SU-8 and Si substrate was the increase in the soft bake and the exposure times. Nevertheless, the results were exactly the same as the ones presented in **2.3.1**.

- **HMDS Vapor Prime**

HMDS deposition is typically used to enhance adhesion of photoresist on a wafer surface, therefore this pre-step was performed before coating SU-8 on Si substrate. However the results were once again very similar to the ones obtained without any previous treatment on the silicon substrate (**2.3.1**).

- **HF treatment of Silicon wafers**

Despite the fact that in the MicroChem SU-8 datasheets [56] mentioned that the silicon substrate should only be cleaned with Piranha solution (thus the surface keeps hydrophilic), it was not known if the adhesion between SU-8 and Silicon substrate was higher using a hydrophilic or a hydrophobic silicon surface.

To make the Si surface hydrophobic, the native oxide layer that forms over the silicon substrate when it was exposed to the air was removed using for this purpose Hydrofluoric Acid (HF). This method proved to be more efficient when compared to the previous methods performed to increase the adhesion between SU-8 and Silicon substrate because the microchannels with widths between one hundred and ten micrometers were successfully obtained (see Figure 2.24). The only group of channels that were not perfectly obtained were those with widths of 5 μm, as it is shown in the following figure:

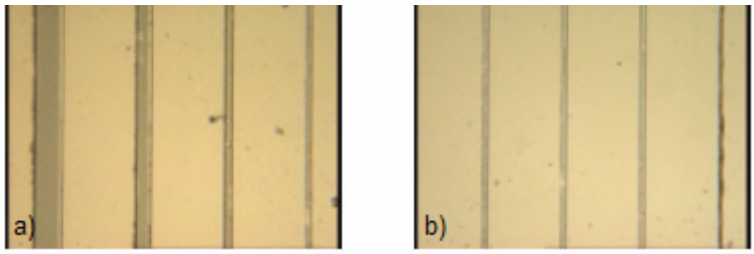

Figure 2.24 - Master mold made of SU-8 using HF to make the surface of Si hydrophobic. a) Microchannels with decreasing widths (from left to right, 100, 50, 20,10 μm). b) Microchannels, the three on the left with widths of 10 μm and the one on the right 5 μm wide.

To confirm the effectiveness of this method, it was attempted to repeat it but the results were not reproducible, and this time only the channels up to 10 μm were obtained. Although the HF treatment of silicon wafers could not be used in this project, because it was important to have channels with widths similar to the size of the yeast cells, this approach demonstrated the highest efficiency in terms of adhesion of the SU-8 photoresist in a hydrophobic Si surface.

- **Deposition of an amorphous silicon layer**

Another method that was tested to increase the adhesion between SU-8 and Silicon substrate was the deposition of an amorphous silicon layer over the silicon substrate. The silicon wafers available in INESC-MN were highly polished and are flat and smooth enough to support optical photolithography. For this reason the deposition of an amorphous silicon film intended to create some roughness on the flat surface and thereby increase the adhesion of the photoresist (Figure 2.25).

Figure 2.25 - Master mold made of SU-8 using an amorphous silicon film over the Si substrate before coating the negative photoresist. Microchannels with decreasing widths (from left to right, 100, 50, 20 and 10 μm).

Using this method to enhance the adhesion between SU-8 and Si substrate, the channels with widths greater than 10 μm were obtained but the small channels, with widths down to 10 μm, presented some irregularities along the channels. Furthermore, as shown in Figure 2.25, the sidewalls of the channels were not vertical as they were in the first method described to fabricate the microchannels (**2.3.1)**, where no previous treatment was done before coating the SU-8 photoresist on the Si substrate.

- **Coating of PMMA layer**

The last method tested to increase interfacial bonding of SU-8 onto silicon substrate was the use of PMMA. It was proved before [59] that using highly polished poly(methyl methacrylate) (PMMA) as substrate instead of silicon, the adhesion between PMMA and the overlying SU-8 is enhanced dramatically. However it is important to refer that in this paper only microchannels with a width of 100 μm were tested.

As described in section **2.2.2.2**, the PMMA used in this experiment was liquid E-Beam Resist PMMA 600K and not a solid substrate, and therefore the results could not reproduce exactly the results shown in that paper. Using this methodology only the bigger channels, up to 20 μm wide, were obtained.

2.3.3 Fabrication of microchannels using polymeric materials as substrate

Because polymeric materials are becoming more and more important for the realization and commercial success of new microcomponents and microsystems, some polymers were tested to substitute the traditional silicon substrates. Two different thermoplastic polymer films were used for this purpose: Polyimide (PI) and Polyethylene (PET). Despite the similarity of both materials, PET proved to be a better substrate when compared to PI because using Polyimide,

only the channels with widths of 100 µm were obtained and even these channels did not always present a regular shape (see Figure 2.26). PET had shown to be a good polymeric material to use as substrate to be coated with SU-8. Microchannels with widths up to 10µm were well defined, however the results were not the same throughout the master mold (see Figure 2.26). In some group of channels the microchannels were all well defined, except channels with widths of 5 µm, while other groups presented irregularities in almost all the channels. Despite the fact that this technique could not be use in this project due to channel widths limitation, such methodology could be extremely advantageous to replace the traditional Si substrates which are much more expensive comparing to polymeric materials. In this work, we used Si as a back support of the polymeric materials to keep them flat during fabrication but silicon could be replaced by other cheaper flat surfaces. On the other hand, if we use polymeric substrates with a higher thickness, these flat surfaces were no longer needed for support.

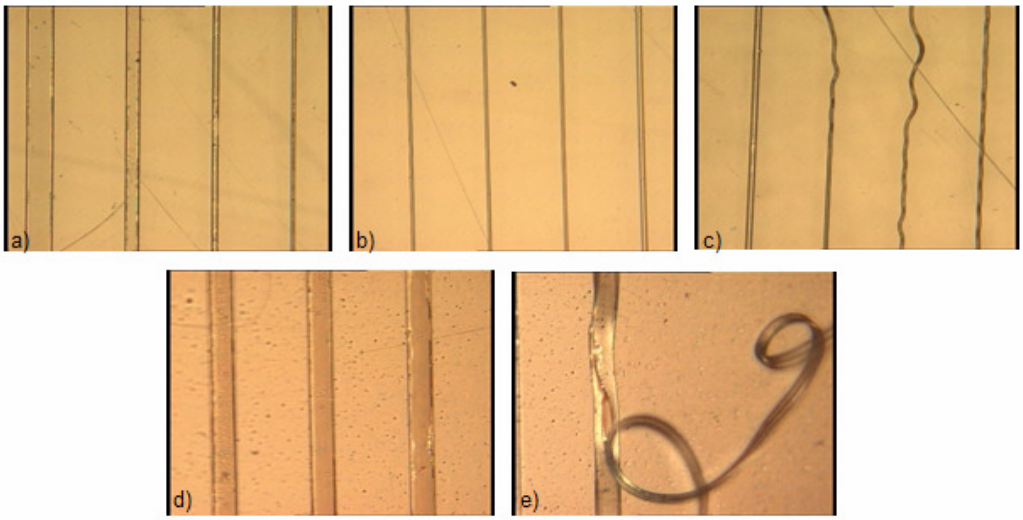

Figure 2.26 - Master mold made of SU-8 2015 using PET (a) to c)) and PI (d) and e)) as substrates. a) Microchannels with decreasing widths (100,50,20 and 10µm). b) Microchannels with widths of 10µm and the last one with a width of 20µm. c) The first channel has a width of 20mm and the last ones (with irregular shapes) have widths of 10µm. d) Microchannels with a 100µm wide. e) Microchannels with 100µm wide presenting irregularities.

2.3.4 Fabrication of microchannels using the positive photoresist AZ 4562

Another way to fabricate the master mold was the use of the positive photoresist AZ 4562. The steps required to make the mold were very similar to the ones used in SU-8 (see **2.2.2.1**). The great advantage of AZ 4562 when compared to SU-8 2015 is the capability of coating very thin films, until 5 µm (which is adjusted with the aim of this work) according to the spin speed conditions [60]. AZ 4562 is more recent than SU-8 therefore is not widely used in microfluidics

fabrication despite being cheaper. The run-sheet of this photoresist is more time consuming mainly because of the prebake and post bake times. Moreover, the exposure step takes longer because it has to do small steps of 7 seconds alternating with waiting times of 15 minutes to avoid bubble formation. The results are shown in Figure 3.6.

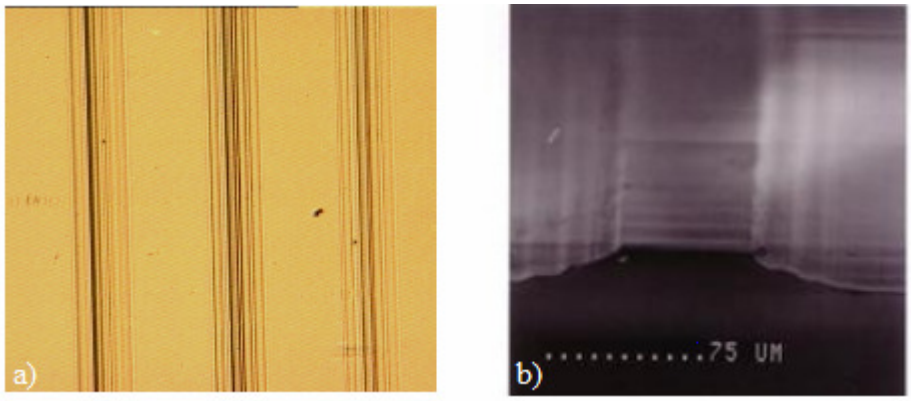

Figure 2.27 - Master mold made of AZ-4562. a) Microchannels with different widths. c) SEM photograph showing the profile of a microchannel.

From figure 2.27 one can verify that the microchannel walls were sloping with a *stair* shape. It seems that the reason for these poor sidewalls could be due to the reflection and refraction phenomena when the light crosses the quartz mask during the exposure step in the UV chamber. As a consequence, the upper edges of the resist are exposed but the light does not have sufficient energy to expose the lower ones. Possibly, the quartz substrate that was used to do the mask was too thick (2 mm).

2.3.5 Microfluidic channels using four layers of positive photoresist PFR 7790G 27cP

The last method used to fabricate the master mold involved the use of the photoresist PFR 7790G 27cP. As mentioned earlier, this photoresist is usually used in DWL machine for mask making and direct writing, however, the state of the art technology of this system can also create complex 3D structures in thick photoresist. Each layer of the photoresist could have the maximum thickness (according to the spin speed) of 1.5µm. Thereby, to achieve an appropriate thickness so that the cells could enter the channels, an overlapping of 4 layers of this photoresist was necessary.

The implementation of this method to fabricate the master mold had the great advantage of creating the required pattern given by the input file, without the need of any mask. With this method the microchannels with widths between one hundred and five micrometers were obtained with a very high precision and without any irregularities, as it is shown in Figure 2.28a) and b).

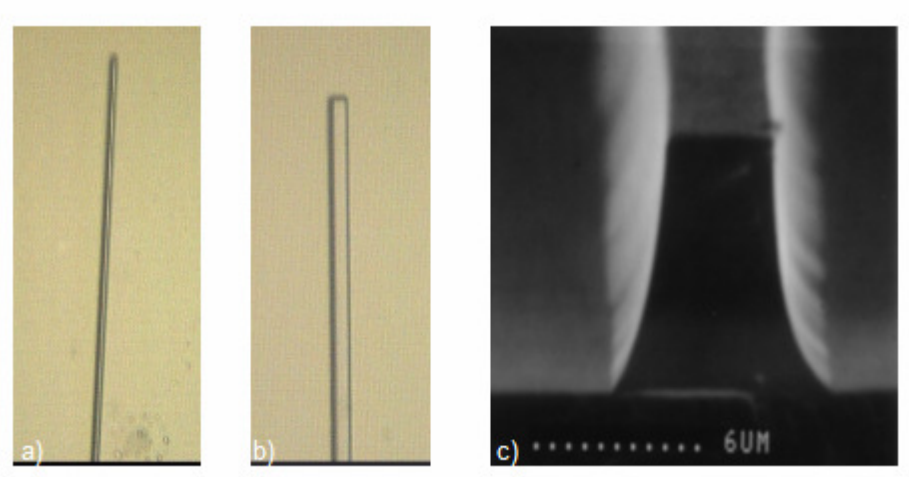

Figure 2.28 - Microchannels made of 4 layers of photoresist PFR 7790G 27cP. a) Microchannel with a width of 5 µm. b) Microchannel with a width of 10 µm. c) SEM photograph showing the profile of a microchannel.

Looking at the figure 2.28c) we can see that the sidewalls were not completely vertical possibly due to an underexposure of the PR lower layers. However, for the goals of the present project it was not absolutely essential to obtain perfectly defined walls, and therefore this methodology was implemented to fabricate the final master mold.

The only critical step of this method that was needed more care was the development phase because its time was adjusted for only one layer of the PR and therefore, to avoid the loss of some small structures the development was carried out in small steps.

The drawback of this new method was the fact that the mold was less resistant when compared to the master mold made of SU-8. Some tests were made to find out how many channels broke after peeling the PDMS off. The first master mold fabricated, after 8 uses presented 18,8% of broken cannels. The method of peeling the PDMS off was optimised in order to apply the least amount of force possible. Using this approach the maximum percentage of broken channels per mold, after 8 uses, was 10%.

2.3.6 General considerations about the microfluidic device

During the present work, the microfluidic device was undergoing changes according to the aims proposed (see section **2.2.4**). Figure 2.29 shows the evolution of the master mold and its PDMS microfluidic device:

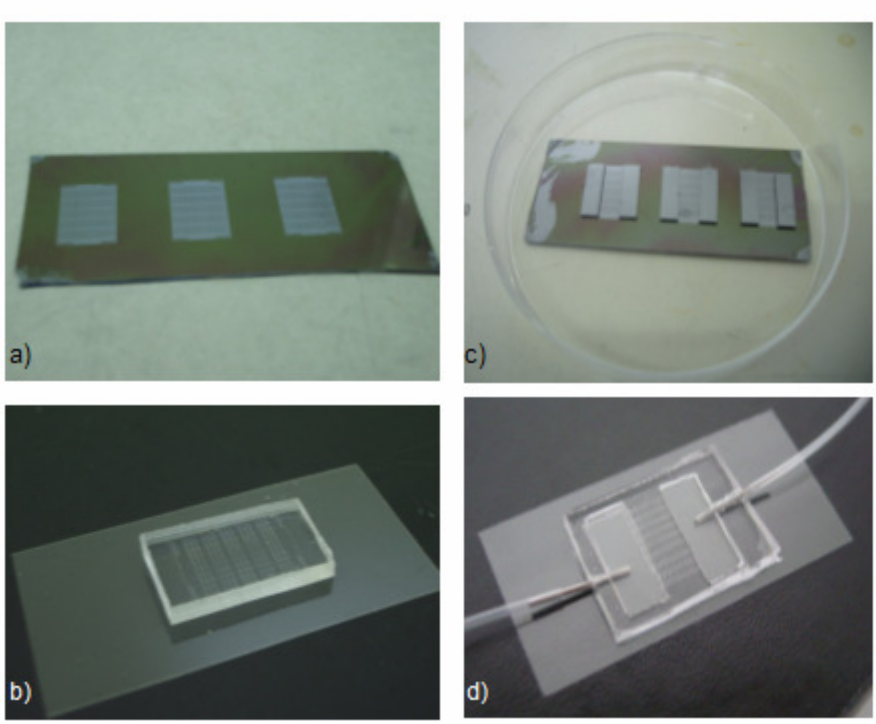

Figure 2.29 - Evolution of the master mold and the microfluidic device. a) Master mold only with microchannels and b) its microfluidic device. c) Final master mold with reservoirs made of rectangular pieces of silicon and d) its microfluidic device with external tubage.

As described in section **2.2.4**, rectangular pieces of silicon were used to act the mold for the inlet and outlet reservoirs. Ideally, the device should have been done all integrated by soft lithography including the reservoirs. However, using the methodology of mold fabrication described in **2.2.1.5.** it was not possible to achieve a photoresist thickness greater than 6 microns and thus, to obtain reservoirs with a significant capacity, the area of these ones had to be very high. As it was said before, using reservoirs with great areas when compared to the height, PDMS sag and close off the fluidic channels when in contact with the glass substrate. It was described in the literature [27] that to avoid the collapse of the reservoirs, one could add some support structures (pillars) uniformly distributed along the reservoirs. However, the capacity of the reservoirs would decrease significantly and for the aim of this project this situation would be disadvantageous.

Another possibility to fabricate the master mold with the reservoirs already included could be the use of photoresists (mainly SU-8) with different standard viscosities to have multi-height structures in the master mold according to the applications desired [23,40]. However, this methodology was much more complex and the photoresist used to fabricate the mold in this project (PFR 7790G 27cP) was only available in INESC MN in one standard viscosity.

Using the methodology developed in the present project to do the mold for the reservoirs, they have much higher capacity when compared to reservoirs made of any photoresist due to the higher thickness. This capacity could also be increased/decreased by simply changing the

dimensions of the silicon pieces used to make the reservoirs.

Usually, in microfluidic devices the reservoir holes were simply punched through the PDMS using sharpened needles, thereby such reservoirs would be open to the atmosphere [23,31,37,40]. Using the methodology developed in this project to make the mold for the reservoirs, the device has close reservoirs avoiding any cell contamination. Furthermore, a fully closed microfluidic device is also very important in cells experiments because it allows a completely controlled environment. The major advantage of this microfluidic device, together with the tubes that constitute the external fluidic system, is the capability of making a vacuum inside it, which force the fluid/cells to enter the microchannels.

Despite the fact that the new methodology to fabricate the master mold developed in this project was very efficient for the goals of this work, it could have some disadvantages that incapacitate its use for more specific and complex patterns. For example, channels with small lengths (≤1000 μm) could be difficult to obtain due to the proximity of the silicon reservoirs and therefore one has to be very careful when peeling the PDMS over the mold. For more specific applications, some experiments could require microchannels with an exact length and using the method developed in this project, the alignment of the Si reservoirs had to be forcibly performed using a microscope to ensure the perfect alignment.

In terms of the design of the microfluidic device, with microchannels alongside two reservoirs, it is very difficult to guarantee that all the channels were hydrophilic after Corona Discharge because this treatment was made on the reservoirs and not channel by channel and thus it was difficult to ensure that corona treatment covered all the channels. Initially, when we were testing the optimal width of the channels, it was very clear the rays of the Corona Discharge entering the microchannels with widths up to 50 μm. However, with channels with a range of widths between 10 and 5 μm it is impossible to see this phenomenon.

3 Yeast cell experiments

Saccharomyces cerevisiae yeast cells were used in this project to test the effectiveness of the microfluidic device to analyse single cells. In section **3.1** we will refer the different strains used in this project and the cell growth conditions. Section **3.2** will be dedicated to the description of the methodologies used to study some basic aspects in the cell behaviour. The methodology employed to introduce the cells within microchannels will be described as well as their growth inside such structures and αsyn-GFP protein expression with Galactose. Finally in section **3.3** several results will be presented and discussed. Some approaches related to the temperature control in cell experiments will be discussed as an outlook for future work.

3.1 *Materials*

The yeast cells used in this project were provided by the group of Dr. Tiago Outeiro at the IMM (Instituto de Medicina Molecular). Since the process of yeast transformations is outside the scope of this project, in the following paragragraphs just a brief description of the method will be given. For more detailed information see **ANNEX 1.**

3.1.1 Strains and Plasmids

Transformations of yeast were carried out using the standard lithium acetate procedure (Annex 1). This process was performed in order to introduce in *Saccharomyces cerevisiae* strain W303.1A (*MAT***a;** *can1-100; his3-11 15; leu2-3 112; trp1-1; ura3-1; ade2-1*) [63] two 2μ multicopy plasmids, one with GFP-αSyn fusion protein under the control of a galactose-inducible promoter and the other with a RFP protein under the control of a methionine-repressible promoter. According to their auxotrophies, cells carrying 2μ plasmids were grown in synthetic medium (2% Glucose and 0,67% yeast nitrogen base without amino acids) lacking uracil and leucin for plasmid selection.

Another strain was also used, VSY72 (a kind gift from Vicente Sancenon, Gladstone Institute of Neurological Disease, San Francisco, USA) made in the W303.1A background and has the following genotype: *MAT***a;** *can1-100; his3-11 15; leu2-3 112; ade2-1; GAL1pr-SNCA*(WT)-*GFP::URA3; GAL1pr-SNCA*(WT)-*GFP::TRP1.* On this strain two copies of the SNCA (WT), that encodes α-Syn, were inserted directly in the genome, and these genes encode αSyn-GFP fusion protein, jointly with two other genes: URA3 and TRP1, under the control of *GAL* inducible promotor. In this case, this strain is auxotrophic for hystidin, leucin and adenin.

3.1.2 Growth Conditions and Media

Before starting with the experiments, yeast strains were pre-grown for 24 hours at 30 ºC in raffinose medium. Raffinose was used as a carbon source, at the place of glucose, so that the cells could adapt to galactose. Both galactose and raffinose are secondary sources and therefore needed to induce carbon limitation responses.

The cells used in the experiments were in the exponential phase and concentrated to a final OD_{600} of approximately 3.4 by short centrifugation. Before loading the cells into the device a vigorous vortex was made.

3.2 *Methods*

3.2.1 Introduction of the cells into microchannels

Since the microfluidic channels have a width very similar to the size of the cells they did not enter through the channels only by capillarity. Therefore, a similar process like the one described in **2.2.5** to force the water to enter the microchannels (vacuum step), was performed.

Before introducing the cells in the reservoirs, they were previously emptied due to the fact that they were full of water to avoid PDMS hydrophobic recovery. The solution with the cells was then introduced through the inlet reservoir and a vacuum was applied through the outlet (connecting one 1 ml syringe with the polyethylene tube and pulling carefully the plunger) to force the cells to flow along the channels. A syringe pump could also be used to control the flow rate because if the vacuum is too strong, cells will accumulate at the entrance of the channels stopping other cells to enter the channels. After cell insertion, the presence of cells in the channels was verified using the optical microscope to verify their distribution along the channel.

3.2.2 Cell growth within microchannels

To compare the growth rate of yeast cells within microchannels and in traditional *macro* cultures, the cells were introduced in the microfluidic channels by following the procedure described in 3.2.1.1. A few cells in different channels were selected and their positions registered (with the help of the *ruler*) in order to visualize their growth over time.

Two different experiments were performed with the two different yeast strains available. In the first experiment, we used cells carrying two 2μ plasmids (W303.1A). Images were acquired every 1.5 hours for 3 hours. After acquiring such images, the device was placed over a heated aluminium plate at 30ºC until the time new images were acquired. In the other experiment, cells carrying two copies of the αSyn-GFP fusion protein inserted in the genome were used (VSY72).

Cells were grown overnight in an incubator, at 30ºC, and were only visualized after 18 hours.

3.2.3 αsyn-GFP/GFP-αsyn expression induction with Galactose

In this section the two yeast strains available, W303.1A and VSY72, were used in order to visualize the expression levels of αSyn-GFP fusion protein (GFP-αSyn in the case of the strain W303.1A) and RFP protein when stimulated with galactose inducer. It is necessary to recall that these proteins were under the control of a galactose-inducible promotor and methionine-repressible promoter, respectively. Thus, since the cells were grown without galactose or methionine, it was expected that in the case of the strain W303.1A cells would express only the red protein (RFP) and in the strain VSY72, they would not express any protein.

The expression of αSyn-GFP/GFP-αSyn fusion protein was induced in galactose medium. Cells were previously centrifuged and resuspended in galactose (1%) medium. Immediately after resuspension, the cells were inserted in the microfluidic device using a 1 ml syringe. The method previously described in point **3.2.1.1** was used to force the cells to flow through the microchannels. The device was positioned on the stage of the microscope, and some cells in different channels were selected in order to study the protein expression levels along time. The location of the cells during different times was monitored using the *ruler* near the channels which allows the rapid recognition of such cells. Cells were then imaged with a Axiovert 200 model inverted microscope from Zeiss equipped with a digital camera Axiocam MRm from Zeiss every 1.5 hours for 3 hours in the case of the strain W303.1A and for 4.5 hours in the case of the strain VSY72. GFP has an excitation wavelength of 484 nm and a 510 nm emission wavelength and RFP has an excitation wavelength of 557 nm and a 585 nm emission wavelength. The microscope was equipped with GFP and RFP filters. The microscope images were 63x magnifications. Images were analyzed using ImageJ program. For each image, the fluorescence intensity was measured and the background was subtracted.

3.3 *Results and Discussion*

3.3.1 Introduction of the cells into microchannels and optimization of the Optical Density

After the preliminary cell experiments had been carried out (see section **2.2.4**), it was possible to conclude that the phenomenon of capillarity was not sufficient for the cells to go through the channels and they remained at the beginning of the channels.

The microfluidic device was improved in such a way that the cells were forced to enter the channels by vacuum. Initially a very strong vacuum was made using one 1mL syringe and the cells accumulated at the beginning of the microchannels as shown in Figure 3.1. Afterwards, the vacuum was made very carefully (pulling on the plunger carefully just one time) to avoid cells accumulation.

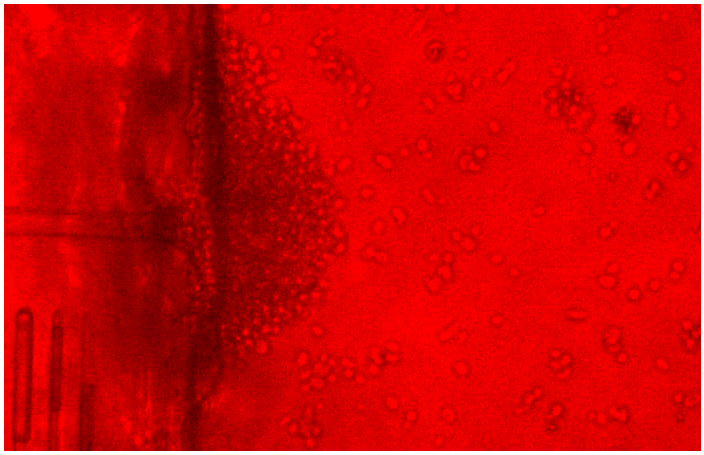

Figure 3.1 - Cluster of cells accumulated at the entrance of a microchannel.

Despite the cluster of yeast cells at the entrance of the channels not being beneficial for this work, because avoid other cells flowing through the microchannels, the vacuum step in the reservoir opposite the reservoir where the cells were, could be very important to other experiments for example to concentrate the cells in a specific place without the need for any electric field.

After improving the methodology of introduction the cells in the microchannels, the main challenge was to find the optimal optical density (OD) in which the cells entered the microchannels and stayed as sparse as possible. Firstly, an OD_{600} around 10 tested. After applied vacuum to force the cells to go through the channels in many of them the results were similar to the shown in figure 3.2.

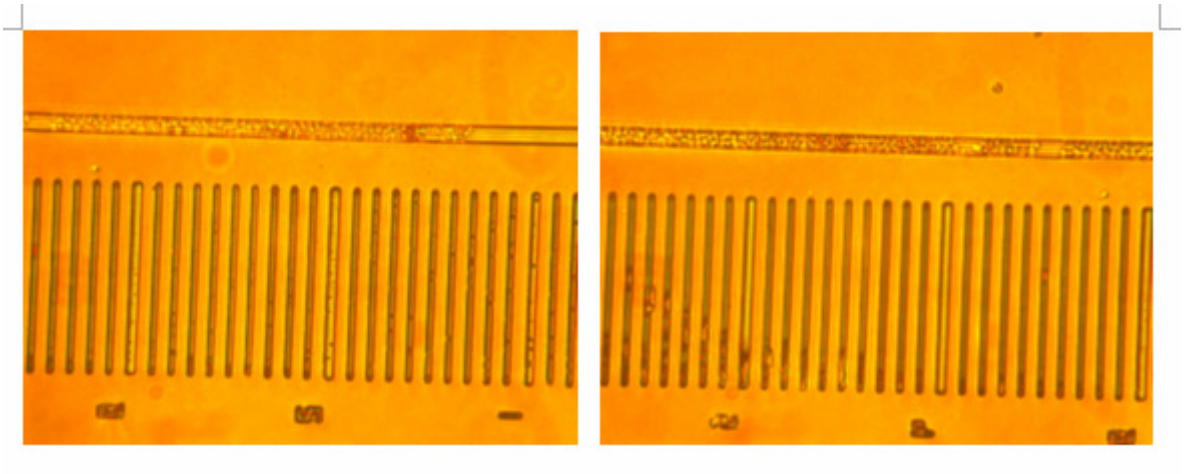

Figure 3.2 - Clusters of yeast cells inside a microchannel with 5 µm wide.

For the purpose of this project, yeast cells should be visualized individually in order to identify them over time. Looking at figure 3.2, it was clear that the OD should be much smaller and thus several tests were performed to find the optimal range of OD values. It was difficult to achieve an optimal OD value for the cells because when they were to concentrate a large quantity entered the channels. On the other hand, if the optical density was too low, the probability that the cells went through the channels would be much smaller. In all the further experiments we worked with an OD_{600} of approximately 3.4 (Figure 3.3).

Since the cells came into the channels in big clusters, which made their movement along such channels difficult, before introducing the cells into the device a vigorous vortex was applied to separate them from each other.

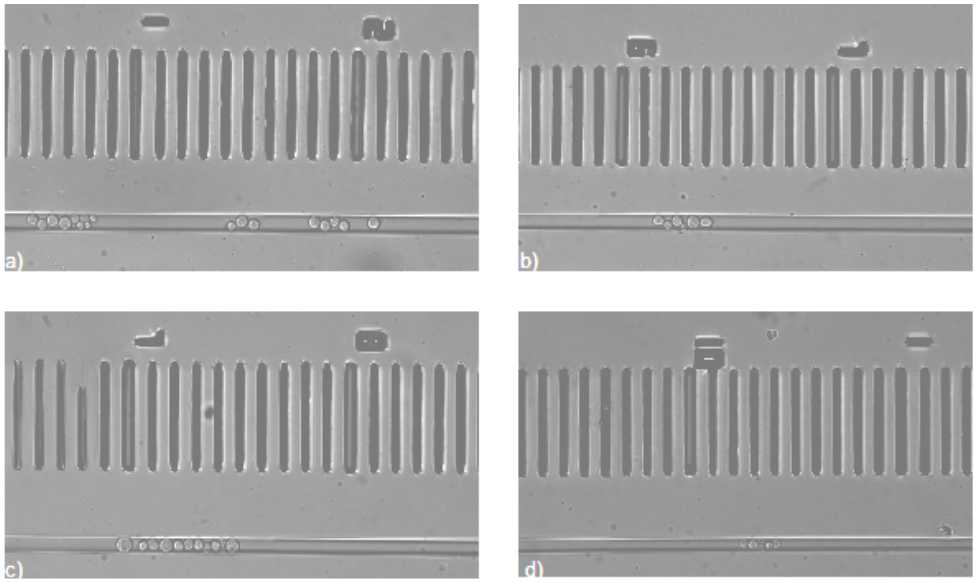

Figure 3.3 - Yeast cells inside microchannels with an OD_{600} of 3.4 and after a vigorous vortex.

3.3.2 Approaches to identify a particular cell over long periods

For experiments involving the visualization of individual cells over long periods, the *ruler* made close to each channel (see section **2.2.4**) proved to be a very efficient way to localize the cells. In all the cell experiments performed in this project, a few channels were selected according to the best cell distribution (and their location registered), and images of the cells inside these channels were acquired over long periods, therefore, the *ruler* was essential to allow the quick recognition of a particular cell in a particular channel. Despite the effectiveness of the ruler to identify the same cell over long periods, some cells were weakly adherent to the glass substrate and therefore during the time of the experiments some of them changed their positions and it was difficult to localize them again.

Researchers have been very inventive in developing mechanical obstacles or barriers to sieve a particular object from a fluid suspension by providing a passage for the fluidic only [27]. This hydrodynamic trapping has the advantages that cell immobilization is rapid compared with chemical trapping and that the devices are often simple and inexpensive.

Although the microfluidic channels made in this project work as traps due to their small widths, a simple approach was performed to test the efficiency of a simple trap. A new mold was fabricated in which one group of channels presented small traps along the channels in order to narrow them in particular places like it was shown in Figure 3.4.

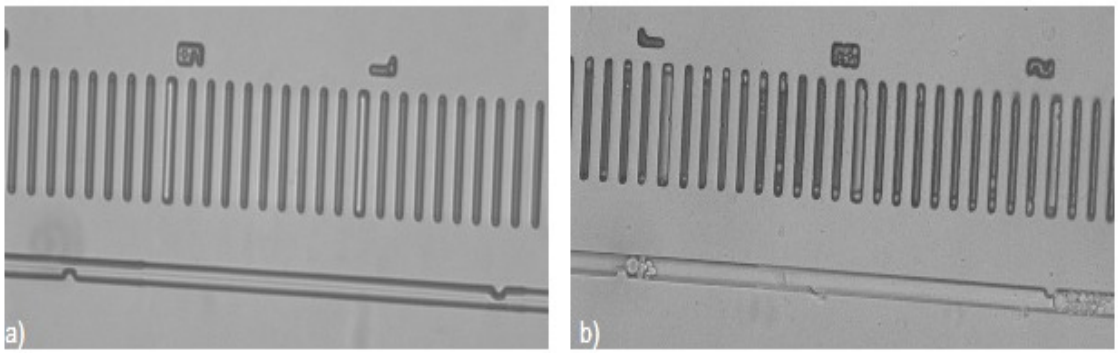

Figure 3.4 - Hydrodynamic traps. a) Microchannel with 2 traps. b) Yeast cells trapped inside a microchannel**.**

This simple method had shown to be efficient to trap cells, however one has to be more careful when working with these particular microchannels because if a cluster of cells get stuck in the first trap, no more cells could enter the channels and they start to accumulate at the beginning of this channel. Because this method was done at the end of the project, there was no time to improve such methodology.

3.3.3 Cells growth within microchannels

Some experiments were performed to visualize cells growth within the microchannels. To facilitate the counting of the cells, individual or a small number of cells were selected to observe them along time (see Figure 3.5). The division time of wild type cells is about 120 minutes (in minimum medium) in traditional culture flasks (S. Tenreiro, personal communication).

The first cell growth experiment (described in section **3.2.2**), in which the cells were carrying 2μ plasmids, was only performed in the visible mode because we intend only to visualize the cells growth within microchannels and not the expression levels of the fluorescent proteins. Furthermore, since cells were in raffinose medium, they were not expressing GFP-αSyn protein (because this protein is under the control of a galactose-inducible promoter) and thus it was not relevant to visualize them in fluorescence mode.

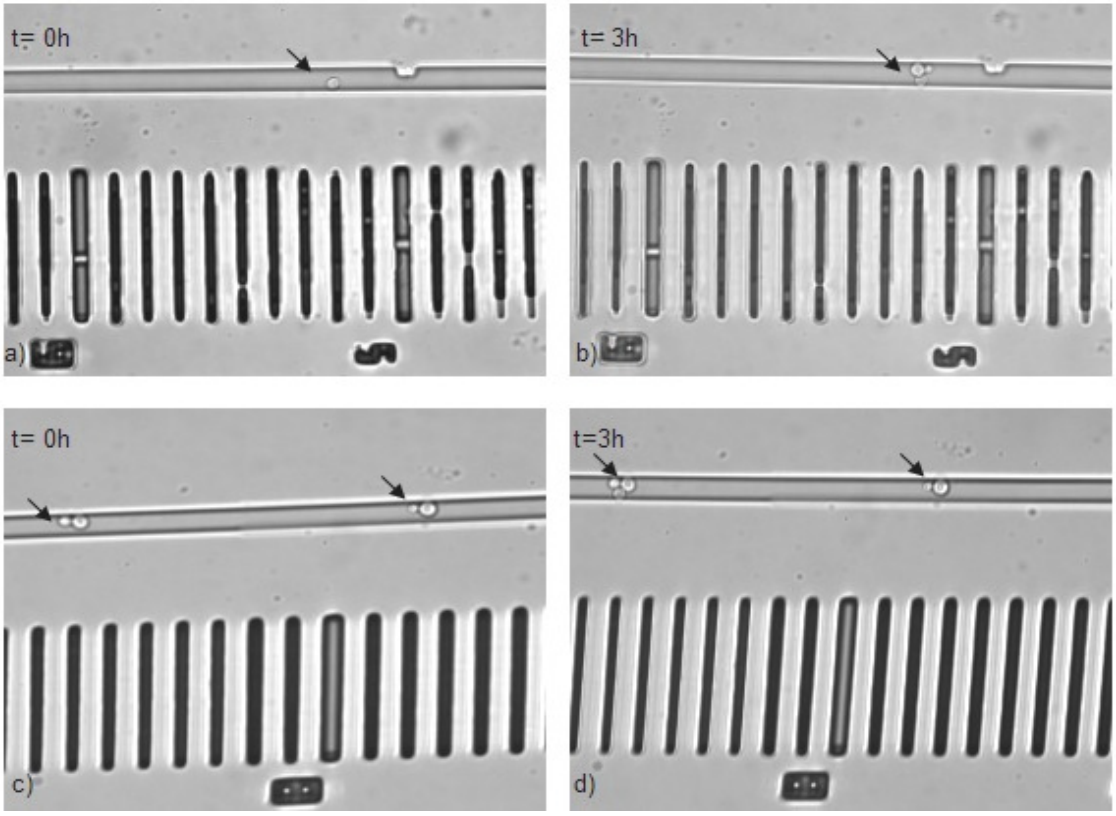

Figure 3.5 - Yeast W303.1A cells growth within microchannels. Individual cells were selected (a) and c)) and the same cells were visualized after 3 hours respectively in (b) and d)).

After three hours of experiment, it was found that yeast cells divided once, twice or even did not divide at all. These results were somewhat according to the expectations because all the cells were in different stages of growth and thus it was not expected that they divided all at the same time that is to say in a synchronized way. Besides that, individual cells present different cellular rhythms that could also explain such variability on division time.

Compared to traditional cell cultures, in microfluidic platforms we were able to visualize

relatively small number of cells, however, because a group of cells can more easily maintain a local environment within microchannels than in *macroscale* culture flasks, cells can grow significantly slower in microchannels [20,64].

The same experiment was performed to visualize cells growth within the microchannels but this time the cells used were the ones with two copies of the genes that encode α-syn-GFP fusion protein inserted in the genome (strain VSY72), to compare the division times between this strain and wild type cells. Cells were grown in galactose medium to express α-syn-GFP protein to see if they express this protein at the same intensity in cells genetically identical. Some cells were previously selected along different channels and afterwards the device was placed in an incubator at 30ºC overnight (Figure 3.6 and 3.7).

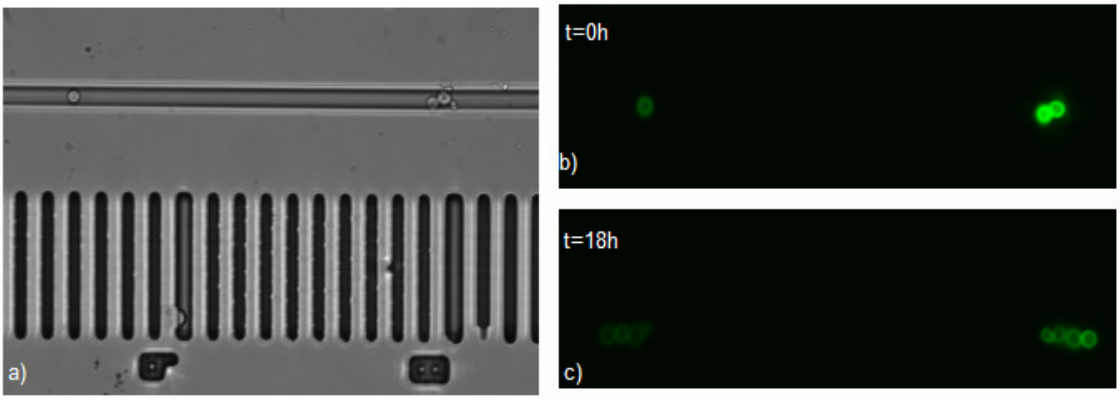

Figure 3.6 - Yeast VSY72 cell growth within microchannels expressing α–syn-GFP fusion protein. a) Visible micrograph of cells previously selected within microchannels at t=0h. b) Fluorescence micrographs of the same cells at t=0h and c) t=18h.

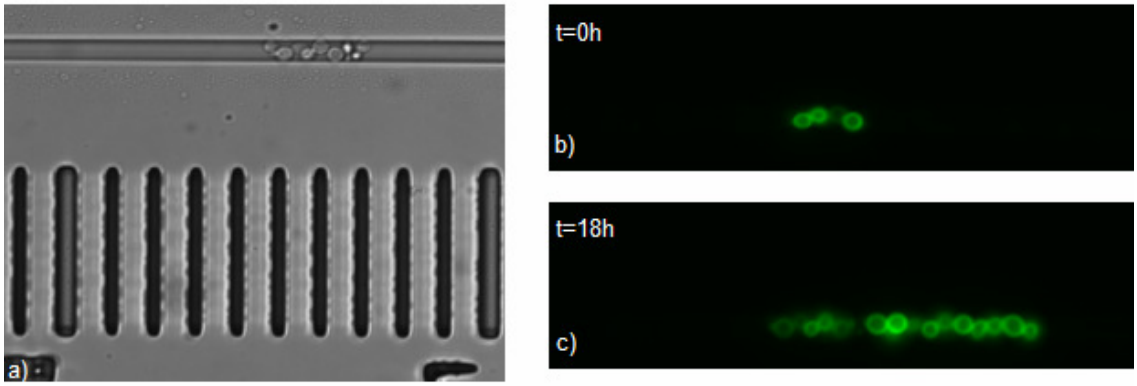

Figure 3.7 - Yeast VSY72 cell growth within microchannels expressing α-syn-GFP fusion protein. a) Visible micrograph of cells previously selected within microchannels at t=0h. b) Fluorescence micrographs of the same cells at t=0h and c) t=18h.

Before examining the division time of the cells it is important to observe that α-syn-GFP is clearly located in the plasma membrane in all the cells (Figure 3.6 and 3.7) after 18 hours of incubation which led us to conclude that the cells were viable inside microchannels and were constantly induced by galactose medium. This and other assays helped us to prove the

effectiveness of the microchannels as an appropriate environment for the study of single cells.

The generation time (based in cell number counting before and after 18 hours of incubation at 30ºC) is around 4.5 hours, a value that is in agreement with previous experiments carried out in IMM (in traditional cultures flasks) revealing that the division time of such cells was approximately five hours. Accordingly, we verified that when overexpressed (two copies), α–syn inhibited growth if we compare to the division time of wild-type cells. The inhibition of growth when α–syn is overexpressed may be evidence of the toxicity of this protein, as observed before by Outeiro and Lindquist [53]. One aspect that is also interesting is the similarity in phenotypic terms among cells genetically identical (Figure 3.7), as it was expected.

This type of studies, when we intend to observe the successive generations of a particular cell, is an added value of this type of microfluidic devices since we were able to visualize several individual cells along different channels for long periods in the same experiment. In *macrocultures,* this kind of studies was only possible to perform if we have a couple of cells in the same field since it is not possible to change it because it would be very difficult to localize the same cells again.

3.3.4 The importance of the temperature control in biological studies

When a certain device is being developed for biological studies, it is very important to recall that all biological species have an optimal temperature range in which they grow best. Particularly, the optimal temperature of *S. Cerevisiae* is about 30 ºC. Therefore, the microfluidic setup should have incorporated a system to control temperature with high precision within microchannel environments.

As it has already been referred, in the experiment involving cells growth (**3.3.3**), the microfluidic device was placed on a heated aluminium plate or in an incubator at 30ºC. However, the first method has a drawback which is the fact that during microscope visualization the microfluidic device could not be over the hot plate and thus the device temperature was not kept constant during the time of the experiment. In the second method, the device was placed in a incubator overnight and thus it was not subject to temperature variations. However, for more accurate studies, when it is necessary to visualize cells in small periods of time, this methodology would not be advantageous.

Approaches to accurate temperature control within microfluidic systems have been varied. Some examples will be given with the aim of integrating such systems, or similar approaches, over the long term in our microfluidic devices for biological applications.

Charvin and co-workers [28] found a way to regulate the temperature during the experiments: the whole microfluidic setup was clamped onto a heated aluminium alloy stage using screws

attached to an aluminium top and thus heating the stage as well as the objective using thermoelectric modules ensuring a constant temperature (see Figure 3.8a)).

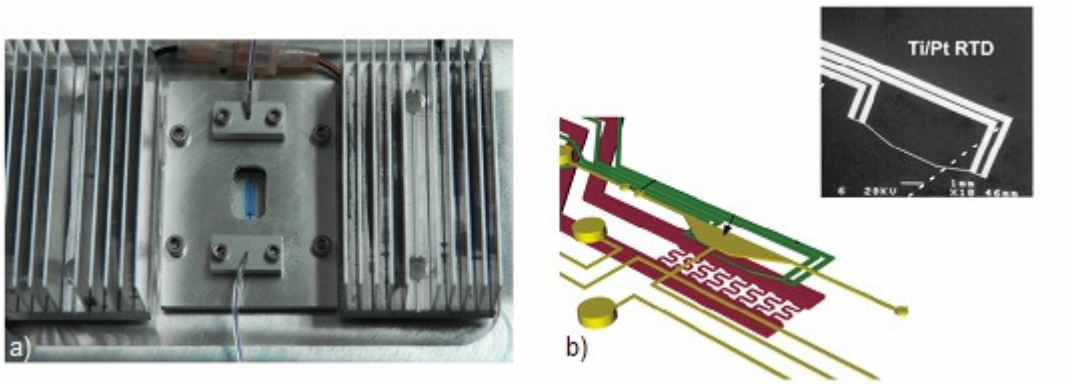

Figure 3.8 - Examples of experimental setups to control the temperature in microfluidic devices. a) Heated aluminium alloy stage using thermoelectric modules in which the microfluidic device was clamped [28]. b) Microfabricated heating elelments made of Ti/Pt [65].

Lagally and colleagues [65] reported the integration of microfabricated heaters and resistance temperature detectors in PCR microsystems that improves the heating and cooling rates, and increase the accuracy of the temperature measurements. The heating elements are a parallel serpentine design and are made of Ti/Pt and are placed parallel to the PCR chamber to facilitate the temperature measurements in the thermal place of interest (Figure 3.8b)).

3.3.5 αsyn-GFP/GFP- αsyn expression induction with Galactose

The expression of α–syn was induced in galactose both in the strains W303.1A and VSY72. The first experiment (using the strain W303.1A) was carried out for three hours and, as already been described in **3.2.3**, some cells in different microchannels were selected (with the help of the ruler) and images of such cells were acquired every 1,5 hours. Selected results are shown in Figures 3.9, 3.10 and 3.11.

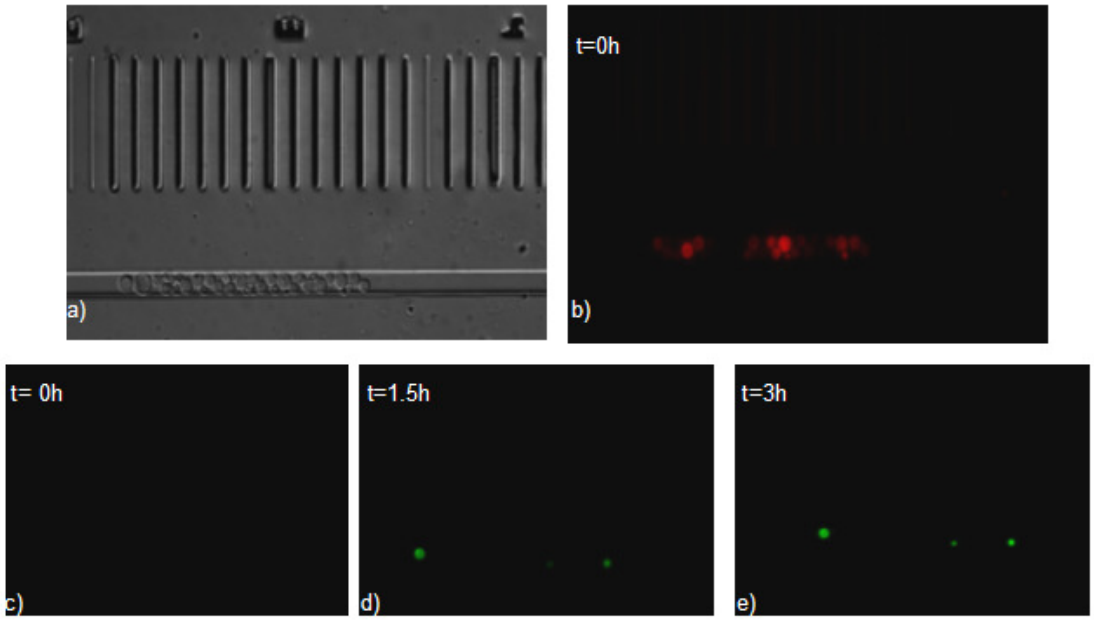

Figure 3.9 – Yeast W303.1A expression levels of RFP and GFP-αsyn proteins within microchannels. a) Visible micrograph of cells previously selected within microchannels at t=0h.b) Fluorescence microscopy of cells expressing RFP protein at t=0h. c) Fluorescence micrographs of yeast cells expressing GFP-αsyn protein at t=0h d) 1.5h and e) 3h after galactose induction.

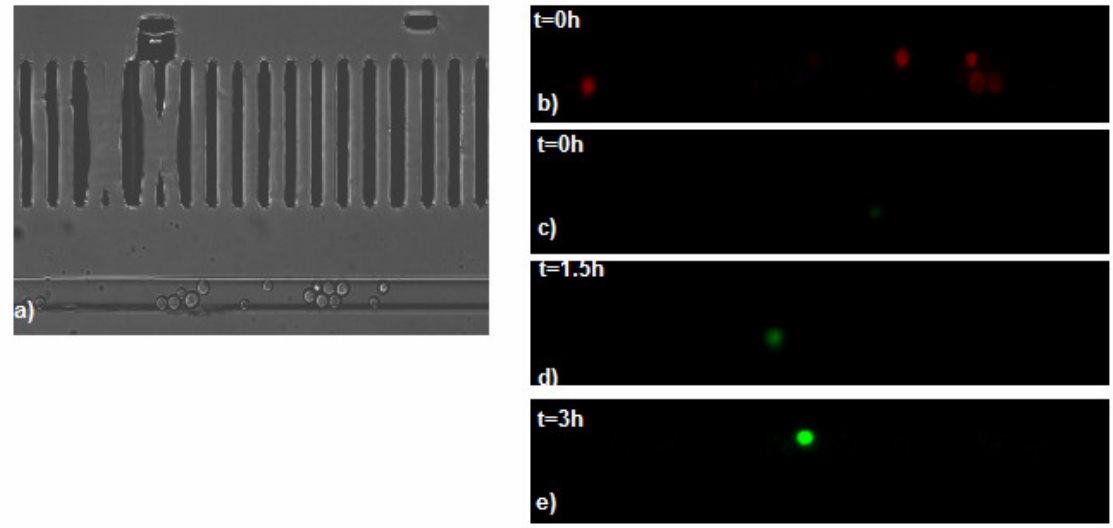

Figure 3.10 - Yeast W303.1A expression levels of RFP and GFP-αsyn proteins within microchannels a) Visible micrograph of cells previously selected within microchannels at t=0h.b) Fluorescence microscopy of cells expressing RFP protein at t=0h. c) Fluorescence micrographs of yeast cells expressing GFP-αsyn protein at t=0h d) 1.5h and e) 3h after galactose induction.

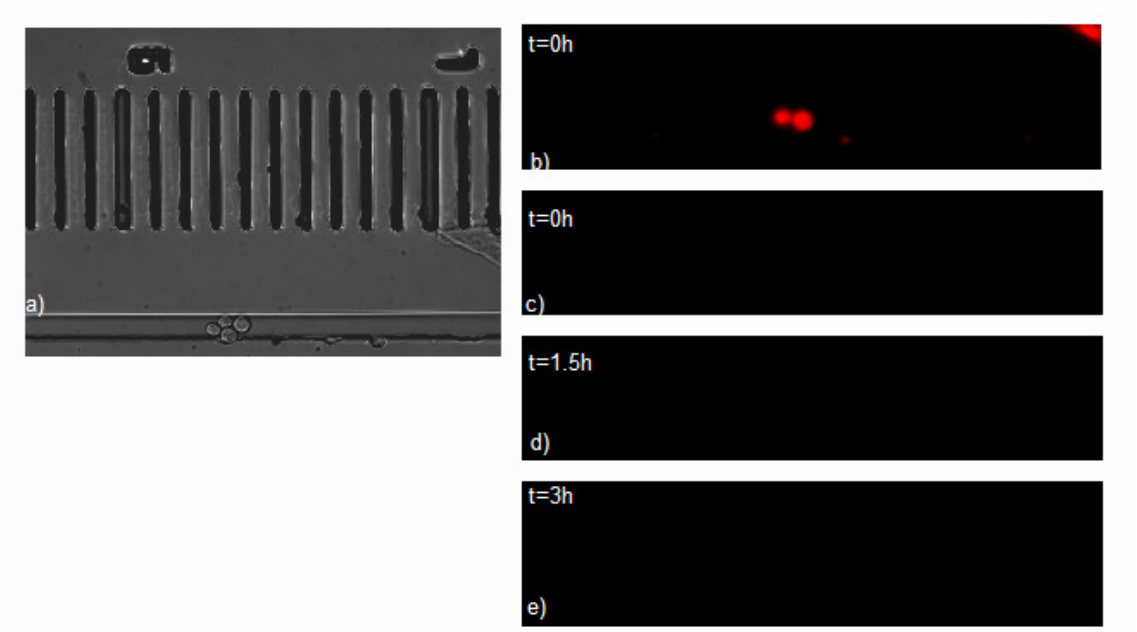

Figure 3.11 - Yeast W303.1A expression levels of RFP and GFP-αsyn proteins within microchannels a) Visible micrograph of cells previously selected within microchannels at t=0h.b) Fluorescence microscopy of cells expressing RFP protein at t=0h. c) Fluorescence micrographs of yeast cells expressing GFP-αsyn protein at t=0h d) 1.5h and e) 3h after galactose induction.

Looking at the previous figures one can immediately verify the heterogeneity of the results obtained. Starting with the analysis of the RFP protein, we can conclude that in the absence of methionine the cells express this protein as it was expected. However, RFP expression levels varied between individual cells. Gene expression is already known to vary stochastically between individual cells [66,67]. The reactions underlying gene expression involve small numbers of molecules (e.g., transcription factors, DNA, and mRNAs) and may therefore exhibit stochastic fluctuations that could generate population variation when phenotypic diversity would be advantageous.

As it was referred previously, W303.1A cells were carrying two 2μ plasmids, one with GFP-αsyn fusion protein and the other with a RFP protein. The type of transformation based on plasmids, instead of the integration into the genome, could explain in part the variability of the expression levels between individual cells since the copy number per cell could vary over a population of cells and therefore the expression levels of the proteins could also be different. To eliminate this variability, some experiments with cells carrying two copies of α-syn-GFP inserted directly in the genome (strain VSY72) were performed to compare the variability of expression levels among individual cells inside microchannels.

To serve as control for the experiments in the microfluidic device, cells were previously visualized in a glass slide to confirm the effectiveness of the galactose in the induction of the α-syn-GFP protein (Figure 3.12).

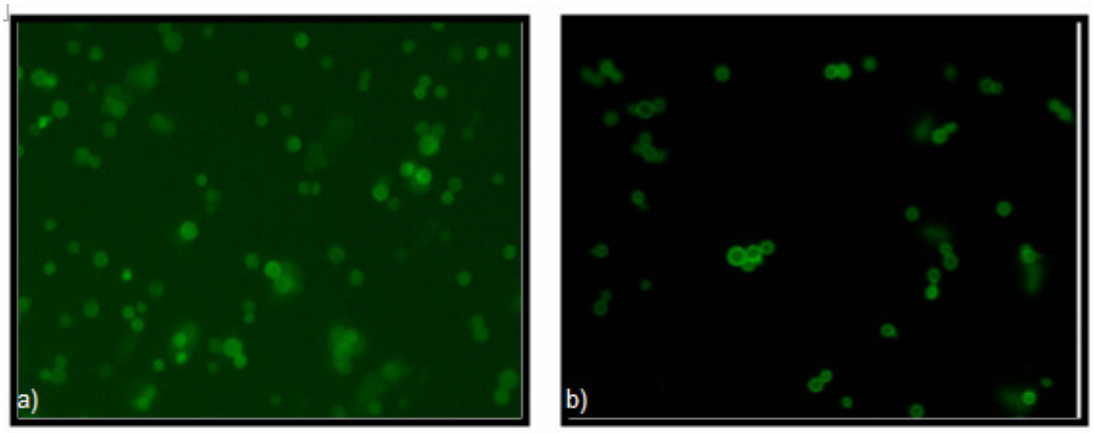

Figure 3.12 - Fluorescence microscopy of *S. cerevisiae* VSY72 cells expressing a α-syn-GFP fusion protein under the control of *GAL1* promoter, grown in a) raffinose (negative control of α-syn-GFP fusion protein expression) or in b) galactose medium (positive control of α-syn-GFP induction by galactose).

The yeast cells carrying two copies of α-syn-GFP inserted in the genome were previously visualized in raffinose medium as a negative control (Figure 3.12 a)). The fluorescence observed did not come from the αSyn-GFP because the intrinsic fluorescence is diffuse and it was not located in the plasma membrane as it was possible to see in galactose medium (Figure 3.12b).

Within the microchannels the results were shown in figures 3.13 and 3.15.

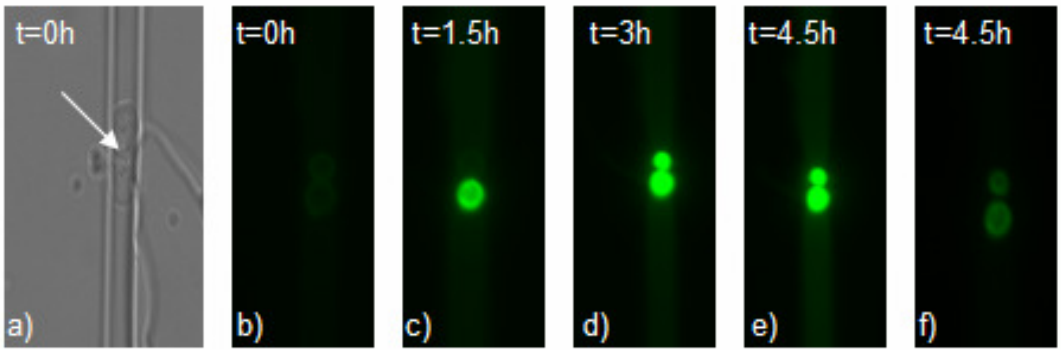

Figure 3.13 - Expression levels of α-syn-GFP protein in VSY72 yeast cells within a microchannel (width= 6μm) when subject to galactose induction. a) Visible micrograph of cells previously selected within a microchannel at t=0h.b) Fluorescence microscopy of cells at t=0h, c) t= 1.5h d) t= 3h and e) t= 4.5h with an exposure time of 114ms. f) Fluorescence microscopy of cells at t=4.5h with an exposure time of 23ms with the aim of locating the source of fluorescence inside the cells.

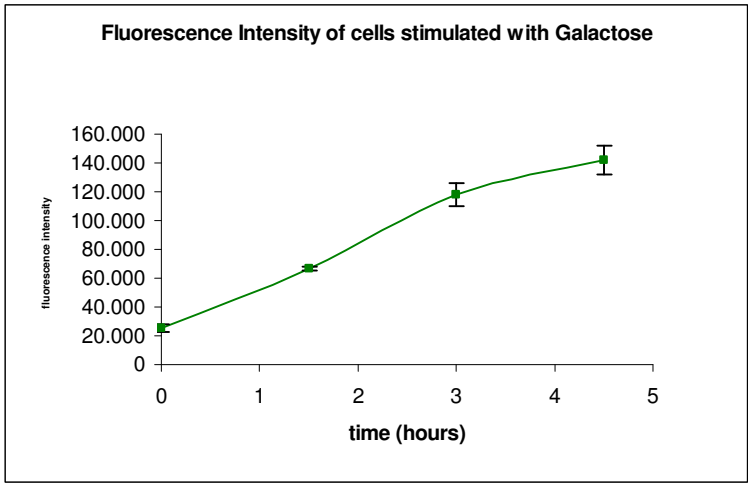

Figure 3.14 - Chart showing the evolution of the fluorescence intensity of α-syn-GFP fusion protein of the VSY72 cells of Figure 3.23 along time when induced by the galactose inducer Fluorescence measurements were obtained with ImageJ software.

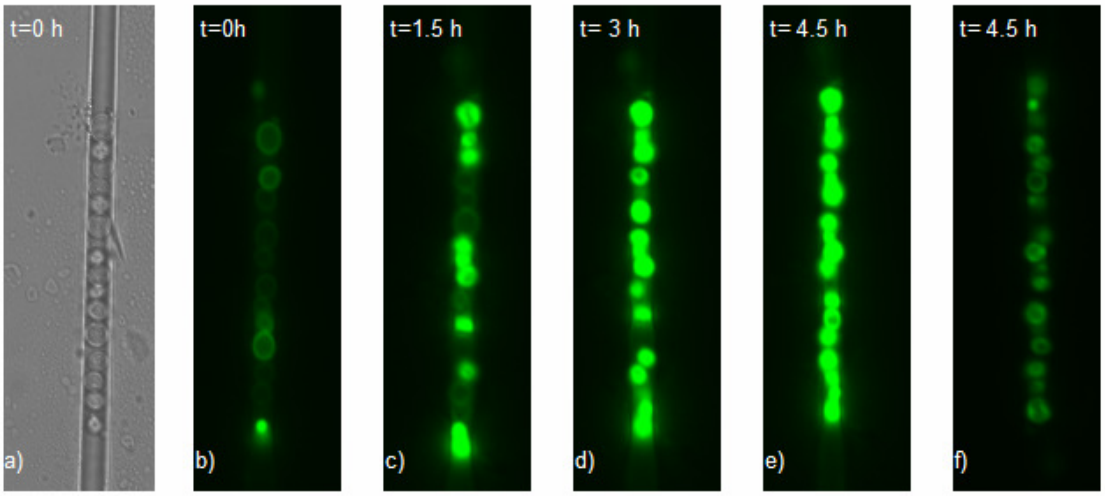

Figure 3.15 - Expression levels of α-syn-GFP protein in VSY72 cells within a microchannel (width= 5µm) when subject to galactose induction. a) Visible micrograph of cells previously selected within a microchannel at t=0h.b) Fluorescence micrographs of cells at t=0h, c) t= 1.5h d) t= 3h and e) t= 4.5h with an exposure time of 194ms. f) Fluorescence microscopy of cells at t=4.5h with an exposure time of 87ms with the aim of locating the source of fluorescence inside the cells.

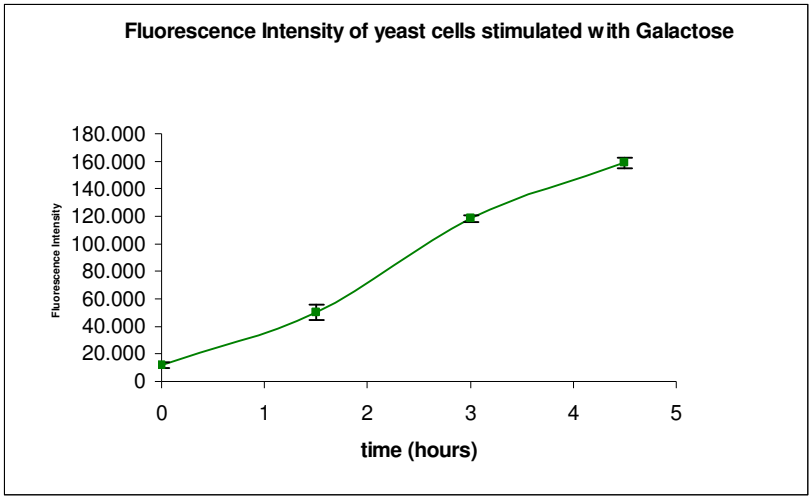

Figure 3.16 - Chart showing the evolution of the fluorescence intensity of αSyn-GFP fusion protein of the cells of Figure 3.25 along time when induced by the galactose inducer. Fluorescence measurements were obtained with ImageJ software.

From figures 3.13 and 3.15 we can clearly see that at *time zero* some cells have already started to express α-syn-GFP in the plasma membrane but in reduced levels. The expression increased gradually and after 4.5 hours all the cells expressed this protein almost at the same intensity. The expression levels are so high that it was difficult to localize the origin of such fluorescence inside the cells using the same exposure time as at t=0h. For this reason, at 4.5 hours another image was acquired but with a lower exposure time, to confirm that the fluorescence was located in the plasma membrane (Figure 3.13f) and 3.15f)). The increase in fluorescence over 4.5 hours could be quantitatively analysed by the charts in figures 3.14 and 3.16. In both charts it is possible to verify that the fluorescence intensity increased almost linearly in relation to the galactose exposure time.

Comparing the previous results to those referred to the cells carrying GFP-αSyn in a 2μ plasmid, we can immediately verify the difference in terms of protein expression variability. All the cells that have two copies of αSyn-GFP protein in the genome presented a very similar level of fluorescence intensity that did not happen in the cells carrying 2μ plasmids. Therefore, we can conclude that for future studies involving the comparison of the expression levels of such protein when subject to a certain molecular gradient, the insertion in the genome is a better choice since the variability factor associated with the plasmid maintenance and copy number per cell is eliminated.

4 Generation of a Stable Gradient inside the channels

A wide range of chemical and biological phenomena are influenced by gradients of molecular species. One of the main goals of this project was the establishment of a steady-state gradient in the microchannels so that in the medium term it would be possible to visualize the effect this molecular gradient on the protein expression levels over time.

This chapter will be dedicated to the description of the methodology applied to generate a stable gradient in the microfluidic device platform developed in this project. In section **4.1** the experimental setup for such purpose will be presented as well as the methodology used to create a gradient inside microchannels over long periods. Results will be shown and discussed in section **4.2**.

4.1 *Materials and Methods*

The basic design of the microfluidic device developed in this project consists of two reservoirs with the same capacity connected by a number of microchannels. The dimensions of the microchannels were significantly smaller (6 µm high and 5-10 µm wide) than the reservoirs (700 µm high and 15 mm wide). Due to this size difference, we expected that the fluidic resistance in the microchannels would be much higher than that of the reservoirs, thus minimizing the likelihood of convection through the microchannels. Diffusion would thus be the predominant mode of transport across the microchannels. When a molecular species is introduced in one of the reservoirs and buffer in the other, molecules diffuse across the microchannels to the place of lower concentration, and generate a gradient.

The experimental setup consists of 1 syringe pump carrying two syringes, each one connected to the reservoirs of the microfluidic device by polyethylene tubes. In the other side of the reservoirs they are connected to *eppendorf* tubes, in which the molecular species (dye) and the buffer are stored (Figure 4.1 and 4.2).

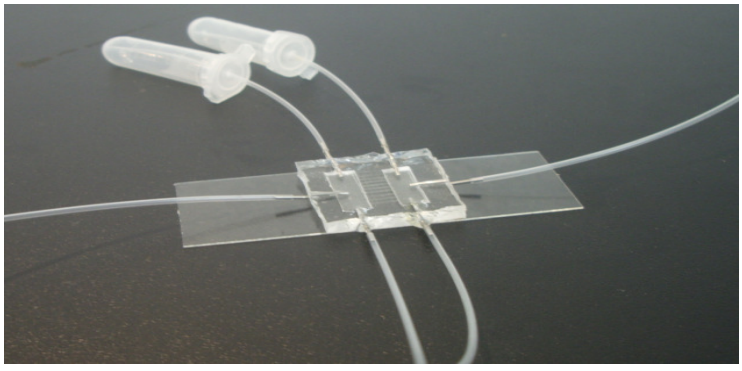

Figure 4.1 - Microfluidic device with the tubing responsible for the external fluidic system.

Figure 4.2 - Experimental setup: 1 syringe pump carrying two syringes, each one connected to the reservoirs of the microfluidic device by polyethylene tubes.

4.1.1.1 Generation of stable gradients using the fluorophore FITC

Gradients were characterized using fluorescence microscopy. Carbonate buffer was loaded into one *eppendorf* tube for the reservoir and a 389 mM FITC solution (from Sigma-Aldrich) in $NaHCO_3$ was loaded into the other *eppendorf* tube for the opposite reservoir. Flow rates of 5.5 µL/min were maintained by withdrawing the fluids from the reservoirs using the syringe pump. Gradient evolution was monitored. Images were analyzed using ImageJ program. For each image, the fluorescence intensity was measured and background-subtracted. The *ruler* near each microchannel was an essential tool for the analysis of the fluorescence intensity along the channels due to the rapid recognition of the same points in each frame.

4.1.1.2 Generation of Methionine and Galactose gradients

After inserting the cells into the microchannels (described in **3.2.1**) the same procedure was followed as described in **4.1.1.1** to create a gradient of methionine and galactose. One of the *eppendorf* tubes was filled with rafinose medium and the other one was filled with galactose + methionine medium to form a gradient of these species inside the channels. Before starting the gradient, a few cells were selected by optical microscope observation in different channels with the help of the *ruler* with the aim of studying the protein expression levels according to the gradient generated along the channels. Afterwards, the evolution of intensity of green (GFP) and red (RFP) fluorescence of these cells (which corresponds to the expression levels of these proteins) were monitored by acquiring images every 1 hour.

4.2 *Results and Discussion*

4.2.1 Generation of a stable gradient using fluorophores

From the literature it was possible to conclude that there are two main approaches that have been described to generate molecular gradients:
- forming gradients perpendicular to continuously flowing streams of varying concentration [40,68].

- forming gradients along a channel by free-diffusion between a source and a sink [37].

The first method is advantageous for producing stable complex gradients and the second one, because it relies on free diffusion, the gradient profile changes with time, and it is difficult to obtain a steady-state gradient over long periods. Therefore, in this project it was decided to form a gradient according to the first method because it was necessary to guarantee a stable gradient over 2-3 hours in order to visualize changes on the expression levels of some proteins when induced/repressed to such gradients.

The microfluidic device developed in the present work was capable of generating gradients across microchannels between inlet and outlet reservoirs. Convective flow into the microchannels was minimized by designing the height of the channels (6μm) to be significantly smaller than the reservoirs (700μm). This large difference yields an even greater difference in fluidic resistance, causing flow to take the path of least resistance rather than entering the channels, allowing only diffusive transport.

The generation of stable gradients inside microchannels was maintained by constantly withdrawing the fluids from the reservoirs using the syringe pump. Continuously replenished source and sink is advantageous over static reservoirs because their concentration can be kept constant, and thus the gradients can be maintained at a constant profile in steady-state (Figure 4.3).

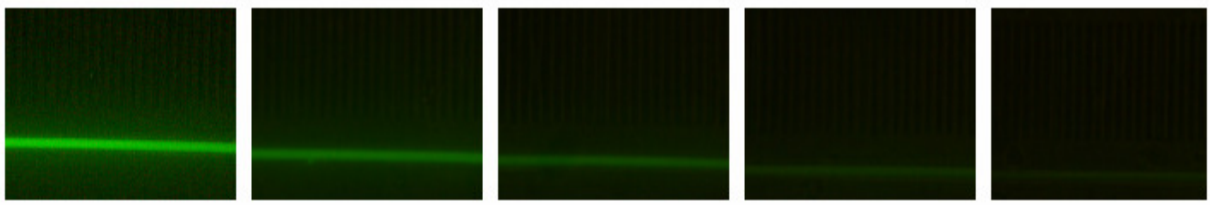

Figure 4.3 - FITC Gradient inside a microchannel.

The first step before finding the optimal flow rate in which the gradient could remain stable over 2-3 hours was simply the view of the formation of a gradient within the channels in order to demonstrate the effectiveness of the methodology used, without regarding the flow rate. Afterwards, we began to gradually reduce the flow rate until the optimal one was reached in

which the time window for the gradient was approximately the time necessary for the cells to express/repress the proteins according to the inducible/repressible gradient. The stepper-motor-based syringe pump (stepper motors convert electrical signals into discrete mechanical rotational movements) available on INESC MN has an interface menu in which the user can chose the value of the desired pulse.

Initially, the flow rates were set to be constant in the inlet and outlet reservoirs with a value of approximately 5,5 µL/min. However, during the experiments using FITC it was verified that after this fluorophore crossed the channels it started to accumulate on the outlet reservoir close to the end of the channels (due to the small flow rate) and thus the diffusion phenomenon inverted direction and FITC molecules started to diffuse to the opposite side. To overcome this situation, one had to increase the flow rate of the solution in the outlet reservoir (buffer) to avoid FITC accumulation. Because the syringe pump available on INESC MN was only capable of establishing a unique flow rate for both syringes and due to the fact that only one syringe pump was available, the only solution found to increase the flow rate in only one reservoir was to use a syringe with a greater capacity (3mL) compared to the one used for the inlet reservoir (1mL) (Figure 4.4). This way, the flow rate on the outlet reservoir was three times higher compared to the flow rate on the inlet reservoir, which allows the renewal of the solution faster than the one in the inlet reservoir.

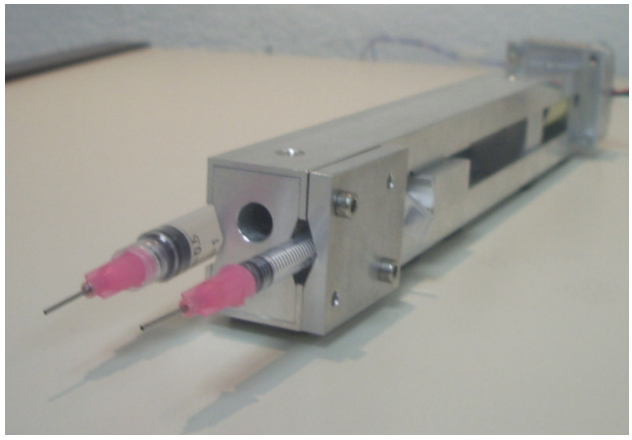

Figure 4.4 - Syringe pump carrying two syringes with different capacities (1mL and 3mL).

It must be emphasized that the gradient stability is dependent on the flow, and remains stable as long as the flow is maintained in the reservoirs. The flow rates and outside reservoir volumes determine the time window for stable gradients. With typical outside reservoir sizes (vol=2 mL each reservoir), and flow rates of 5.5 µL/min and 20 µL/min in inlet and outlet reservoir respectively, the gradients can be maintained for 2,5 h.

By looking at the figure 4.5 it was possible to verify that a steady-state gradient was achieved, because the gradient remained stable, after 16 minutes. Moreover, two distinct points across the channels were selected in order to observe the variation of the fluorescence intensity over

time (Figure 4.6). It was found that in each point the fluorescence intensity converged to a stable value, showing that the gradient remained stable.

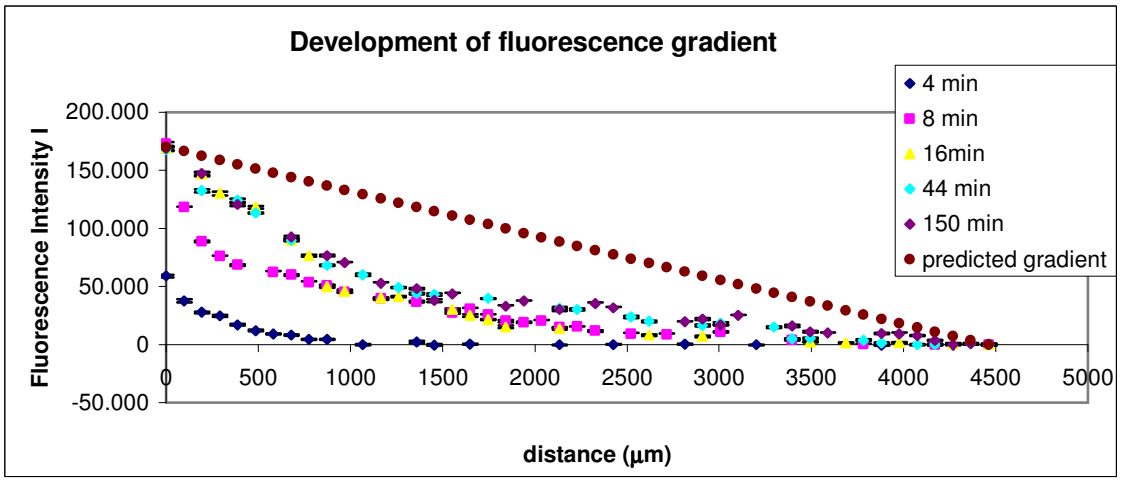

Figure 4.5 - Chart showing the fluorescence intensity profile across a microchannel (width=6 µm) at different times. A stable gradient was established after 16 minutes.

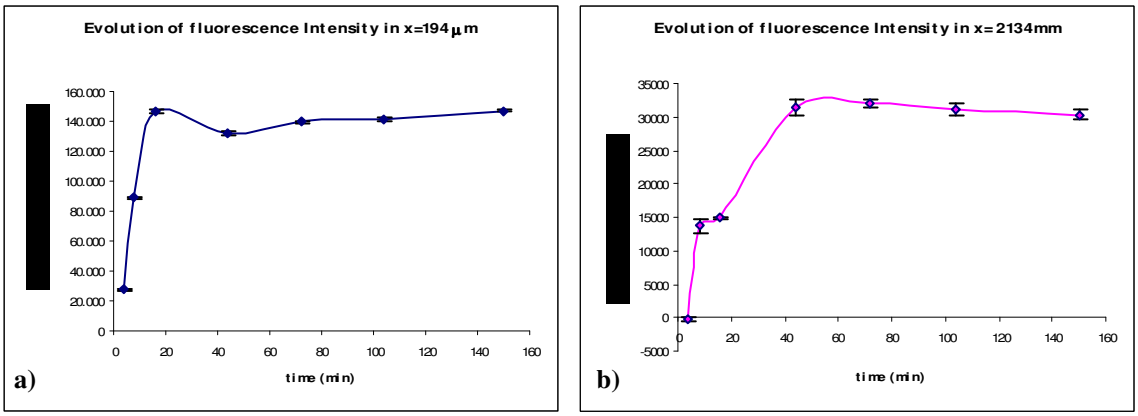

Figure 4.6 - Charts showing the evolution of the fluorescence intensity in the same microchannel in a) x = 194µm and x = 2134 µm.

However, the experimental results were not in good agreement with the theoretical predictions (see Figure 4.5). After reaching a steady-gradient, a linear concentration of the fluorophore should have been established, according to the following equation [40]:

$$C = \frac{(C_r - C_l)}{L} x + C_l \qquad (5)$$

where C is the concentration of the diffusing molecule, Cr is the concentration in the inlet reservoir, Cl is the concentration in the outlet reservoir, L is the length of the channel and x is the position across the channel.

We believe such deviations could be mainly attributed to the following aspects:

- Imperfections in the microchannels resulting from the lithography process. Moreover, in this project, for reasons already outlined, the microchannels had to be fabricated with a very high length and therefore the probability of such imperfections appearing was greater.
- Convection was not completely eliminated inside microchannels. Despite the fact that the convection was minimized due to the design of the microfluidic device, it could also be possible that this phenomenon could not have been completely avoided and thus the gradient was not generated only by diffusion transport across the microchannels.
- The fact that the syringe pump works with a stepper motor may also have led to deviations from the theoretical predictions because both FITC solution and buffer crossed the reservoirs not in continuous flow but in discrete steps.

After having established a stable-gradient using FITC, another fluorophore was used in order to verify if the results were similar or not. Alexa 430 is a fluorescent dye with emission/excitation values of 430/520 nm [69]. Alexa Fluor dyes are typically used as cell and tissue labels in fluorescence microscopy and cell biology. However, the fluorescence intensity of this molecule is very low when compared to FITC and thus the values measured for the fluorescence intensity were very similar to each other across the channel making it impossible to establish a valid gradient.

The method to establish a stable gradient implemented in this project has one disadvantage related to the constant flow because the cells were weakly adhered on the substrate and some cells did not adhere at all therefore during experiments some cells changed positions over time and it was very difficult to localize them again.

The establishment of a steady-state gradient inside the microchannels was a truly challenge because there were many obstacles to overcome in order to generate a stable gradient over long periods. One of these obstacles was the variations in cross sectional area among microchannels due to the imperfections in microfabrication. Even more, despite PDMS Replica being cleaned with HCl before bonding to the glass substrate, some waste particles were present inside the channels and thus, the diffusion of the solute particles was interrupted in that place. Some of these particles are so small that they were not visible during the experiments, and one only realised about their presence when the solute started to accumulate in that place (Figure 4.7). For these reasons, it was very difficult to obtain the same gradient among different channels.

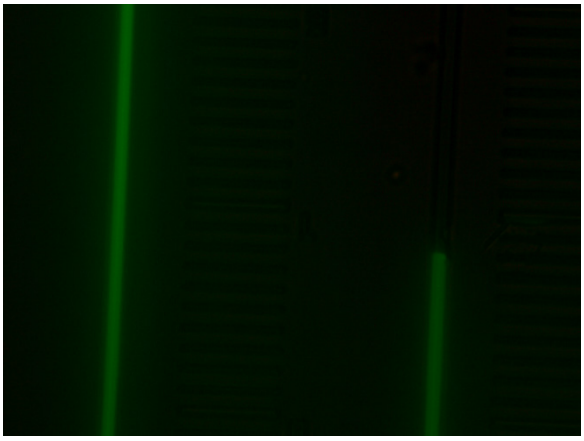

Figure 4.7 - Fluorescence micrograph of two microchannels showing a defect in the PDMS walls in one microchannel which stops the passage of the fluid along the rest of the microchannel.

Considering the microfluidic devices that have been made for the generation and characterization of stable gradients, they did not have outside reservoirs for the liquid supply but these reservoirs were made by punching the PDMS using a sharpened needle. These reservoirs were then connected to two main channels that are continuously replenished by flow and a gradient–generating region is located between the source and the sink channels [40]. One could have made a similar approach, however, since the microfluidic device was already done and optimized for the study of yeast cells, it was decided to adapt this microfluidic for the generation of a gradient inside the channels. What is more, using *eppendorf* tubes (with different capacities) as outside reservoirs, one could have a much higher flow supply when compared to the holes made directly on the PDMS.

4.2.2 Generation of methionine and galactose gradients within microchannels

The last goal of this work was the visualization of the expression levels of αSyn-GFP and RFP protein when subject to a molecular gradient of galactose and methionine.

Some experiments were performed in the INESC-MN, however, since the microscope available has a filter that covers both green and red fluorescence, it was not possible to visualize separately the repression of the RFP protein and the induction of the GFP-αSyn fusion protein (data not shown). We had originally intended to install the syringe pump in the IMM because the microscope available has two distinct filters for the different fluorescences. However, due to the fact that the syringe pump started to malfunction, and due to time limitations, we decided to discontinue this approach.

5 General Considerations

After several experiments had been carried out, including the cell and the gradient experiments, some general aspects were verified which could lead to some unwanted results. The two major aspects were the hydrophobic surface of the PDMS and the fluidic resistance at the entrance of the microchannels. The last paragraphs will be dedicated to other microfluidic components, besides microchannels, that could be important to incorporate in the medium term, in the microfluidic platform developed in this project.

5.1.1 Hydrophobic surface of the PDMS

In the field of Microfluidics, a number of efforts have been made to modify the surface of PDMS microchannels to enhance hidrophilicity, which limit its applicability for analytical devices.

Oxygen plasma has been widely used to modify the surfaces of PDMS [60,71]. However this property is quickly lost through hydrophobic recovery caused by diffusion of unreacted oligomer to the surface. This aspect associated with most of the currently employed treatments is one of the current issues limiting the use of PDMS for microfluidic devices. Nevertheless, keeping the oxidized PDMS in contact with a polar liquid, water for example, its hydrophilic surface could be preserved, although the long-term stability is unknown [4]. Oxygen plasma treatment could be used to bond the PDMS over the glass substrate, however this method would not be capable of rendering the microchannels hydrophilic since all the microfluidic device is irreversibly bonded to the glass microscope slide. For this reason, in this project, as it has already been said, a Corona portable system was used both to improve the adhesion between PDMS and glass (using a two and a half inch wire electrode) and to modify the hydrophobic surface of the microchannels (using a needle type electrode). Due to the geometric design of the microfluidic device, with a series of microchannels fabricated alongside the reservoirs, the corona treatment could not be completely efficient in the microchannels hydrophilization step.

Recent reports had presented other alternatives to modify the surface of the PDMS, namely the fabrication of permanently hydrophilic surfaces via controlled grafting of HEMA [72,73,74]. Functional HEMA monomers were spin coated onto the surface of the PDMS and exposed to the oxygen plasma to obtain long-term hydrophilic surfaces with a cross-linked network of grafted monomers. This chemical modification proved to be the most efficient in terms of hydrophilic stability with surfaces stable over 10 days [72] (see Figure 5.1).

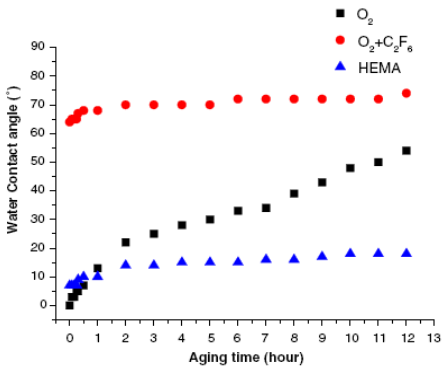

Figure 5.1 - Graph of water contact angle vs. Aging time for PDMS modified with oxygen plasma, O_2 + C_2F_6 plasma and HEMA (from [72]).

5.1.2 Fluidic resistance at the entrance of the microchannels

During the experiments it was verified that almost all the soluble components had a great resistance at the entrance of the microchannels. The big question that arises is to know if such resistance is due to inefficient Corona discharge or if the channels were so small compared to the reservoirs that the high fluidic resistance in all the microchannels hinders flow entrance.

Considering eqn. (6) [75], the fluidic resistance is inversely proportional to the cubic of tube height h (considering a rectangular tube):

$$R = \frac{12\mu L}{w h^3} \tag{6}$$

where R = fluidic resistance, L = length of tube and μ = fluid viscosity and w=channel width.

From the previous equation one can verify that considering the dimensions of the reservoirs (700μm high and 15.000μm length) and the microchannels (6μm high and 5000μm length) the resistance in the microchannels will be 4.41×10^8 higher than in the reservoirs which could explain the fluidic resistance at the entrance of the microchannels. To decrease this resistance, the reservoirs should have been fabricated in such a way that their height would be similar to the height of the microchannels. However, during the fabrication of the microfluidic device one had to face many problems related to the reservoir capacities and to overcome that situation such reservoirs were made using rectangular silicon pieces with a thickness of 700μm. There was a need to find a balance between the optimum reservoir capacities and the resistance that such reservoirs would cause.

A simple approach to ensure that all the channels were filled with a soluble component would be the fabrication of a microfluidic device in which each channel had two reservoir holes punched through the PDMS [76], similar to the following figure:

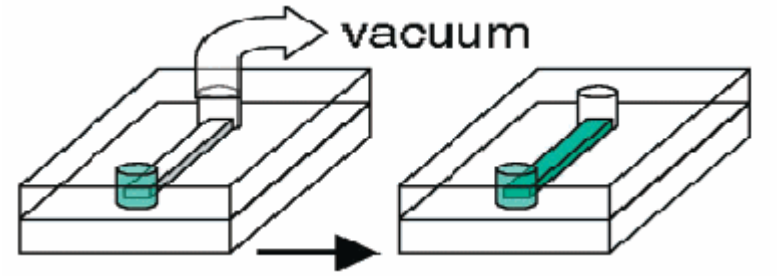

Figure 5.2 - Schematic representation of a method for filling microfluidic channels in a PDMS device (from [76]).

Using this approach, the method for filling microchannels would be easier because a vacuum could be easily made directly on one of the holes. Moreover, with this design one could guarantee the effectiveness of the corona treatment because such discharge would be applied directly on the holes and therefore on the channel. However, the method described above was not appropriate for the generation of a stable gradient. Furthermore, the results of an experiment in only one channel, especially when studying cell behaviour, makes it impossible to compare to other channel results. The same experiment could be done at different times to make them reproducible; nevertheless the conditions would not always be the same.

5.1.3 Microfluidic components which could be incorporated in the microfluidic device

Besides the aspects previously described to improve the microfluidic device developed in this work, some other key microfluidic elements could have also been added to the device. For example, valves are widely used in microfluidic approaches because the release volume must be accurately controlled with them to minimize macroscopic fluid flow and fluctuations in the gradient profile [39,77].

In the experimental setup developed in this project, the gradient can only be maintained within the microchannels with constant flow, and the cells were constantly exposed to shear stress. If valves were used on this microfluidic device, one could have temporal control over the initiation of the biomolecule gradient. What is more, one could have made other interesting experiments to observe the cell behaviour when exposed to different biomolecules in different times.

6 Conclusion

A microfluidic device made of PDMS and glass was successfully created during this project. Methods to fabricate the master mold were improved, namely the most widely used based on the patterning of SU-8 photoresist on Si wafers. A new method to fabricate the master mold was also implemented in which it was not necessary to make a photomask because the positive patterning is directly made by double exposure on a Direct Laser machine (DWL). Using this new method, the time spent to produce the microfluidic device decreased significantly and the fact that the master mold was fabricated in such a way that allows the fabrication of three PDMS replicas simultaneously also increase the effectiveness of such methodology. The new microfabrication technique developed in this project allowed us to overcome many drawbacks of the traditional master mold techniques, including the obtaining of very small structures (≤10μm).

The fabrication of microfluidic devices in PDMS had shown to present several advantages when compared to the devices made of glass or silicon. In biological applications, a device should only be used once per experiment because it is difficult to wash it every time it is used and is almost impossible to ensure that no cells were adhered to the glass or PDMS surface. Therefore, using elastomeric materials make all the process more cost effective comparing to other materials used in the fabrication of microfluidic devices.

The design of the microfluidic chip was improved throughout the project and an important tool, *the ruler*, was added to allow the recognition of a particular cell over long periods. Without this tool it would be very difficult to analyse many cells in different channels in the same experiment. Furthermore, the ruler was also essential to measure the fluorescence intensity along the channels during the gradient experiments.

The microfluidic device developed in this project was tested with yeast cells genetically modified with the aim of understanding the effect of a soluble component in the protein expression levels of such cells.

The study of single cells inside a microfluidic platform allowed us to understand some fundamental aspects in the field of Biology that would be impossible to comprehend in the traditional *macro* culture techniques. One of these essential aspects was the cellular heterogeneity among a population of yeast cells carrying 2μ plasmids in terms of fluorescence protein expression levels. This variability decreased significantly in yeast cells carrying the gene encoding the protein of interest directly in the genome. In accordance with the objectives of the present work, the cells that will be more useful will be the ones with genomic insertions of the SNCA gene. Furthermore, with this device it was also possible to visualize other important aspects such the division time of a particular cell within microchannels and the successive generations of the same cell in a very controlled environment. The increasing in the division time of VSY72 cells comparing to WT cells proved the toxicity of αSyn when overexpressed.

Despite having been tested with yeast cells, the platform developed in this work could also be used for many other applications:

- Since the methodology used to fabricate the microchannels (with widths between 5-10μm) was also efficient to produce any range of widths ≥ 3μm, this device could also be used to study other cells such as *Escherichia coli (2* μm long and 0.5 μm in diameter*)* and almost all the microrganisms, and some mammalian cells whose diameter does not exceed 5-6μm.
- By making use of this gradient-generator platform, chemotaxis studies could be carried out to study many effects in the cell behaviour such as those referred in **1.5.2.**.

7 Future Work Perspectives

In the short term some measurements and changes could be made in order to improve the results in the present project:

- Finish the gradient experiments with galactose and methionine in order to visualize the differences on the expression/repression levels of αSyn-GFP and RFP proteins along the channels. Since the variability on the expression levels in very high among cells carrying aSyn-GFP and RFP proteins in 2μ plasmids, it might be advantageous to study such gradients in cells that carry these proteins in the genome.
- Fabricate a microfluidic device using the microfabrication technique developed in the present work, but change the design mask in such a way that it could be possible to test a wide range of lengths and widths. The variation in these dimensions, namely in the length of the microchannels, could give us different profiles of the gradient generated. Possibly one could find the optimal length in which the steady-state gradient is linear. A simple approach could be similar to the Figure 7.1. The geometry of the reservoirs could be difficult to obtain using Si, but we could substitute this material to another one (PDMS for example).

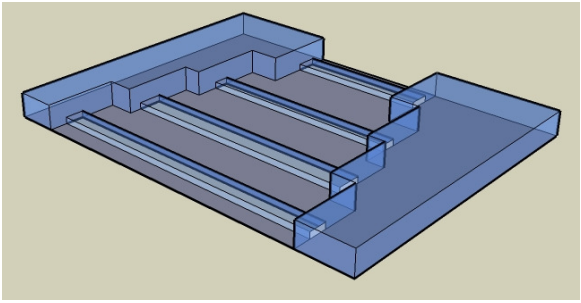

Figure 7.1 - Microfluidic device with microchannels of different lengths to test the influence in the gradient profile.

- Find a way to immobilize the cells inside the microchannels either by hydrodynamic trapping, improving the methodology that we started by narrowing the channels in specific places (see section **3.3.2**) or including more complex mechanical barriers/obstacles, or by chemical trapping. One approach could be the micro patterning technique providing discrete places for the cells to adhere and inhibit cell attachment in the surrounding areas. This last technique has already been improved in INESC MN for the immobilization of *Escherichia coli,* but not inside microchannels.

In the long term, as it has already been referred, it would be advantageous to integrate in the device some other components besides microchannels that would be very important for more accurate results:

- A temperature sensor that could maintain an optimal temperature for biological applications.
- PDMS microvalves to control the fluid flow in microchannels that could also act as switches.

- Integrate this microfluidic device in sensors that were being developed in INESC-MN. These sensors will be able to detect and measure protein expression levels.

Fabricate a fully integrated device in which the reservoirs are made in PDMS and thus eliminating *eppendorf* tubes to the setup. A similar approach to the one showed in the Figure 7.2 could be implemented. In a platform like that the reservoirs could be isolated from the rest of the device by valves that could switch off and on depending on the application desired. Using a similar approach cells could be exposed to different molecular solutes at different times and it could be possible to visualize changings in the cell behaviour according to specific stimulations.

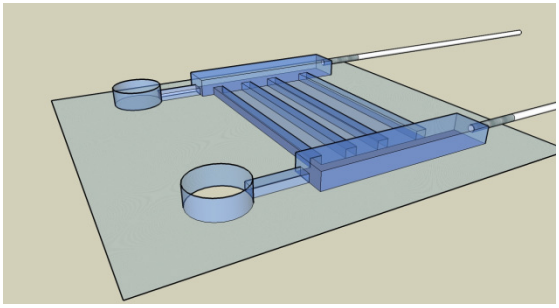

Figure 7.2 - Long term microfluidic platform.

In biological terms, a long term line to follow would be:

- After the creation of a linear gradient inside the channels, it would be important to establish a relation between the galactose concentration and the expression levels of α–Syn. This way, it could be possible to have cells in different expression levels according to the concentration of galactose in the same microchannel.
- Transformation of yeast cells carrying out the sequence of different possible suppressors of αSyn under the action of regulatable promotors. Once established the gradient of their respective metabolites, such supressors would be in different levels along the channels and therefore it could be possible to find the optimal concentration of the regulators in which the supressors could change the expression levels of α-Syn.

8 References

[1] J. Urbanski, W. Thies, C. Rhodes, S. Amarasinghe and T. Thorsen. Digital microfluidics using soft lithography. Lab on a chip. 2006, 6, 96–104.

[2] G. M. Whitesides. The origins and the future of microfluidics. NATURE , 442(2006).

[3] F. A. Gomez. Biological applications of Microfluidics. ed., John Wiley & Sons, Inc., 2008.

[4] J. C. McDonald, D. C. Duffy, J. R. Anderson, D. T. Chiu, H. Wu, O. J. Schueller, G. M. Whitesides. Fabricatin of microfluidic systems in poly(dimethylsiloxane). Electrophoresis, 2000, 21, 27-40.

[5] J. El-Ali, P. K. Sorger and K. F. Jensen. Cells on chips. NATURE, 442(2006).

[6] J. Ouellette. A new wave of microfluidic devices. American Institute of Physics. 2003, 14-17.

[7] http://www.wou.edu/las/physci/ch462/BouncingPutty.htm

[8] G. M.Whitesides, E. Ostuni, S. Takayama, X. Jiang and D. E. Ingber. Soft Lithography in Biology and Biochemistry. Annu. Rev. Biomed. Eng. 2001, 3, 335–73.

[9] J. C. Lötters, W Olthuis, P H Veltink, P Bergveld. The mechanical properties of the rubber elastic polymer polydimethylsiloxane for sensor applications. J. Micromech. Microeng. 1997, 7 145-147.

[10] J. Pihl, J. Sinclair, M. Karlsson, and O. Orwar. Microfluidics for cell-based assays. 2005 VOL. 8 No 12.

[11] http://faculty.washington.edu/yagerp/microfluidicstutorial/basicconcepts/basicconcepts.htm.

[12] http://www.niherst.gov.tt/scipop/sci-bits/microfluidics.htm.

[13] http://www.ims.tnw.utwente.nl/masters/docs/softlitho.doc/.

[14] B. Michel, A. Bernard, A. Bietsch, E. Delamarche, M. Geissler, D. Juncker, H. Kind, J.-P. Renault, H. Rothuizen, H. Schmid, P. Schmidt-Winkel, R. Stutz, H. Wolf. Printing meets lithography: Soft approaches to high-resolution Patternig, IBM J. RES. & DEV., 2001, Vol. 45, No. 5.

[15] B. Michel. Printing Meets Lithography. American Institute of Physics, 2002

[16] Y. Xia and G. M. Whitesides. Soft Lithography. Annu. Rev. Mater. Sci. 1998, 28,153–84.

[17] http://dougrobello.pluggedin.kodak.com/.

[18] D. Roy, P. K. Basu, S. V. Eswaran. Photoresists for Microlithography. RESONANCE, 2002, 44-53.

[19] M. A. Unger, H. Chou, T. Thorsen, A. Scherer, S. R. Quake Monolithic Microfabricated Valves and Pumps by Multilayer Soft Lithography, *Science*. 2000: Vol. 288. no. 5463, pp. 113 – 116.

[20] C. Yi, C. Li, S. Ji, M. Yang. Microfluidics technology for manipulation and analysis of biological cells. Analytica Chimica Acta, 560 (2006), 1–23.

[21] H. Yu, I. Meyvantsson, I. A. Shkelab and D. J. Beebeb Diffusion dependent cell behavior in microenvironments. Lab Chip, 2005, 5, 1089–1095.

[22] P.J. Lee, P. J. Hung, R.Shaw, L. Jan, L. P. Lee. Microfluidic application-specific integrated device for monitoring direct cell-cell communication via gap junctions between individual cell pairs. American Institute of Physics. 2005, 86, 1-3.

[23] A. M. Taylor, Blurton-Jones, S. W. Rhee, D. H. Cribbs, C. W. Cotman, N. L. Jeon. A microfluidic platform for CNS axonal injury, regeneration and transport. Nature Methods. 2005, Vol. 2 nº8, 599-605.

[24] D. D. Carlo, L. Y. Wu, L. P. Lee. Dynamic Single cell culture array. Lab Chip. 2006, **6**, 1445 - 1449,

[25] D.Longo, J. Hasty. Dynamics of single-cell gene expression. Molecular Systems Biology. 2006, 64.

[26] S. Cookson, N. Ostroff, W. L. Pang, D. Volfson, J. Hasty. Monitoring dynamics of single-cell gene expression over multiple cell cycles. Molecular Systems Biology. 2005.

[27] J. Ryley,O. M. Pereira-Smith. Microfluidics device for single cell gene expression analysis in *Saccharomyces cerevisiae. Yeast.* 2006; 23: 1065–1073.

[28] G. Charvin, F. R. Cross, E. D. Siggia. A Microfluidic Device for Temporally Controlled Gene

Expression and Long-Term Fluorescent Imaging in Unperturbed Dividing Yeast Cells. PLoS ONE. 2008.

[29] T. M. Keenan, A. Folch. Biomolecular gradients in cell culture systems. Lab Chip, 2008, 8, 34–57.

[30] N. Zaari. Photopolymerization in microfluidic gradient generators: Microscale control of substrate compliance to manipulate cell response. Adv. Mater. 2004, 16(23–24), 2133.

[31] N. L. Jeon , H. Baskaran , SK. Dertinger , GM. Whitesides , L. Van de Water , M. Toner . Neutrophil chemotaxis in linear and complex gradients of interleukin-8 formed in a microfabricated device. Nat. Biotechnol., 2002, 20(8), 826–830.

[32] H. Mao, P. S. Cremer, M. D. Manson, A sensitive, versatile microfluidic assay for bacterial chemotaxis, Proc. Natl. Acad. Sci. U. S. A., 2003, 100(9), 5449–5454.

[33] J. Diao, L. Young, S. Kim, E. A. Fogarty, S. M. Heilman, P. Zhou, M. L. Shuler, M. W., M. P. DeLisa. A three-channel microfluidic device for generating static linear gradients and its application to the quantitative analysis of bacterial chemotaxis, Lab Chip, 2006, 6(3), 381–388.

[34] S. Koyama, D. Amarie, H. A. Soini, M. V. Novotny, S. C. Jacobson. Chemotaxis assays of mouse sperm on microfluidic devices, Anal. Chem., 2006, 78(10), 3354–3359.

[35] W. Saadi, S. Wang, F. Lin, N. L. Jeon. A parallel-gradient microfluidic chamber for quantitative analysis of breast cancer cell chemotaxis, Biomed. Microdev., 2006, 8(2), 109–118.

[36] G. M. Walker, M. S. Ozers, D. J. Beebe. Cell infection within a microfluidic device using virus gradients. Sens. Actuators B: Chem., 2004, 98(2–3), 347–355.

[37] K. A. Fosser, R. G. Nuzzo.Fabrication of Patterned Multicomponent Protein Gradients and Gradient Arrays Using Microfluidic Depletion. Anal. Chem. 2003, 75, 5775-5782.

[38] V. V. Abhyankar, M. A. Lokuta, A. Huttenlocher, D. J. Beebe. Characterization of a membrane-based gradient generator for use in cell-signaling studies. Lab Chip, 2006, 6, 389–393.

[39] B. G. Chung, F. Lin, N. L. Jeon. A microfluidic multi-injector for gradient generation. Lab Chip, 2006, 6, 764–768.

[40] B. Mosadegh,C. Huang, J. W. Park, H. S. Shin, B. G. Chung, S. Hwang, K. Lee, H. J. Kim, J. Brody, N. L. Jeon. Generation of Stable Complex Gradients Across Two-Dimensional Surfaces and Three-Dimensional Gels. Langmuir. 2007, 23, 10910-10912.

[41] N. L. Jeon, S. K. W. Dertinger, D. T. Chiu, I. S. Choi, A. D. Stroock, G. M. Whitesides. Generation of Solution and Surface Gradients Using Microfluidic Systems. Langmuir 2000, 16, 8311-8316.

[42] M. A. Holden, S. Kumar, E. T. Castellana, A. Beskok, P. S. Cremer. Generating fixed concentration arrays in a microfluidic device. Sensors and Actuators, 2003, 199–207.

[43] http://diffusion.wikidot.com/

[44] J. Berthier, P.Silberzan. Microfluidics for Biotechnology. Arthec House Microelectromechanical systems (MEMS) series, Norwood, 2006.

[45] H. Song, M. R. Bringer, J. D. Tice, C. J. Gerdts, R. F. Ismagilova. Experimental test of scaling of mixing by chaotic advection in droplets moving through microfluidic channels. *Appl Phys Lett*. 2003;, 83(12): 4664–4666.

[46] http://en.wikipedia.org/wiki/Yeast.

[47] http://www.yeastgenome.org/VL-what_are_yeast.html.

[48] A. Gofieau, B. G. Barrell, H. Bussey, R. W. Davis, B. Dujon, H. Feldmann, F. Galibert, J. D. Hoheisel, C. Jacq, M. Johnston, E. J. .Louis, H. W Mewes, Y. Murakami, P Philippsen, H. Tettelin, S. G. Oliver, Life with 6000 genes. Science, 1997, Volume 274, Issue 5287, 546,563-567.

[49] S. Ostergaard, L. Olsson, J. Nielsen. Metabolic Engineering of *Saccharomyces cerevisiae.* Microbiology and Molecular Biology Reviews,2000, 64, 34–50.

[50]http://www.sfn.org/index.cfmpagename=brainBriefings_alphaSynucleinAndParkinsonsDisease

[51] http://nmnf.epfl.ch/page9109.html

[52] B. L. Schneider, C. R. Seehus, E. E. Capowski, P. Aebischer, S. Zhang, C. N. Svendsen.

Over-expression of alpha-synuclein in human neural progenitors leads to specific changes in fate and differentiation. Human Molecular Genetics, 2007, Vol. 16, No. 6 651–666.

[53] T. F. Outeiro, S. Lindquist. Yeast Cells Provide Insight into Alpha-Synuclein Biology and Pathobiology.Science. 2003 December 5; 302(5651): 1772–1775.

[54] S. Willingham, T. F. Outeiro, M. J. DeVit, S. L. Lindquist, P. J. Muchowski. Yeast Genes That Enhance the Toxicity of a Mutant Huntingtin Fragment or α-Synuclein. Science. 2003 December 5; 302(5651): 1769–1772.

[55] http://www.inesc-mn.pt

[56] MicroChem (www.microchem.com). SU-8 2000 datasheet.

[57] http://www.yieldengineering.com/

[58] G. Spierings. "Wet Chemical Etching of Silicate Glasses in Hydrofluoric Acid Based Solutions", Journal of Materials Science, 28 (1993), pp. 6261-6273.

[59] A. Bubendorfer, X. Liu, A V Ellis. Microfabrication of PDMS microchannels using SU-8/PMMA moldings and their sealing to polystyrene substrates. Smart Mater. Struct. **16** (2007) 367–371.

[60] Microchemicals (http://www.microchemicals.com/). AZ 4500 datasheet.

[61] Dow corning (www.dowcorning.com) Sylgard 184silicone elastomer datasheet.

[62] L. Hung, A. P. Lee. Optimization of droplet generation by controlling PDMS surface hydrophobicity. ASME International Mechanical Engineering Congress and RD&D Expo. 2004.

[63] B. J. Thomas, R. Rothstein. Genetics. 1989,123, 725.

[64] G.M. Walker, M.S. Ozers, D.J. Beebe. Insect cell culture in microfluidic channels. Biomed. Microdevices. 2002, 4, 161.

[65] E. T. Lagally, C. A. Emrich, R. A. Mathies. Fully integrated PCR-capillary electrophoresis microsystem for DNA analysis. Lab on a Chip, 2001, 1, 102–107.

[66] J. M. Raser, E. K. O'Shea. Control of Stochasticity in Eukaryotic Gene Expression. Science.

2004 June 18; 304(5678): 1811–1814.

[67] E. M. Ozbudak, M. Thattai, I. Kurtser, A. D. Grossman, A. van Oudenaarden. Regulation of noise in the expression of a single gene. Nature Genetics. May 2002,31, 69-73.

[68] C. Li, R. Chen, M. Yang. Generation of linear and non-linear concentration gradients along microfluidic channel by microtunnel controlled stepwise addition of sample solution Lab Chip, 2007, 7, 1371 – 1373.

[69] Diffusion DataBase (http://diffusion.wikidot.com/values:alexa-fluor)

[70] D. C. Duffy, J. C. McDonald, O. J. A. Schueller and G. M. Whitesides. Rapid Prototyping of Microlfuidic Systems in Poly(dimethylsiloxane). Anal. Chem. 1998, 70, 4974-4984.

[71] K. Haubert, T. Drier and D. Beebe. PDMS bonding by means of a portable, low-cost corona system. Lab Chip, 2006, 6, 1548-1549.

[72] D. Bodas,C. Khan-Malek. Formation of more stable hydrophilic surface of PDMS by plasma and chemical treatments. Microelectronic Engineering. 2006, 83, 1277-1279.

[73] J. A. Vickers, M. M. Caulum, C. S. Henry. Generation of hydrophilic PDMS for high-performance microchip electrophoresis. Anal. Chem. 2006, 78, 7446-7452.

[74] D. Bodas, C. Khan-Maleck. Fabrication of long-term hydrophilic surfaces of PDMS using 2-hydroxy ethyl methacrylate. Sensors and Actuators. 2007, 120, 719-723.

[75] E. Hilner, S. Stefanou. Soft Lithography. Making a valve in PDMS.2004.

[76] J. Monahan, A. A. Gewirth, R. G. Nuzzo. A Method for Filling Complex Polymeric Microfluidic Devices and Arrays. Anal. Chem. 2001, 73, 3193-3197.

[77] A. R. Abate, D. A. Weitz. Single-layer membrane valves for elastomeric microfluidic devices APPLIED PHYSICS LETTERS. 2008, 92, 243509.

9 ANNEX 1

Preparation of Yeast Cells

(for Transformation)

Day 1:

1. In the morning prepare 30 ml pre-inoculum in YPD, in a 100 ml erlenmyer. Shake at 30ºC and 250 rpm till late afternoon.

2. Dilute X ml of pre-inoculum in 30 ml of YPD, in a 100 ml erlenmyer. Shake at 30ºC and 250 rpm overnight.

Day 2:

3. Check OD. It must be around 0.5-0.7 (G=1.5h).

4. Split the volume of your erlenmyer into two 50 ml centrifuge bottles.

5. Centrifuge for 5 min at 4ºC and 4000 rpm. Discard supernatant.

6. Add 30 ml of sterile water to each bottle. Shake until pellet is dissolved.

7. Centrifuge for 5 min at 4ºC and 4000 rpm. Discard supernatant.

8. Ressuspend each pellet in 1ml of sterile water.

9. Transfer cells into 2 ml epps.

10. Perform a short spin for 30 sec at 4ºC. Discard supernatant.

11. Add 1 ml of **Solution 1**. Ressuspend pellet with pipette. ⚠ do **Not Vortex**. Only use pipette. Cells are very delicate after AcLi is added.

12. Perform a short spin for 30 sec at 4ºC. Discard supernatant.

13. Add 150 µl of **Solution 1** to each epp. ⚠ if culture volume is > 30 ml add 500 µl

14. Put your cells on Ice.

Solutions:

AcLi 10x: 1M AcLi pH 7.5 (adjusted with acetic acid)

TE 10x: 0.1M Tris pH 7.5; 0,01M EDTA pH 7.5.

Solution 1: 1/10 AcLi 10x, 1/10 TE 10x, 8/10 sterile wate

Yeast Transformation (Lithium Acetate procedure)

1. Mark your epps.

2. Add 5 µl (10 mg/ml) of denatured salmon sperm to the bottom of each epp.

3. Add 50 µl of yeast cells to each tube.

4. Add 2 µl (~ 2 µg)of DNA to the corresponding tube. Mix manually.

5. Add 18 µl 0f 5% DMSO ⚠ This step is optional.

6. Add 300 µl of **Solution 2**. Mix manually.

7. Put at 30ºC with agitation for 30 min.

8. Transfer the epps to a 42ºC bath for 20 min.

9. Spin down and remove supernatant.

10. Add 500 µl of sterile water. Invert several times until pellet is dissolved.

11. Spin down and remove supernatant.

12. Add 500 µl of sterile water to the tubes with DNA and 100 µl to the control tube.

13. Plate 50 µl on one plate and the remaining 450 µl on another.

Solutions:

AcLi 10x: 1M AcLi pH 7.5 (adjusted with acetic acid)

TE 10x: 0.1M Tris pH 7.5; 0,01M EDTA pH 7.5.

Solution 2: 1/10 AcLi 10x, 1/10 TE 10x, 8/10 PEG 50% (w/v)

Salmon Sperm DNA: Boil for 10 min. Place immediately on ice for 5 min. (Sonication not necessary)